ABSTRACT

CHEMISTRY

GATIMU, ENID N. B.S. CLARK ATLANTA UNIVERSITY, 1994

A DIFFUSE REFLECTANCE FOURIER TRANSFORM INFRARED STUDY OF THE ADSORPTION AND DECOMPOSITION OF DIMETHYL METHYLPHOSPHONATE ON COPPER OXIDE SUPPORTED γ-ALUMINA

Advisor: Dr. Mark Mitchell

Dissertation dated May, 2003

The adsorption and decomposition characteristics of dimethyl methylphosphonate (DMMP) were studied over copper oxide supported γ-alumina using diffuse reflectance fourier transform infrared spectroscopy. Our studies indicate that DMMP adsorbs molecularly on the surface of the alumina samples that contained a copper oxide content of less than 1%. This molecular adsorption was primarily via the P=O bond on the DMMP molecule to a surface site on the metal oxide surface. At copper oxide coverages of higher than 1%, dissociative adsorption of DMMP was observed. There are two mechanisms identified for the dissociative adsorption of DMMP on the surface. One that involves the P=O bond attaching to a Lewis site on the surface of the supported metal oxide and the other that involves a nucleophilic attack of the phosphorus atom of the DMMP molecule by a surface hydroxyl or oxygen atom.

A DIFFUSE REFLECTANCE FOURIER TRANSFORM INFRARED STUDY OF THE ADSORPTION AND DECOMPOSITION OF DIMETHYL METHYLPHOSPHONATE ON COPPER OXIDE SUPPORTED γ-ALUMINA

A DISSERTATION

SUBMITTED TO THE FACULTY OF CLARK ATLANTA UNIVERSITY

IN PARTIAL FULFILLMENT OF THE REQUIREMENTS FOR

THE DEGREE OF DOCTOR OF PHILOSOPHY IN CHEMISTRY

BY

ENID NYAKARURA GATIMU

DEPARTMENT OF CHEMISTRY

ATLANTA, GEORGIA

MAY 2003

R = x T = 97

ACKNOWLEDGEMENTS

I wish to express my sincere gratitude to my advisor and mentor, Dr. Mark Mitchell, for guiding and mentoring me through this project. Thank you to Dr. Viktor Sheinker for his help in experiment setup, sample preparation, for running my samples, and invaluable discussions related to my work. Thank you to Dr. Mark White for his encouragement, discussions and suggestions on the direction of my work. I am grateful to Dr. Michael Williams, Dr. James Reed and Dr. Lebone Moeti for being on my thesis committee.

I want to thank my family, especially Linda Njeri Gatimu, and friends for their prayers, encouragement and support. None of this would have been possible without you.

TABLE OF CONTENTS

ACKNOWLEGEMENTS.....ii

LIST OF FIGURES.....vii

LIST OF TABLES.....x

CHAPTER1 INTRODUCTION.....1

1.1 Introduction.....1

1.2 Scope of study.....3

CHAPTER 2 LITERATURE REVIEW.....5

2.1 Dimethyl methylphosphonate.....5

2.1.1 Physical properties.....5

2.1.2 Structure of DMMP.....5

2.2 Adsorption and decomposition reactions of DMMP on metal oxides and supported metal oxides.....8

2.3 Spectroscopy.....11

2.3.1 Diffuse Reflectance Infrared Fourier Transform Spectroscopy.....11

2.3.2 Theory of diffuse reflectance.....11

2.4 Nature of alumina.....16

2.4.1 Copper Oxide on alumina.....18

2.4.2 Characterization of supported copper catalysts.....20

2.4.3 Carbon monoxide adsorption.....21

2.4.4 Nitric Oxide adsorption.....23

CHAPTER 3 MATERIAL AND METHODS.....25

3.1 Material and methods.....25

3.2 Catalyst synthesis.....25
3.2.1 Non-aqueous impregnation.....25
3.2.2 Aqueous impregnation.....26
3.3 Diffuse reflectance infrared spectroscopy experiments.....26
3.3.1 Vacuum manifold.....28
3.3.2 DMMP gas mixture.....28
3.4 Sample Preparation for the DRIFTS cell.....29
3.5 Micro-reactor experiments.....30
3.6 Carbon dioxide adsorption..... 30
3.7 Nitric Oxide (NO) experiments.....32
3.8 X-ray diffraction data.....32
CHAPTER 4 RESULTS AND DISCUSSION.....33
4.1 Physical characteristics of studies samples.....33
4.2 γ-alumina.....34
4.2.1 DRIFTS results of DMMP adsorbed on γ-alumina.....34
4.2.2 Micro-reactor experiments of DMMP and alumina.....38
4.3 Non-aqueous impregnation samples and their interaction with DMMP.....42
4.3.1 DRIFTS spectra of DMMP on NAQ4.....42
4.3.2 Interaction of DMMP with the surface of sample NAQ9.....43
4.3.2.1 DRIFTS results of NAQ9 at 50 °C.....46
4.3.2.2 DRIFTS results of the interaction of DMMP with the hydrated surface of NAQ9.....48
4.3.3. DMMP and its interaction with the surface of sample NAQ11.....49

4.3.3.1. Carbon monoxide adsorption on the surface of NAQ11.....49

4.3.3.2. DRIFTS results of reduced NAQ11 and DMMP.....50

4.3.3.3 DMMP adsorption the surface of NAQ11 at 25 °C.....51

4.3.3.4 DMMP adsorption the surface of NAQ11 at 50 °C.....52

4.3.3.5. Heating at high temperatures.....53

4.3.3.6. Hydration experiments.....55

4.4 Aqueous Impregnation samples and their interaction with DMMP.....56

4.4.1 DMMP interaction on the surface of sample AQ1.....56

4.4.1.1 Carbon monoxide adsorption on AQ1.....56

4.4.1.2 Adsorption of DMMP on AQ1.....57

4.4.2 Interaction of the surface of sample AQ2 and DMMP.....58

4.4.2.1 Carbon monoxide adsorption on the surface of sample AQ2.....58

4.4.2.2 DMMP adsorption on AQ2.....60

4.4.2.3 Addition of CO on oxidized AQ2 after DMMP addition.....62

4.4.3 Sample AQ3 and its interaction with DMMP.....63

4.4.3.1 X-ray diffraction data of AQ3.....64

4.4.3.2. Carbon monoxide adsorption.....64

4.4.3.3 Nitric oxide adsorption.....67

4.4.3.4 Micro-reactor experiments.....67

4.4.3.5 DRIFTS spectra of AQ3 with DMMP.....70

4.4.3.6.DMMP addition on the oxidized surface of AQ3 at 25 °C.....72

4.4.4 Sample AQ4 and its interaction with the DMMP molecule.....77

4.4.4.1 X-ray diffraction results.....78

4.4.4.2 CO adsorption on the surface of AQ4.....78

4.4.4.3 Nitric oxide adsorption on the surface of AQ4..... 81

4.4.4.4 Interaction of DMMP and AQ4 using micro-reactor experiments.....83

4.4.4.5 DRIFTS spectra of AQ4 with DMMP.....85

CHAPTER 5 CONCLUSIONS.....90

5.1 Future work.....92

BIBLIOGRAPHY.....93

LIST OF FIGURES

Figure 1. Methyl stretch region of Liquid DMMP in CCl_4.....7

Figure 2. Lower frequency region of liquid DMMP in CCl_4.....7

Figure 3. Mechanism of dissociative adsorption of DMMP on alumina.....8

Figure 4. Harrick DRS optics schematic diagram.....12

Figure 5. Dehydration pattern on alumina..... 17

Figure 6. Proposed structures of surface hydroxyl groups on γ-alumina.....18

Figure7. Schematic diagram of vacuum manifold.....28

Figure 8. Methyl stretch region of DMMP adsorbed on γ-alumina.....35

Figure 9. Lower frequency region of DMMP adsorbed on γ-alumina.....36

Figure 10. Loss of hydroxyl groups as DMMP adsorbs on the surface of γ-alumina..... 37

Figure 11. Decomposition product distribution of DMMP over γ-alumina at 25 °C.....39

Figure 12. Breakthrough point curve of DMMP over γ-alumina.....40

Figure 13. Methyl stretch region of DMMP adsorbed on the surface of NAQ4 43

Figure 14. Methyl stretch region of DMMP adsorbed on the surface of NAQ9 at 25 °C 44

Figure 15. Lower frequency region of DMMP adsorbed on the surface of NAQ9 at 25 °C.....45

Figure 16. Methyl stretch region of DMMP adsorbed on the surface of NAQ9 at 50 °C 47

Figure 17. Methyl stretch region of DMMP adsorbed on the hydrated surface of NAQ9 48

Figure 18. Fourier self-deconvolution spectra of 2110 cm^{-1} CO band on reduced NAQ11 50

Figure 19. Methyl stretch region of DMMP adsorbed on the surface of reduced NAQ11 51

Figure 20. Methyl stretch region of DMMP adsorbed on the surface of NAQ11..... 52

Figure 21. DMMP adsorption on the surface of on NAQ11 at 50 °C..... 53

Figure 22. Methyl stretch region of DMMP adsorbed on NAQ11 after heating at 400 °C 54

Figure 23. Methyl stretch region of DMMP adsorbed on the hydrated surface of NAQ11 55

Figure 24. Carbon monoxide adsorbed on surface of AQ1..... 57

Figure 25. Methyl stretch region of DMMP adsorbed on the surface of AQ1..... 58

Figure 26. Adsorption of carbon monoxide the oxidized surface of AQ2..... 59

Figure 27. Carbon monoxide adsorbed on the reduced surface of AQ2..... 60

Figure 28. Methyl stretch region of DMMP adsorbed on surface of AQ2 61

Figure 29. Lower frequency region of DMMP adsorbed on the surface of AQ2..... 62

Figure 30. CO adsorbed on the oxidized surface of AQ2 before and after DMMP adsorption..... 63

Figure 31. Carbon monoxide adsorbed on the oxidized surface of AQ3..... 64

Figure 32. CO adsorbed on the reduced surface of AQ3 and the corresponding Fourier self-deconvolution (FSD) 65

Figure 33. CO adsorbed on the surface of re-oxidized AQ3.....66

Figure 34. DMMP breakthrough data for AQ3 at 25 and 50 °C.....68

Figure 35. AQ3 product distribution as a function of temperature.....69

Figure 36. Lower frequency region of adsorbed DMMP
on the vacuum treated surface of AQ3 at 50 °C.....70

Figure 37. Methyl stretch region of adsorbed DMMP on the
vacuum treated surface of AQ3 at 50 °C.....71

Figure 38. Adsorbed DMMP on the surface of AQ3 during evacuation at 50 °C.....72

Figure 39. Lower frequency region of DMMP adsorbed on the
oxidized surface of AQ3.....73

Figure 40. Methyl stretch region of DMMP adsorbed on the
oxidized surface of AQ3 76

Figure 41. CO adsorbed on the oxidized surface of AQ3 at 25 °C.....77

Figure 42. CO adsorbed on the oxidized surface of AQ4.....80

Figure 43. Carbon monoxide adsorbed on the reduced surface of AQ4.....80

Figure 44. Effect of evacuating gas phase CO on the reduced surface of AQ4 81

Figure 45. NO on the oxidized surface of AQ4.....82

Figure 46. Simultaneous adsorption of NO and CO on the oxidized surface AQ4.....83

Figure 47. Breakthrough point data for AQ4.....84

Figure 48. Decomposition products distribution comparison over AQ4.....85

Figure 49. Methyl stretch region of DMMP adsorbed
on the surface of AQ4 at 50 °C.....86

Figure 50. Lower frequency region of DMMP adsorbed on AQ4 at 50 °C.....87

LIST OF TABLES

Table 1. Chemical structure of some nerve agents.....3

Table 2. Infrared vibration frequencies of DMMP in Hexane.....6

Table 3. γ-alumina hydroxyl group frequency assignments.....18

Table 4. Infrared frequency ranges of different carbon monoxide configurations.....21

Table 5. Assigned infrared adsorption frequencies for Cu-CO surface species.....23

Table 6. Observed infrared vibrations of NO on supported copper oxide alumina.....23

Table 7. Summary of copper samples studies for DMMP interaction.....33

CHAPTER 1

INTRODUCTION

1.1 Introduction

In 1993, after the Gulf War, the chemical weapons convention[1] drafted a treaty to prevent the development, production and stockpiling of chemical warfare and other toxic chemical agents. Russia and the United States have huge stockpiles of chemical warfare agents. Under the Chemical Weapons Convention Treaty, disposal of these stockpiles is mandated. There are two currently accepted methods of chemical warfare disposal: incineration and chemical degradation. In incineration, the unwanted chemicals are burned in a furnace and the effluents passed through scrubbers to ensure that no agents or toxic by-products are released. Chemical degradation on the other hand, seeks to change the chemical make up of the toxic chemical and destroy it or render it harmless.

There are seven locations in the United States of America that house stockpiled chemical weapons. These locations are also possible sites for or have incineration plants for disposal of toxic agents. The building of incinerators and the potential of toxic effluents or accidental spills in the plants during operation have raised grave concerns amongst the public, especially those who reside close to the locations of the incinerators.

As a result of this public outcry, the need to develop alternative technologies for toxic chemical disposal is critical. The critical features that need to be considered in developing these technologies include: a) designing systems that does not have smoke stacks. Smoke stacks are associated with uncontrolled environmental emissions and,
b) development of a portable chemical warfare destruction system that can be used directly in a chemical warfare storage facility. This minimizes the risks associated with transportation and handling of chemical weapons away from their storage or manufacturing sites.

Heterogeneous catalysis has emerged as a viable alternative[2] technology that utilizes chemical degradation as a means of destroying chemical warfare agents (CWA). This technology is attractive since it may have dual applications. It can serve as a means of bulk degradation of toxic chemicals and as a direct method for small scale decontamination efforts such as air filtration in gas masks and ventilation systems in buildings, decontamination of buildings, vehicles and clothing exposed to CWA.

Most CWA are in a class of chemical compounds called organophosphonates. They affect biological processes by depression of the nervous system, inflicting incapacitation or death. They do so by inhibiting the enzyme acetylcholinesterase which is responsible for the release of acetylcholine which aids in neural electrical transmission. Consequently, they are known as nerve agents. Table 1 shows the chemical structures of some common nerve agents.

Other than nerve agents, organophosphates also have useful applications in industry as heavy metal extraction solvents, in medicine (Zoledronic acid)[3] as a drug to

treat hypercalcemia, a common side effect of chemotherapy in cancer patients, and in agriculture as pesticides.

Tabun or GA Ethyl N,N-dimethyl phosphoramidocyanidate	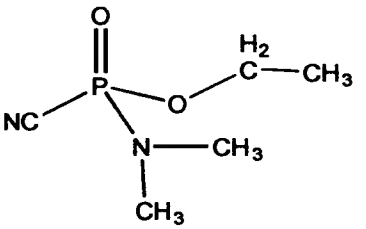
Sarin or GB Isopropyl methylphosphonofluoridate	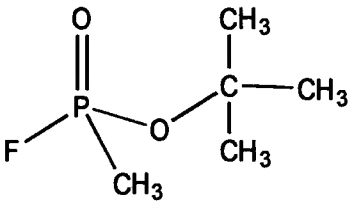
Soman or GD Pinocoyl methylphosphonofluoridate	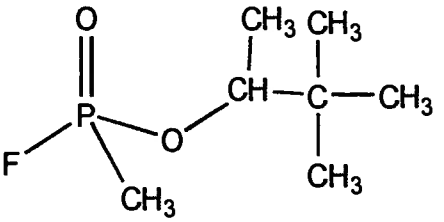
VX O-ethyl S-(2-iisopropylamino) ethyl methylphosphonothiolate	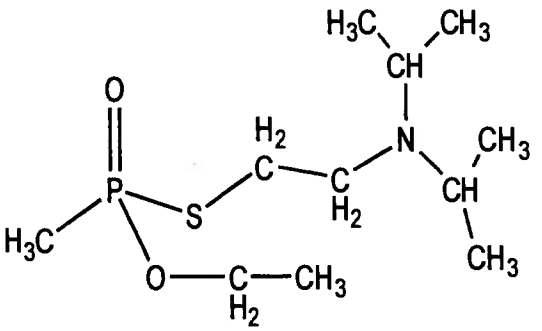

Table 1. Chemical structure of some nerve agents.

1.2 Scope of study

Metal oxides[4] are well known adsorbents, catalysts and catalyst supports in industry and are currently under consideration as decontamination agents. Wagner et al.,[5]

have studied nanosized CaO, MgO and alumina and have shown that these metal oxides hydrolyse GD, VX, GB and other toxic organophosphonates at room temperature. The products of the hydrolysis reaction are non-toxic volatile gases which are evolved and the resulting phosphonic acid derivatives bind to the surface of the metal oxide. This study suggests that these metal oxides can be applied as CWA decontamination agents especially since the products of hydrolysis are retained on the surface of the metal oxide.

Further study of metal oxides in this context is warranted so as to identify other metal oxides and/or supported metal oxides that are suitable for decontamination purposes. In this work, we continue the search for supported metal oxide combinations that effectively work as either adsorbents or decomposition agents for CWA and environmentally unfriendly pesticides. Laboratory use of toxic organophosphonates is hazardous, so non-toxic simulant chemicals are used for study. In this work we chose to use dimethyl methylphosphonate (DMMP) as the simulant molecule of choice. The adsorption and decomposition of dimethyl methylphosphonate on copper oxide supported on γ-alumina and other metal oxides at room temperature is the focus of this study.

CHAPTER 2

LITERATURE REVIEW

2.1 Dimethyl methylphosphonate

Dimethyl methylphosphonate (DMMP) is an organophosphonate that is used in industry as an additive in flame retardants, solvents and low-temperature hydraulic fluids. It is non-toxic and is one of the most widely used simulants for both chemical warfare agents[6] and pesticides[7]. DMMP is the starting material for the manufacture of toxic gases such as sarin and soman and is regulated by the Chemical Weapons Convention under the Dialkyl methylphosphonate section, schedule 2.

2.1.1 Physical properties

Dimethyl methylphosphonate is a clear liquid at 25 °C with a vapor pressure *ca.* 1 Torr. It has a molecular weight of 124.08, a density of 1.15g/cm^3 and a boiling point of 79.5 °C at 20 °C. It possess a dipole moment of about 3 debyes[8]. DMMP is polar and hence soluble in most polar solvents such as water and ethanol.

2.1.2 Structure of DMMP

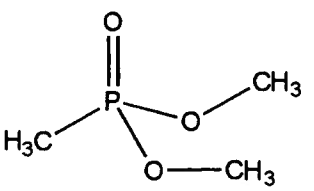

DMMP is a tetrahedral molecule with a van der Waals diameter of 3.25 Å.[9] It possesses 16 atoms and therefore 42 normal modes of vibration. Its molecular point group symmetry is C_1 hence all fundamental vibrations are allowed in infrared spectroscopy. The vibrational spectrum is calculated and confirmed experimentally by Moravie et al., [10] and Van der Veken et al., [11] respectively. Table 2 below shows the IR vibration frequencies for DMMP in hexane.

Vibration Mode	Frequency cm^{-1}.	Vibration Mode	Frequency cm^{-1}.
ν_a (CH_3P)	2992[b]	ν(P=O)	1246
ν_a (CH_3O)	2957[b]	ρ(CH_3O)	1185
ν_s (CH_3P)	2926[b]	ν(CO)	1061
ν_s (CH_3O)	2852	ν(CO)	1033
δ_a (CH_3O)	1467	ρ(CH_3P)	914
δ_s (CH_3O)	1452	ν(PO_2)	820
δ_a (CH_3P)	1421	ν(PO_2)	789
δ_s (CH_3O)	1314	ν(PC)	711

Table 2. Infrared vibration frequencies of DMMP in Hexane

a = antisymmetric, s = symmetric, ν = stretch, δ = deformation, ρ = rock

Infrared spectra of DMMP are shown in Figures 1 and 2. Figure 1 shows the methyl stretch region and Figure 2 shows the lower frequency region showing the peaks identified in Table 2.

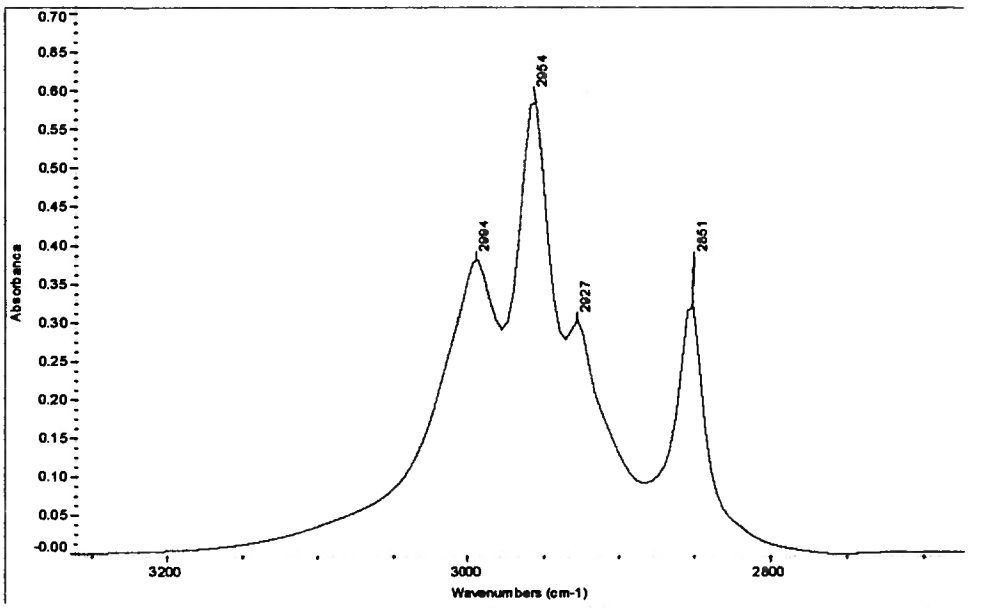

Figure 1. Methyl stretch region of liquid DMMP in CCl_4

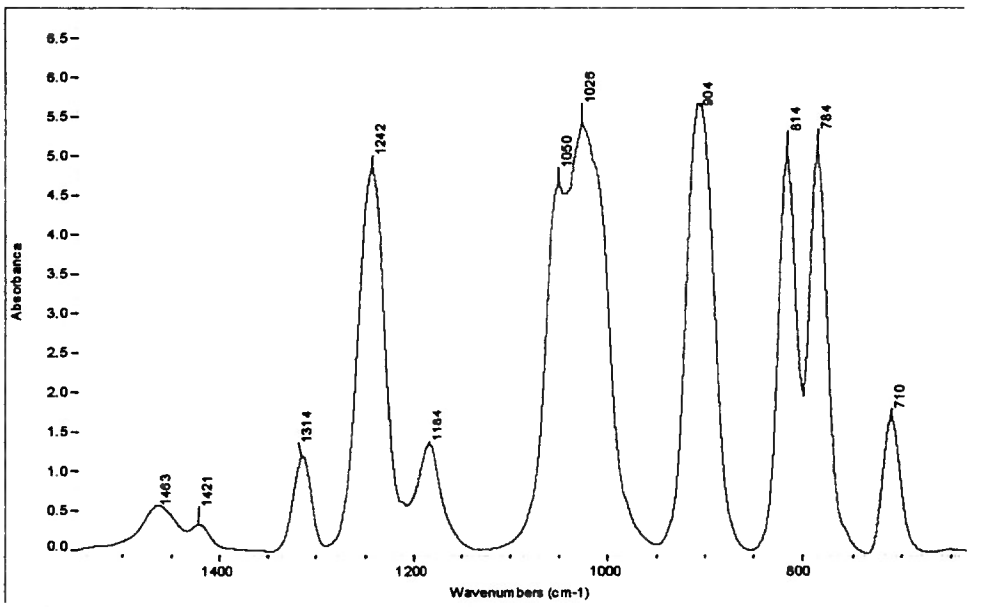

Figure 2. Lower frequency region of liquid DMMP in CCl_4

DMMP can coordinate to a metal oxide surface via the lone pair of electrons on the phosphoryl oxygen atom. This oxygen atom can also form hydrogen bonds with surface hydroxyl groups. Templeton et al. [12] studied DMMP and alumina using inelastic tunneling spectroscopy and showed that DMMP adsorbs molecularly at 200 K and dissociatively at 295 K and above. The dissociative reaction occurs by the phosphoryl oxygen binding to a Lewis acid site on the alumina surface followed by nucleophilic substitution at the phosphorus center by a surface oxygen. This interaction then leads to the formation of a surface phosphonate species and loss of a methoxy group as methanol. The mechanism of this reaction is shown below.

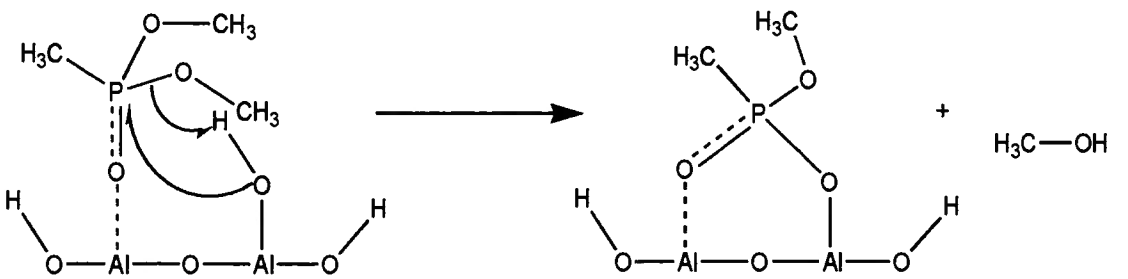

Figure 3. Mechanism of dissociative adsorption of DMMP on alumima

2.2 Adsorption and Decomposition Reactions of DMMP on Metal Oxides and Supported Metal oxides

Adsorption and decomposition reactions of DMMP have been studied over several metal and metal oxide systems at various temperatures.

At room temperature, Tesfai and coworkers[13], studied iron oxide on γ-alumina and reported DMMP decomposition via cleavage of the carbon phosphorus bond on DMMP. They proposed an oxidative mechanism involving the Fe(II)/Fe(III) redox couple where an oxide ion on an oxide surface is made available via a change in the oxidation state of

the metal. This ion then reacts with the adsorbed DMMP to cleave the P-CH_3 bond at room temperature.

Mitchell et al.[14] investigated the interaction of DMMP with four different metal oxide surfaces and found that DMMP binds to acidic sites via the P=O bond. After the DMMP binds to the surface, methanol is evolved and a methyl methylphosphonate (MMP) group is left behind on the surface at temperatures as low as 50 °C.

DMMP has been shown to strongly adsorb on a magnesium oxide[15] surface at room temperature through a Lewis acid site interaction of the oxygen atom on the P=O bond. At temperatures as high as 500 °C, dimethyl methylphosphonate decomposes on the surface of magnesium oxide evolving formic acid and methanol. There was no evidence of phosphorus containing fragments evolving as the reaction occurred indicating that all such species were immobilized on the surface of the magnesium oxide.

Recently other studies have been recorded in which different metal oxides have been supported on alumina and silica and tested for thermocatalytic oxidation of DMMP at high temperatures. Copper, nickel and vanadium[16]oxides on alumina at 673 K show activity for thermocatalytic oxidation of DMMP. Vanadium oxide showed the highest activity for DMMP oxidation possibly due its inability to form a stable phosphate which poisons the copper and nickel oxides. Phosphorus pentoxide, a by-product of DMMP oxidation at these high temperatures was observed to play an important role in assisting in DMMP decomposition as it acts as a dehydrating agent. Vanadium oxide is not affected by the phosphorus pentoxide and when the vanadium was supported on silica, the effectiveness of this new material was enhanced since silica is unreactive towards P_2O_5.

Mixed valent amorphous manganese dioxide[17] (AMO) exhibited photo assisted decomposition of DMMP. DMMP adsorbed on these materials, when irradiated with UV-Vis light, evolves CO_2 and methanol. Phosphorus species from the DMMP molecules accumulate on the surface of the material and poison the catalyst. Manganese dioxide supported on alumina (Mn/Al_2O_3)[18] has been observed to react with DMMP between 200 °C to 400 °C to yield CO_2 and methanol as a by product of decomposition. The presence of the CO_2 is indicative of an oxidation reaction occurring on the surface of (Mn/Al_2O_3).

Activated carbon [19] does not oxidize DMMP in the absence of molecular oxygen even at elevated temperatures as high as 1100 °C. In the presence of O_2 however, DMMP in the initial stages of contact over activated carbon, gives rise to CO_2, methanol and P_2O_5. This reaction is facilitated by acidic sites created on the carbon surface via oxygen interaction with elevated carbon temperature.

DMMP is hydrolysed by titanium dioxide[20] surface hydroxyl groups. This reaction occurs at temperatures higher than 214 K and results in surface-bound methoxy species that come from the cleavage of the P – OCH_3 bond in DMMP. Rusu and Yates[21] found that small coverages of DMMP on the surface of titanium dioxide at temperatures as low as 200 K are photooxidized to yield CO_2, CO and surface formate groups, when irradiated with UV-Vis light. When large coverages of DMMP were adsorbed on titanium dioxide and irradiated with UV-Vis light, non-photooxidation was observed. This suggested that there is a critical amount of surface DMMP coverage that allows for the photo-decomposition process to proceed. Beyond this point, the DMMP shields all

the TiO_2 sites where O_2 initiates the photooxidative process and thus no decomposition occurs.

2.3 Spectroscopy

Molecular spectroscopy has traditional applications in structure identification, purity diagnosis and quantitative analysis. Faster computers, efficient data processing and new technology for specialized spectroscopic equipment have enabled molecular spectroscopy to develop utilization in areas that include chemical kinetics, molecular geometry and conformational analysis, surface characterization and chemistry. These applications are facilitated by collection techniques including photoacoustic spectroscopy (PAS), attenuated total reflection (ATR) and diffuse reflectance infrared fourier transform spectroscopy (DRIFTS).

2.3.1 Diffuse Reflectance Infrared Fourier Transform Spectroscopy

Diffuse Reflectance Infrared Fourier Transform Spectroscopy (DRIFTS) was a term coined by Peter Griffiths.[22, 23] DRIFTS is a technique whereby diffusely reflected radiation from a surface is collected and sent to a detector via a carefully calculated optical arrangement. A schematic diagram of the optical arrangement is shown in Figure 4. Griffiths and his group designed the first set of optics used to collect diffusely reflected radiation from an illuminated surface. Harrick Scientific Inc. later modified the design making an optical system that is easy to use, produces maximum throughput and is easy to maintain.

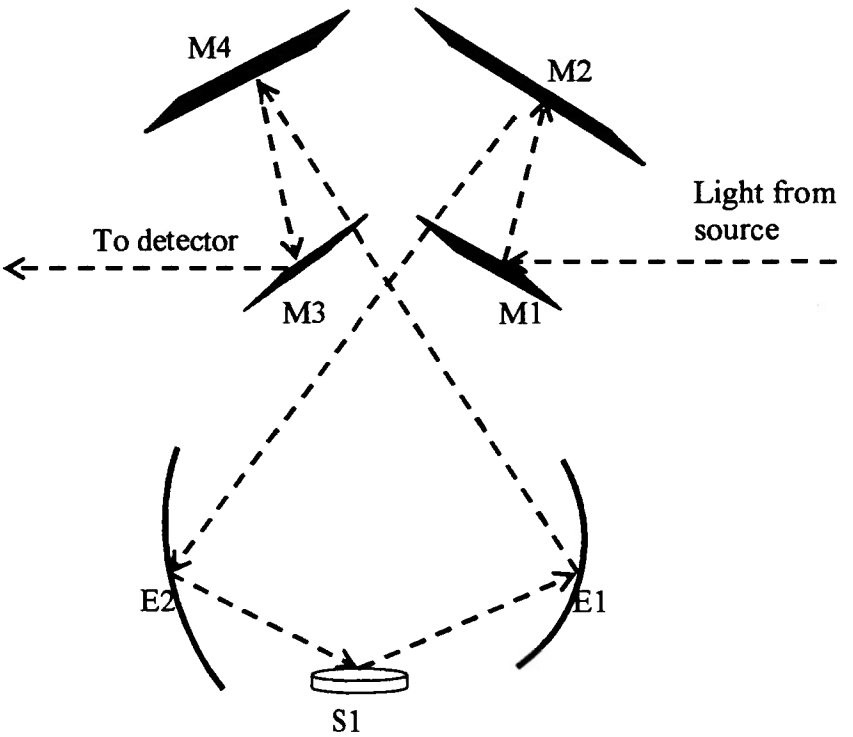

Figure 4. Harrick DRS optics schematic diagram

M1, M2, M3 and M4 are straight mirrors. E1 and E2 are ellipsoidal mirrors. S1 is the sample. Light from the detector is reflected by Mirror M1 to Mirror M2 which then reflects the light onto the ellipsoid E2 which focuses the light in the middle of the sample S1. The light is diffusely reflected by the sample and the radiation is collected by ellipsoidal mirror E1 which then directs the light to Mirror M4. Mirror M4 then collects this light and reflects it to mirror M3 which sends the radiation to the detector

2.3.2 Theory of diffuse reflectance

When a surface is irradiated by light there are two main kinds of reflection that may occur: specular reflection and diffuse reflection. Specular reflection (also known as mirror-like reflection) occurs on smooth shiny surfaces. The radiation does not penetrate

the surface and the angle of incidence is equal to the angle of reflection. This reflection is described by Fresnel equations.

$$R_f = \frac{(n-1)^2 + (n^2k^2)}{(n+1)^2 + (n^2k^2)} \qquad 1$$

where R_f is the Fresnel reflectance, n is the sample refractive index, k is proportional to the absorption index.

Diffuse reflection on the other hand occurs on matte or dull surfaces and is characterized by light that, once incident on a surface, penetrates the surface of the sample and is reflected, refracted and diffracted by the particles of the sample surface to emerge as diffusely reflected radiation. This process is described by Kubelka Munk[24] theory.

In the Kubelka Munk theory, when a sample diffusely reflects light, the ratio of the intensities of the reflected to the incident light is given by

$$R_\infty = \frac{I}{I_o} \qquad 2$$

where R_∞ is the absolute reflectance of an infinitely thick sample, I is the intensity of the reflected radiation, I_o is the intensity of the incident beam. If the sample was a perfect diffuse reflector then $R_\infty = 1$. It is not practical to measure absolute reflectance R_∞ so the relative reflectance is measured instead based on a known reference sample.

$$R'_\infty = \frac{R_\infty sample}{R_\infty reference} \qquad 3$$

The relative reflectance is related to the analyte concentration by the following equation

$$R'_{\infty} = \frac{(1-R_{\infty})^2}{2R_{\infty}} = \frac{k}{s} = \frac{2.303C\varepsilon}{s} \qquad 4$$

where k is the absorption coefficient, s is the scattering coefficient of the sample, ε is the absorptivity, C is the concentration of the analyte. This equation is known as the Kubelka Munk relation and holds true provided the scattering coefficient remains constant.

The Kubelka Munk theory is governed by four assumptions:

1) All fresnel (specular) reflection is ignored.
2) The particles of the sample are smaller than the thickness of the entire sample.
3) The sample thickness is greater than the beam penetration depth.
4) The sample diameter is greater than the focus of the incident beam.

In traditional transmission mode infrared spectroscopy, a sample is pressed into a pellet in a potassium bromide matrix and placed in the path of an IR beam. The resulting spectrum records the radiation adsorbed. The problem with this technique of sample preparation is that if surface chemistry is of interest, the pressure required to press the potassium bromide pellets may alter the sample surface and may cause unwanted reactions to occur.[25] DRIFTS eliminates this problem by collecting data on powder samples without making a pellet prior to data collection.[58] The technique itself is known for superior signal to noise ratio and is more sensitive to very small concentrations of

analyte as a result of the scattering of the radiation which increases the pathlength of the IR radiation.

The most common problem of a spectrum collected via the diffuse reflectance technique is restrahlen bands (which resemble inverted or derivative like bands). These bands are caused by specular reflection and total absorbance which occurs when a sample is a strong absorber. Restahlen bands may be eliminated by diluting the sample in a potassium bromide or potassium chloride matrix and also by loosening the packing of the sample in the sample cup. Tight packing of the sample may lead to a surface that specularly reflects light.

DRIFTS has applications in the pharmaceutical industry as a technique to elucidate drug purity, in environmental studies to identify inorganic and organic species in water, air and soil. Industry has a variety of applications for DRIFTS mostly for quality control purposes. The study of adsorbed species on surfaces to give a mechanistic insight into catalytic processes utilizes DRIFTS as a technique to examine the surface chemistry of the adsorbed species.[57]

2.4 Nature of alumina

Alumina is a term used to describe solids which have the formula $Al_2O_3.n(H_2O)$ where n = 0 to 3. They are derived from heating crystalline ($Al(OH)_3[Al_2O_3.(H_2O)_3]$) and amorphous (AlO(OH) [$Al_2O_3.(H_2O)$]) alumina. Corundum is one of the most thermodynamically stable aluminas known and is obtained by heating naturally occurring or synthetically made alumina hydroxides above 1100 °C. It has very little use as a catalyst or catalyst support for chemical reactions [26]. At temperatures below 1100 °C, depending on the precursor, final temperature and mode of heating, a variety of transition aluminas can be generated. These aluminas include δ and γ-aluminas.

δ-Aluminas are obtained by heating aluminium hydroxides above 600 °C. This class of aluminas include the κ, τ varieties. They are more crystalline than γ-aluminas and possess different physical properties including densities, surface areas, pore volume and diameters.

γ-Aluminas are formed by heating boehmite at temperatures between 400 °C and 500 °C. They are widely used to separate compounds by column chromatography and as supports and/or catalysts for organic reactions. They possess a surface spinel structure and possess a surface area that ranges from 100 – 300 m^2/g or higher. The surface of γ-alumina consists of terminal hydroxyl groups that lie directly above an aluminium ion in the next layer as proposed by Peri. [27] When γ-alumina is heated in the range 100 –150 °C, physisorbed water evolves from the surface. At higher temperatures, the surface hydroxyl groups condense and evolve water, as illustrated in Figure 5, creating three predominant species on the surface;

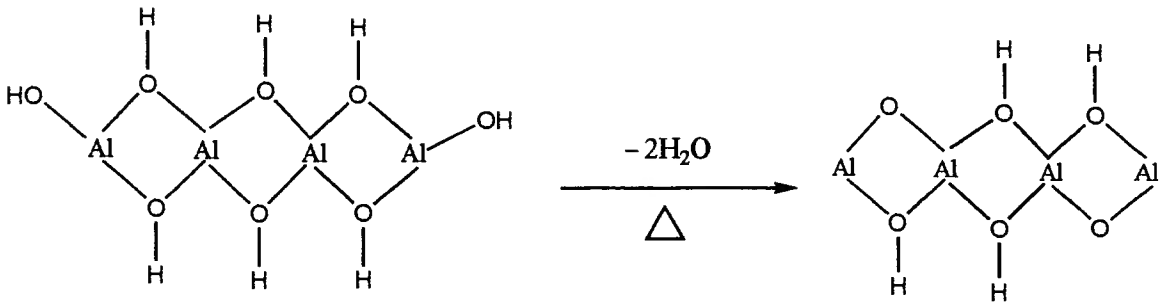

Figure 5. Dehydration pattern on alumina

I. OH sites which may serve as weak Bronsted acids, bases or nucleophiles

II. O^{2-} sites which can function as strong bases or nucleophiles

III. Al^{3+} sites which function as Lewis acid sites or electrophiles

These sites can coexist and act cooperatively to allow a variety of reactions to occur on the surface. Alumina is amphoteric, its acidic or basic characteristics can be enhanced depending on the needs of the reaction to be considered.

Hydroxyl groups on the surface of alumina are not structurally equivalent. Infrared studies have shown that there are up to five OH stretching frequencies that depend on where the OH is situated. Knözinger and Ratnasamy [28] proposed that the five different OH groups are generated depending on whether the hydroxyl group is on a tetrahedral or octahedral aluminium ion. The Figure 6 below shows configuration of the five different types of hydroxyl groups on the surface of alumina. The corresponding infrared frequencies are listed in Table 3.

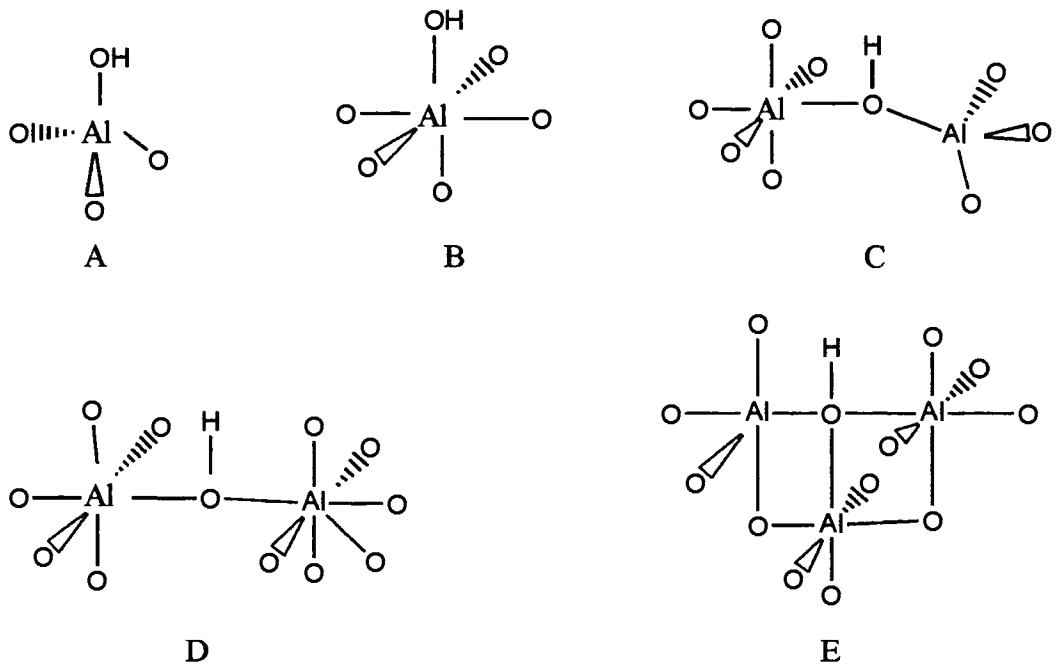

Figure 6. Proposed structures of surface hydroxyl groups on γ-alumina

OH Frequency Assignments	
Structure	ν OH cm^{-1}
A	3760-3780
B	3785-3800
C	3730-3735
D	3740-3745
E	3700-3710

Table 3. γ-alumina hydroxyl group frequency assignments[28]

The most basic group is shown in Figure 6 structure A and the most acidic is in an environment that is similar to that shown by Figure 6 structure E.

The structure of alumina enables it to serve as an ideal surface for adsorption and catalytic reactions as well as a support for metal oxide catalysts.

2.4.1 Copper oxide on alumina

Copper is a well known catalyst for the oxidation of organic molecules by atmospheric oxygen. Supported copper oxide catalysts have been used for selective reduction and oxidation reactions. They are generally prepared by aqueous or non-aqueous impregnations of metal oxide supports such as alumina with a soluable copper salt. The amount of metal oxide and the nature of the dispersion on the surface of the support varies depending on the nature of preparation of the material, the pH of the solution, the nature of the catalyst precursor and the acid base properties of the support.

The use of a thermally stable support such as alumina allows the active CuO phase to be dispersed on the surface. The hydroxyl groups on the alumina surface act as anchoring sites for incoming metal oxides depending on the pH of the solution, the nature of the catalyst precursor i.e., charge of the metallic complex, the pH of the solution and the acid-base properties of the OH groups. Garbowski et. al[29] studied the interaction of copper ions with hydroxyl groups on alumina and observed that there is no specific hydroxyl groups that the copper interacts with on alumina.

Few reports exist in the literature concerning the interaction of DMMP with supported copper oxide. Lee and coworkers[30] studied the interaction of copper substituted calcium hydroxyapatite with DMMP. They observed 100% DMMP conversion over a time interval which is termed as the protection period. The length of the protection period varied with temperature ranging from 5 min to 20 hrs or longer between 373 K and 673 K. During the protection period, the products of conversion were carbon monoxide and water except at 373 K where no products of conversion were observed. After the protection period, methanol and dimethyl ether were observed. During their experiments,

they observed catalyst deactivation and attributed it to surface phosphate residues from DMMP oxidation. The catalyst was temporarily regenerated by heating the sample at temperatures higher than 673 K. At these temperatures, the authors suggested that the phosphate residues migrate to the support re-exposing the active Cu^{2+}/Cu^{+} centers and hence regaining limited ability to continue to decompose the DMMP.

Cao and coworkers[16] studied 10% CuO/Al_2O_3 at 723 K and found that the catalyst had a protection period of 7.5 hours. There was little activity observed after this period due to phosphate residues interacting with the copper to form stable copper phosphates which inhibit further DMMP oxidation.

Trogler and coworkers[31, 32] have done solution chemistry work with copper complexes and their interaction with phosphate esters. Their work shows that the activity of copper catalyst towards phosphate ester hydrolysis is strongly dependent on pH with the catalyst activity decreasing with decreasing pH. They showed that copper 2,2 bipyridine will catalyse the hydrolysis of phosphate diesters in aqueous solution at 75 °C and a pH range 5.8-8.3.

TMEDA [Cu (II)] was one of the first catalysts discovered for the hydrolysis of sarin.[33] Sohn and coworkers incorportated the tetramethylethylenediammine copper complex TMEDA [Cu (II)] into a porous silicon sample and found that this new sample hydrolysed (diisopropylfluorophosphonate) DFP (another CWA stimulant molecule) and produced hydrofluoric acid (HF) which can be detected on the surface of the sample.[34]

2.4.2 Characterization of supported copper catalysts

Several methods were employed to characterize the copper samples that were prepared. Inductively coupled plasma/ mass spectrometry (ICP-MS) was used to determine the elemental composition of the samples. Powder X-ray diffraction spectrometry (XRD) techniques were applied to detect crystalline copper oxide species on the surface and diffuse reflectance infrared spectroscopy was utilized to study small probe molecules such as carbon monoxide and nitric oxide on the surface of the catalysts to determine the surface oxidation states of the supported copper. Surface area measurements were obtained using the Brunnauer Emmett Teller method.

2.4.3 Carbon monoxide adsorption

Carbon monoxide is a small diatomic molecule that has a bond length of 1.131 Å and a polarity of 0.14 Debyes.[36,37] It has the ability to adsorb on transition metal atoms and the resulting M-CO complex shows C-O vibrational frequencies that depend on the metal atom oxidation state. Consequently, carbon monoxide can be used to characterize and determine the surface oxidation states of supported metal catalysts. Carbon monoxide can interact with metal oxides in a bridged or linear configuration. Eischens and his colleagues[46] assigned the infrared frequency of CO adsorbed in a linear configuration to be in the 2000-2100 cm^{-1} range while CO adsorbed in a bridged configuration to be in the 1800-1950 cm^{-1} region. Nguyen and Shepard[47] suggested infrared frequencies ranges for four possible CO configurations shown in Table 4.

Configuration	Frequency region
Terminal or linear	2130-2000 cm^{-1}
Two fold bridged CO	2000-1880 cm^{-1}
Three fold coordinated CO	1800-1880 cm^{-1}
Four fold coordinated CO	1800 cm^{-1} and below

Table 4. Infrared frequency ranges of different carbon monoxide configurations[38]

Several authors[40-42] have documented CO adsorption on supported copper catalysts at room temperature and below. Pritchard and co-workers[48, 49] have done extensive work on CO adsorption on single crystal copper and found a significant correlation between the adsorption maxima and the surface structure of the metal. Busca[35] and his colleagues studied CO adsorption on unreduced Cu/Al_2O_3 using infrared spectroscopy and showed the CO adsorbs very strongly on Cu^+ species. He proposed that the surface of his sample was comprised of both Cu^{2+} and Cu^+ species. London and Bell[36] studied CO adsorption on CuO/SiO_2 samples and observed that CO adsorbs strongly on Cu^+ sites and weakly on Cu^{2+}. Padley and coworkers39 studied CO adsorption on both oxidized and reduced CuO/Al_2O_3 samples and identified four different surface copper species on which CO linearly adsorbs. The four surface species they identified were Cu^{2+}, Cu^+ in a Cu^+ matrix, Cu^+ in a Cu^{2+} matrix and Cu^0 and corresponding infrared frequency adsorptions were assigned at 2137, 2113, 2122 and 2098 cm^{-1} respectively.

Dandekar and Vannice[40] extensively studied the surface oxidation states of several supported copper catalysts using CO as a probe molecule. At 300 K, they observed that CO adsorption occurs reversibly on Cu^+ sites but if the temperature was

lowered to 173 K, CO adsorbed irreversibly on Cu^{2+} and Cu^{+} yielding definitive results regarding the nature of the surface copper species. Table 5 below summarizes the general Cu-CO infrared frequency assignments established in their work.

Adsorbed species	Infrared frequency
Cu^{+}-CO	2140-2110 cm^{-1}
Cu^{2+}-CO	above 2140 cm^{-1}
Cu^{0}-CO	below 2100 cm^{-1}

Table 5. Assigned infrared adsorption frequencies for Cu-CO surface species.

2.4.4 Nitric oxide adsorption

Nitric Oxide (NO) is a diatomic molecule that exists as a free radical in the gas phase. It has the ability to combine with other free radicals to give a stable molecule with paired spins. It has a dipole moment of 0.5 Debye[51] and a bond length of 1.15 Å.[52] NO combines with a number of transition metal ions through the nitrogen atom to form nitrosyl (NO^{+}) complexes which have either a bent or linear geometry.

Infrared studies of NO adsorption on supported copper catalysts have been used to identify the oxidation states and surface composition of copper ions. Table 6 shows the observed vibrational frequencies of copper-NO interactions on copper oxide supported aluminas obtained from literature.

Support	Species	Infrared frequencies cm^{-1}
γ-Al_2O_3	Cu^{2+}-NO^{+}	1875, 1900, 1920 1888, 1863
γ-Al_2O_3	Cu^{+}-NO^{-}	1780, 1800

Table 6. Observed infrared vibrations of NO on supported copper oxide alumina

An infrared spectroscopy study of NO adsorption on copper zeolites -Cu-ZSM-5[53] yielded the following results: - a 1906 cm^{-1} peak that was assigned to NO^{+} species adsorbed on a Cu^{2+} site, an 1813 cm^{-1} peak that was assigned to a NO^{-} species adsorbed on a Cu^{+} site and two peaks at 1827 and 1734 cm^{-1} which were assigned to the symmetric and anti-symmetric vibrations of the anionic dinitrosyl species respectively.

Lokhov et al.[54] observed that on the surface of reduced CuO/γ-alumina, an initial dose of NO caused a peak at 1780 cm^{-1} which they associated with Cu^{+} centers. When the NO was allowed to remain in contact with the surface of the reduced supported copper sample, new peaks appeared at 1880 and 2220 cm^{-1} while the intensity of the 1780 cm^{-1} decreased. They assigned the peak at 1880 cm^{-1} to NO adsorbed on Cu^{2+} sites and the 2220 cm^{-1} to gaseous N_2O. When NO was adsorbed on oxidized CuO/γ-alumina samples, they observed peaks at 1875, 1900 and 1920 cm^{-1}, which were assigned to NO interacting with Cu^{2+} centers. The 1875 cm^{-1} peak was assigned to NO interacting with Cu^{2+} ions in a CuO phase, the 1900 cm^{-1} was assigned to an NO interacting with a Cu^{2+} ion in clusters with a common oxygen ligand while the 1920 cm^{-1} was designated to NO stabilized at interstitial Cu^{2+} in the Al_2O_3 lattice.

Fu and colleagues[55] studied NO adsorption on CuO/γ-Al_2O_3 using infrared spectroscopy at low temperature observed peaks at 1888, 1862 and 1800 cm^{-1}. The 1888 and 1862 cm^{-1} bands were assigned to NO complexes with Cu^{2+} sites and the 1800 cm^{-1} peak was assigned to NO complexes with Cu^{+1} sites. Hierl and coworkers[56] observed a peak at 1863 cm^{-1} when studying NO chemisorption on CuO/γ-alumina and assigned this peak to NO chemisorbed on Cu^{2+} sites in the copper aluminate phase.

It is possible to therefore establish the nature of the supported metal oxide on the surface of the alumina using small probe molecules such as carbon monoxide to establish the presence of Cu^{+} species and nitric oxide to establish the prescence of Cu^{2+} species.

CHAPTER 3

EXPERIMENTAL

3.1 Material and methods

The following gases were obtained from Holox Ltd and used as is: 99.99 % carbon monoxide, 1% nitric oxide in helium, 20 % oxygen in helium, 99.99% methane. γ-alumina was obtained from Goodfellow and $Cu(NO_3)_2.3\ H_2O$ from J.T. Baker Chemical Co. Copper acetylacetonate, dimethyl methylphosphonate and acetonitrile were purchased from Sigma-Aldrich and iron III acetylacetonate from STREM chemicals.

3.2 Catalyst synthesis

3.2.1 Non-aqueous impregnation

The impregnation of copper was carried out by mixing measured quantities of copper (II) acetylacetone and 5 g of alumina in 100 ml of acetonitrile and stirring for 24 hours on a magnetic stirrer. The filtered solids were dried in a vacuum oven for 24 hours at 80 °C. The samples were calcined at 500 °C in air.

3.2.2 Aqueous impregnation

Alumina supported copper oxides were synthesized from aqueous solution. To make these samples, 1.5579 g of $Cu(NO_3)_2.3\ H_2O$ were dissolved in 50 ml of diionized water. To this solution, 5 g of γ-alumina were added and the mixture stirred for approximately 4 hours. The solution was filtered, and the residue dried at room temperature overnight and calcined at 400 °C for 6-8 hrs. For the synthesis of samples with higher metal content, the freshly impregnated calcined solid was then placed back into a new copper nitrate solution containing ca. 1.5 g of the nitrate and process was repeated.

3.3 Diffuse reflectance infrared spectroscopy experiments

The diffuse reflectance studies were performed using a Harrick Scientific Corp. high–vacuum temperature-controlled stainless steel reaction chamber (HVC) diffuse reflectance accessory shown in the appendix. This accessory was fitted in a Nicolet 750 Magna FT-IR. The accessory was fitted with two sodium chloride windows and an optical grade fused-silica viewing window, an iron-constantan thermocouple, and a cartridge heater positioned directly below the sample cup. Gas inlet and outlets were fitted to the accessory for vapor dosing. To obtain spectra, 250 interferograms were co-added at 8 cm^{-1} resolution, transformed and apodized with a Happ-Genzel function. The gas inlets and outlet were connected to stainless lines wrapped in heating tape maintained at a temperature of ~70 °C. Manometers were connected at the entrance and at the exit of the HVC chamber. The line attached to the inlet of the HVC chamber delivered gas from

the vacuum manifold. The line attached to the outlet of the HVC delivered gas to a roughing and diffusion pump vacuum system.

3.3.1 Vacuum manifold

The vacuum manifold is made of glass compartments which consist of a sample tube, a 2.01L bulb, a liquid nitrogen trap, a gas inlet, outlet and vacuum pump connection all fitted with valves attached to a long glass tube. The schematic diagram of the layout of the different compartments of the vacuum manifold is shown in Figure 7. Each compartment can be isolated or connected to the rest of the manifold by opening or closing the valves attached to them. A Baratron Manometer with a 1000 Torr maximum pressure range monitors the pressure in the manifold. It is critical that the manifold has no air leaks. To do this one must evacuate the manifold and seal off the liquid Nitrogen trap, and then monitor any pressure increases in the manifold over a period of time.

3.3.2 DMMP gas mixture

DMMP was stored in liquid form in the sample tube in the vacuum manifold. Several freeze, pump, thaw cycles were necessary to remove any higher vapor pressure components.

The DMMP gas mixture (1:1000) was made by opening the DMMP sample tube to the manifold and the 2 L bulb. The vapor pressure of DMMP was allowed to equilibrate to about 0.7 -0.8 Torr. The bulb was then isolated and the DMMP sample tube

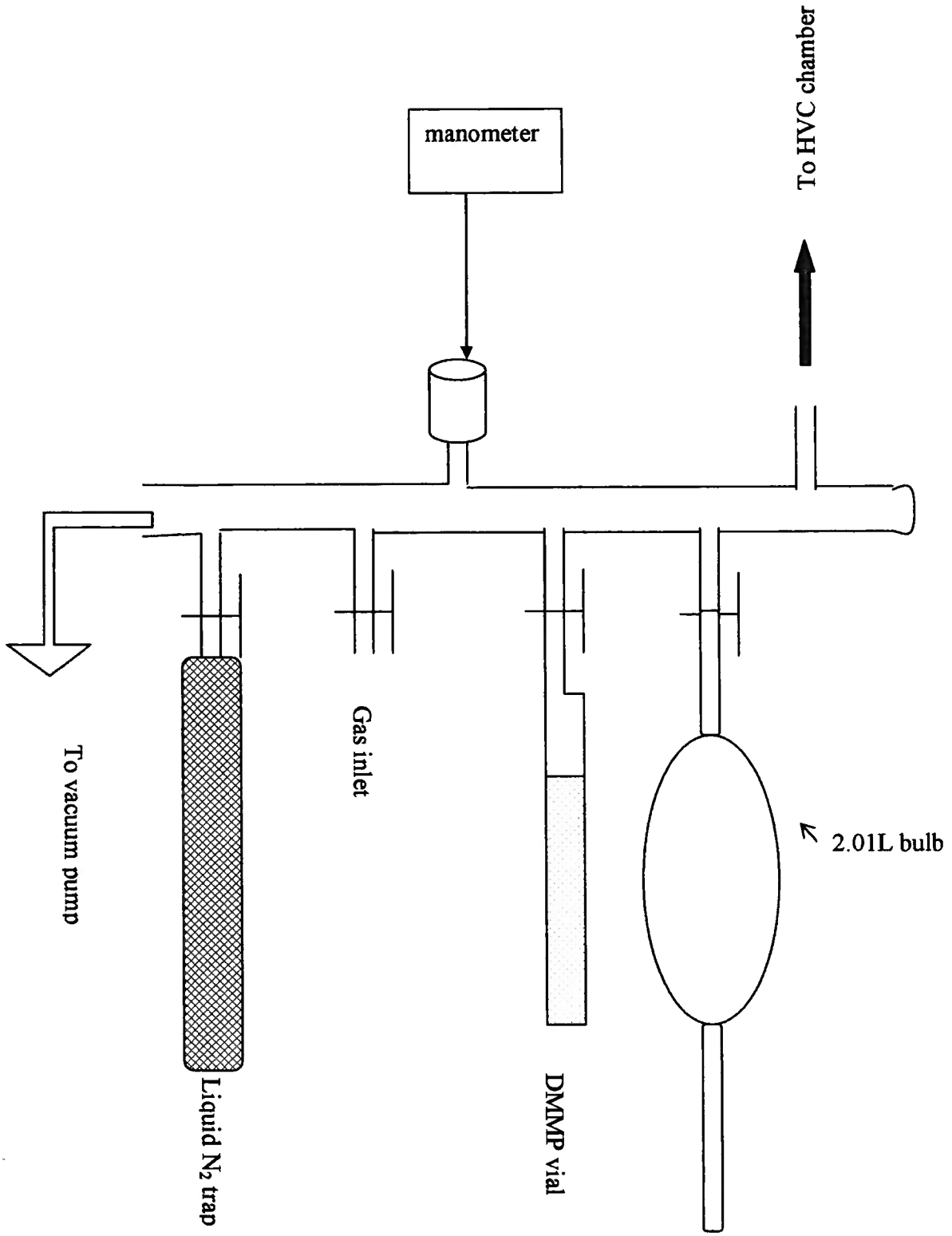

Figure 7. Schematic diagram of vacuum manifold

closed. The rest of the manifold was evacuated. The manifold and the 2 L bulb were then pressurized to 700 Torr with oxygen (20% in helium). The 2 L bulb was isolated, the rest of the manifold evacuated and the gas mixture delivered to the HVC via stainless steel lines heated to ~ 70 °C with heating tape. A measure of the total amount of DMMP that accumulates on the surface of the sample was estimated using the pressure drop observed from the vacuum manifold as the gas mixture flowed through the cell and assuming perfect gas law PV = nRT.

3.4 Sample preparation for the DRIFTS cell

The sample to be tested in the DRIFTS cell was crushed and sieved in a 63μm sieve. Approximately 10 mg of the sample were placed in the sample holder of the HVC. The sample was flattened with a flat spatula, making sure not to pack the sample too tightly and sealed. The sample was evacuated using a roughing pump until the pressure was 1 Torr. The sample was then opened to the diffusion pump and evacuation continued as the temperature in the cell was raised to 400 °C. The sample was kept at this temperature for 1 hour and then cooled to 50 °C or 25 °C depending on the experimental requirements. DMMP was delivered into the sample making sure the pressure in the cell did not rise above 1 Torr as the gas was flowing through the cell. Spectra were collected every 1.5 min at the very beginning of the experiment and every 3-5 min after the first 10 min of experiment until molecular DMMP appeared on the surface of sample, indicating that any surface reaction has ceased. The gas flow was then stopped and the sample chamber evacuated. Spectra were collected in 5-10 min intervals during evacuation.

3.5 Micro-reactor experiments

In a stainless steel U tube, 60 mg of the sample were calcined in 20% O_2/Helium mixture at 400 °C for 1 hour. The sample was then cooled to reaction temperature in helium and DMMP (0.9 μmoles of DMMP /ml) was then flowed through the sample at 30 ml/min. The products of reaction were then monitored in an infrared gas cell mounted in a Nicolet Avatar FT-IR instrument. The rate of product flow, breakthrough points and total amounts of product formed were calculated from the data obtained from these experiments.

3.6 Carbon monoxide adsorption

To characterize the copper oxide supported alumina samples, carbon monoxide and nitric oxide adsorption experiments were performed. All carbon monoxide (CO) adsorption experiments were performed using 99.99 % CO obtained from Holox. The sample was exposed to varying amounts of CO from 10 to 150 Torr CO and spectra collected at each exposure after the appropriate pre-treatments.

3.6.1 Untreated sample

To observe the interaction of carbon monoxide on the untreated sample, the sample was kept under vacuum for 1 hour and 100 Torr of carbon monoxide (CO) was admitted into the cell and spectra collected over a period of 60 min. After this period the CO was evacuated and spectra collected during the evacuation.

3.6.2 Pre-treated sample

Sample pretreatment was carried out by heating the sample in vacuum at 400 °C for 60 min. The temperature was raised to 400 °C at a rate of (25 °C/min) and maintained at 400 °C for 60 min. The sample was then cooled to room temperature and 100 Torr CO admitted into the cell and spectra collected over a period of 60 min. The CO was then evacuated and spectra collected during and after evacuation.

3.6.3 Oxidized sample

To oxidize the sample, 300 Torr of O_2 was placed in the cell and the sample heated at 400 °C in the flow of O_2 maintaining the cell pressure at 300 Torr. The sample was then cooled to room temperature and CO added in 10 Torr increments to a total of 100 Torr. Spectra were collected at each step. The sample was then evacuated and spectra collected during and after evacuation.

3.6.4 Reduced sample

To reduce the sample, 300 Torr of methane was added to the cell, and the sample was heated in a static environment at 450 °C for 60 min. The sample was then cooled to room temperature and CO was then added in 10 Torr increments and spectra collected at each step. The carbon monoxide gas was evacuated 15 minutes after the pressure of the gas reached 100 torr. Spectra were collected during and after evacuation.

3.7 Nitric oxide (NO) experiments

NO adsorption experiments were only performed on oxidized samples. After heating at 400 °C for 1 hour, the sample was cooled to 25 °C in oxygen. The oxygen was

then evacuated from the cell and NO (1% in helium) was added to the cell until the cell pressure reached 400 Torr and spectra collected.

3.8 X-ray diffraction data

X-ray diffraction data were obtained using a Phillips X'PERT diffractometer with CuK α-radiation and nickel filters. The samples were first ground into fine powders and then packed into the aluminium sample holder. The X-ray source was a CuK α–anode, and the voltage and current were maintained at 40 KV and 50 mA, respectively. The diffractometer was programmed to scan diffraction angles from 0 to 80 (2θ) at a step size of 0.4 and a step time of 10 sec.

CHAPTER 4

RESULTS AND DISCUSSION

4.1 Physical characteristics of studied samples

The table below summarizes the synthesis and physical characteristics of the copper samples prepared and studied for interaction with DMMP.

Sample	color	method of preparation	batch impregnation cycles	BET surface area m^2/g	% copper content
γ-alumina	white			148	0
NAQ4	blue	non-aqueous impregnation	4	-	-
NAQ5	blue	non-aqueous impregnation	5	-	2.8
NAQ8	grey green	non-aqueous impregnation	8	122	3.8
NAQ9	grey green	non-aqueous impregnation	9	121	4.3
NAQ11	brownish grey	non-aqueous impregnation	11	112.5	6.23
AQ1	blue	Aqueous impregnation	1	139	0.64
AQ2	green	Aqueous impregnation	2	138.8	1
AQ3	grey	Aqueous impregnation	3	132.8	1.5
AQ4	black	Aqueous impregnation	4	128	3.67

Table 7. Summary of copper samples studies for DMMP interaction

The results of the following samples will be discussed: NAQ4, NAQ9, NAQ11, AQ1, AQ2, AQ3, AQ4 and γ-alumina, the support. The aqueous impregnation samples were also characterized using X-ray diffraction techniques and small probe molecules

such as carbon monoxide and nitric acid were adsorbed on the surface of the samples to obtain information concerning the nature of the metal species present on the surface of the material.

4.2 γ-alumina

The interactions of DMMP and γ-Alumina have been the extensively studies by several authors. [8, 11] It was chosen as the support for this work because it has good adsorption characteristics towards DMMP and at room temperature has been shown to adsorb DMMP dissociatively yielding volatile products such as methanol[8] and dimethyl ether.

4.2.1 DRIFTS results of DMMP adsorbed on γ-alumina

The infrared spectrum of various amounts of DMMP adsorbed on alumina are shown in Figures 8 and 9. In the methyl stretch region, shown in Figure 8, the peaks at 3002 and 2926 cm^{-1} are assigned to the symmetric and anti-symmetric C-H stretches of the methyl group attached directly to the phosphorus atom and the peaks at 2962 and 2858 cm^{-1} are assigned to the symmetric and anti-symmetric C-H stretches of the methyl group directly attached to the oxygen atom.[10,11]

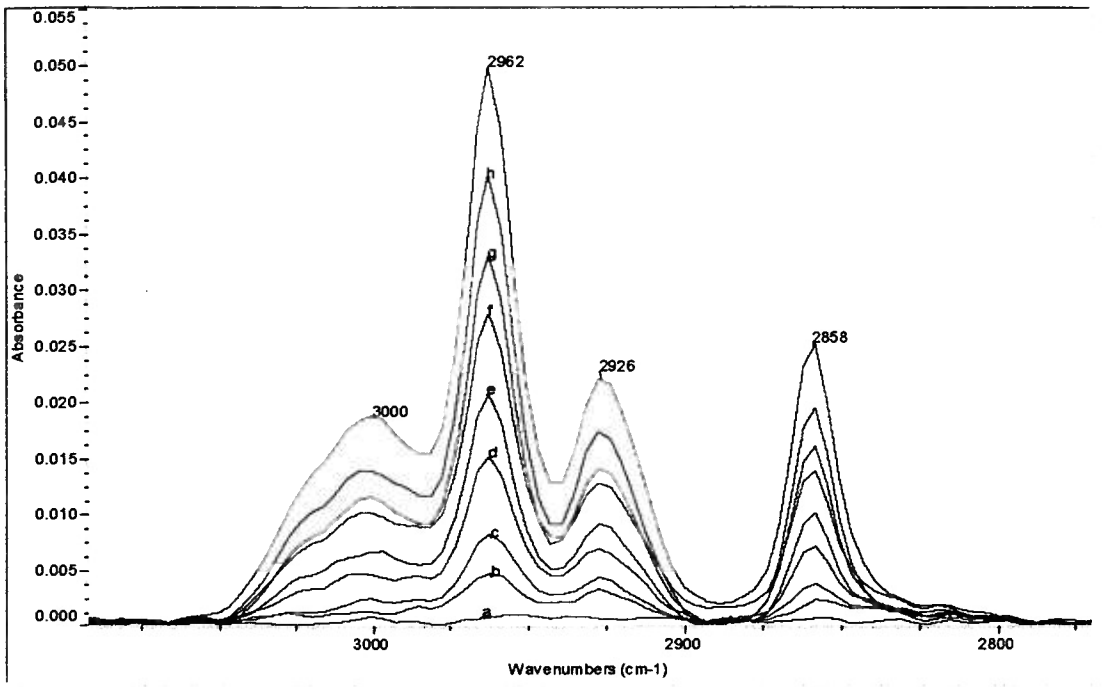

Figure 8. Methyl stretch region of DMMP adsorbed on γ-alumina. Spectrum a = 0 μmoles DMMP, spectrum b = 0.35 μmoles DMMP, spectrum c = 0.41μmoles DMMP, spectrum d = 0.48 μmoles DMMP, spectrum e = 0.52, spectrum f = 0.59, spectrum g = 0.64, spectrum h = 0.7, spectrum i = 0.78

In the lower frequency region, Figure 8, the 1467 and 1420 cm^{-1} bands are methoxy deformation bands. The band at 1317 cm^{-1} is the deformation mode for the methyl group attached directly to the phosphorus atom. The frequencies of the methyl groups of DMMP when adsorbed on alumina do not differ compared to the corresponding frequencies of liquid DMMP in CCl_4. However, the P=O bond stretching frequency is shifted down to 1226 cm^{-1} before evacuation and 1216 cm^{-1} after evacuation from 1242 cm^{-1} for liquid DMMP. This indicates that the main interaction of DMMP with the surface is through the P=O bond and not through the methyl groups.

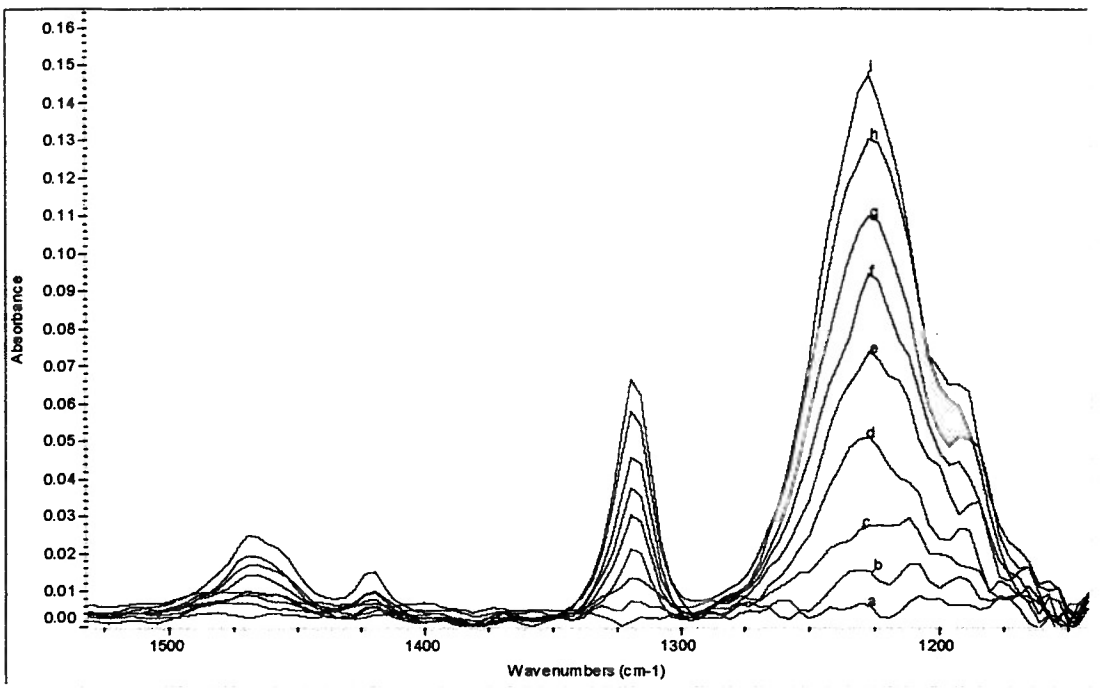

Figure 9. Lower frequency region of DMMP adsorbed on γ-alumina. Spectrum a through i represent 0, 0.35, 0.41, 0.52, 0.59, 0.64, 0.7, 0.78 μmoles of DMMP on the surface of alumina respectively.

The two main modes of adsorption on the surface of alumina are physisorption and chemisorption. Physisorbed species are generally characterized by weak bonds that can easily be broken by washing the surface with a gas such as helium or nitrogen or by evacuating the sample. Chemisorbed species on the other hand are characterized by strong bonds that cannot simply be broken by simple process such as washing or evacuation. The band at 1226 cm^{-1} shifts to 1216 cm^{-1} on evacuation. This leads to the conclusion that species that adsorbs at 1226 cm^{-1} may be assigned to a weakly adsorbed DMMP molecule on the surface, and that which adsorbs at 1216 cm^{-1} is due to species that is more strongly bound to the surface.

Templeton and Weinberg[8] postulated that DMMP adsorbs onto the surface of γ-alumina via the oxygen of the P=O bond. This oxygen donates or shares electrons with a

Lewis acid site on the surface of the alumina or hydrogen bonds to the surface hyrdroxyl groups on the alumina surface. The second interaction can be verified by the loss of free standing hydroxyl group infrared frequencies shown in Figure 10.

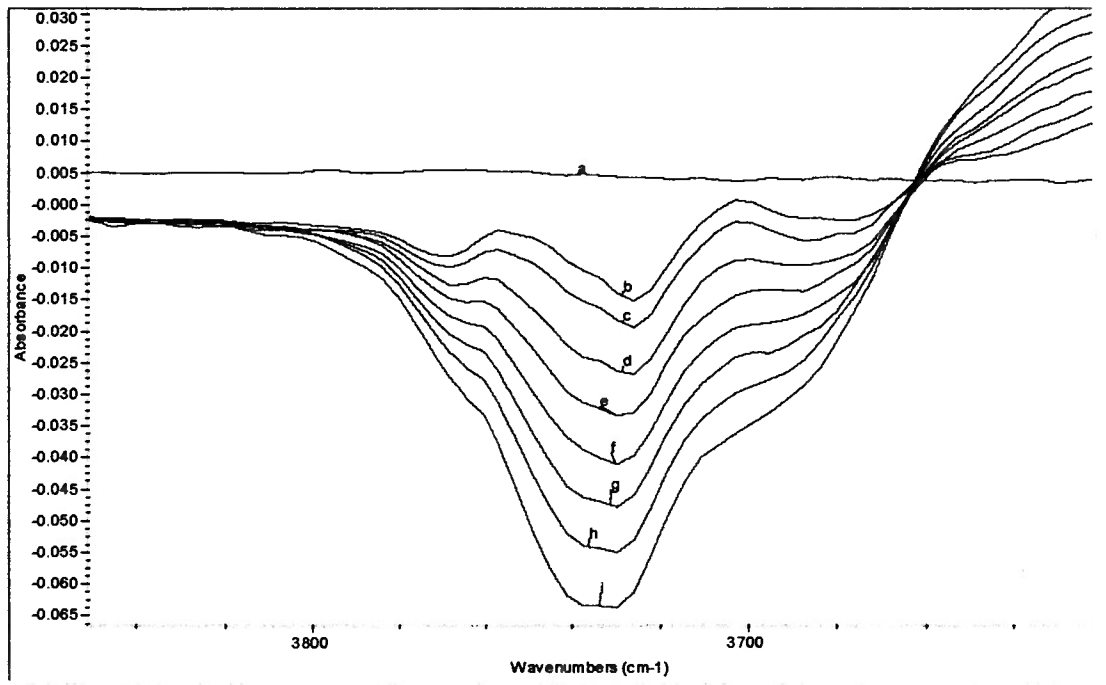

Figure 10. Loss of hydroxyl groups as DMMP is adsorbed on the surface of γ-alumina. Spectrum a through i represent 0, 0.35, 0.41, 0.52, 0.59, 0.64, 0.7, 0.78 μmoles of DMMP on the surface of alumina respectively.

The first hydroxyl groups that begin to disappear are those at 3725 cm^{-1} which are neutral hydroxyl groups. As more DMMP is added to the surface this band broadens as the other hydroxyl groups take part in the reaction between DMMP and the surface. The surface interaction between the surface hydroxyl groups and the DMMP is shown below.

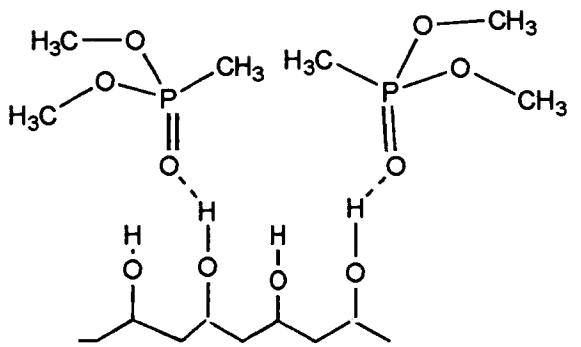

4.2.2 Micro-reactor experiments of DMMP and alumina

Figure 10 shows the results obtained from reacting DMMP with γ-alumina in the microreactor. Methanol and dimethyl ether are the two decomposition products observed. The total amount of methanol and dimethyl ether evolved is shown on the graph on the right with indicates about 6.5 μmoles of methanol and dimethyl ether were produced. To generate these graphs, the total number of volatile carbon species were calculated as illustrated in the equation below.

2 x (μmoles of $(CH_3)_2O$) + μmoles of CH_3OH = Total number of volatile carbon species produced. 5

This number was then plotted against the total number of μmoles of DMMP that had passed through the sample at each point. Figure 11 is a plot that shows the DMMP signal in the FT-IR cell as a function of the total amount of DMMP flowed through the sample. The point at which DMMP is detected in the detector is called the breakthrough point.

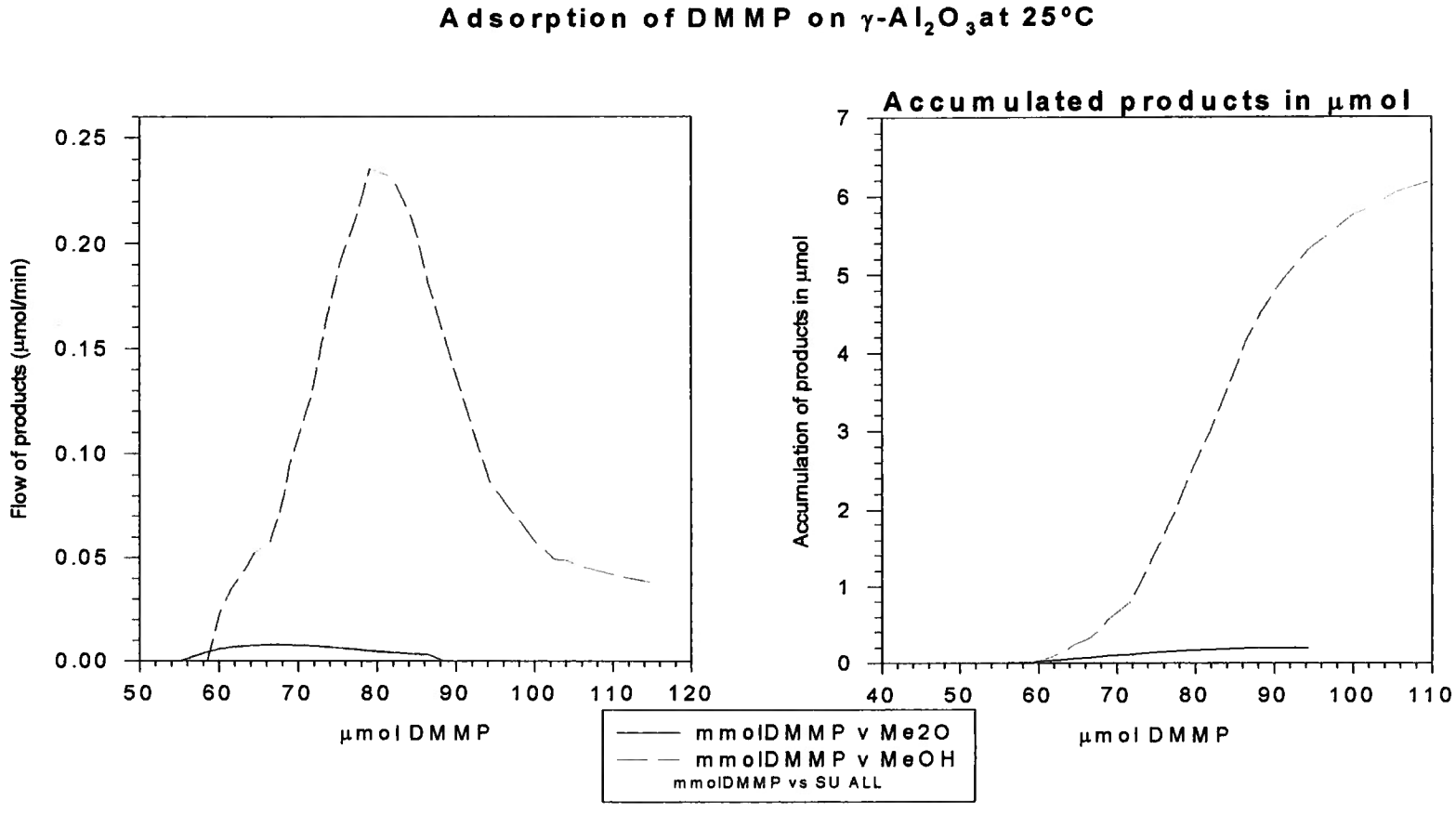

Figure 11. Decomposition product distribution of DMMP over γ-alumina at 25 °C.

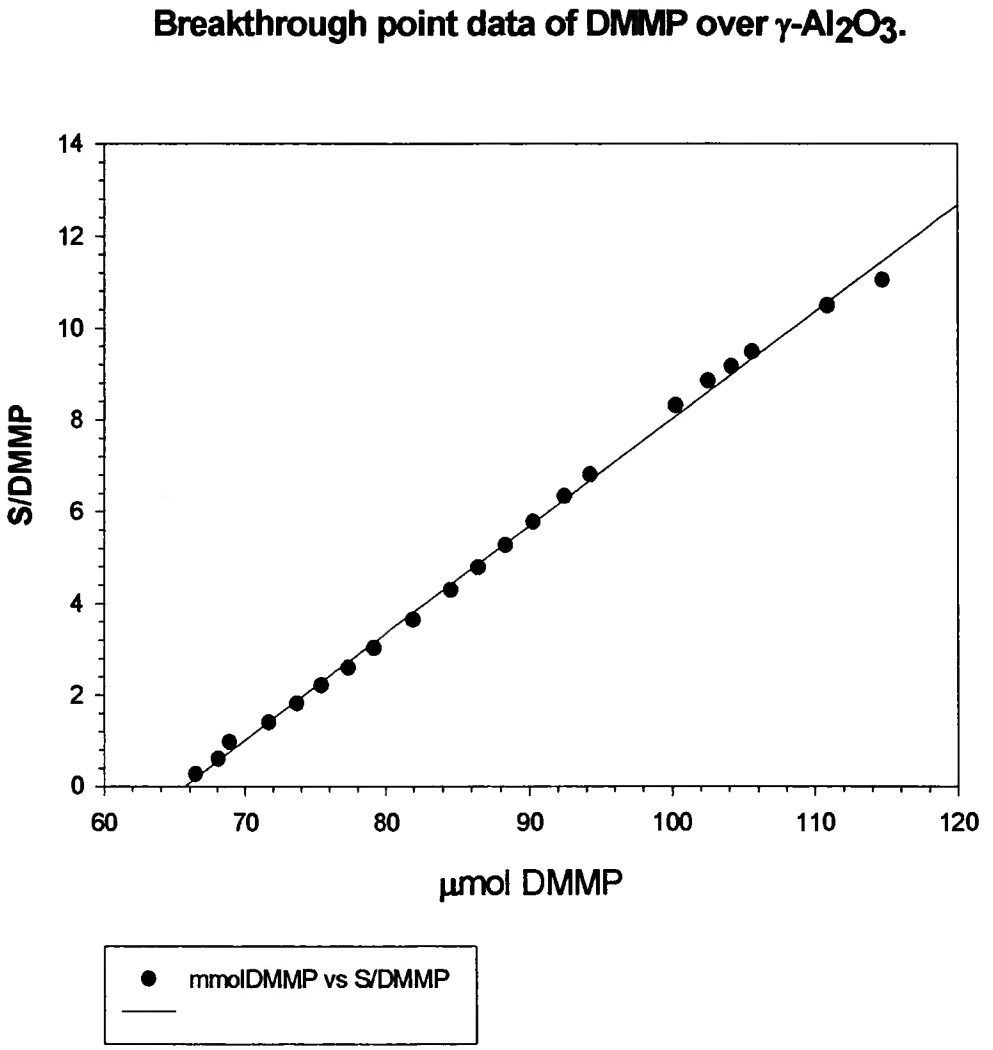

Figure 12. Breakthrough point curve of DMMP over γ-alumina

DMMP adsorbs on the surface of alumina according to the microreactor experiments in a dissociative manner yielding methanol and dimethyl ether. Since the DRIFTS technique looks at surfaces and the reactions that occur on the surface of powders, it is expected that fragments of DMMP adsorbed on the surface of alumina

would appear in the spectra collected as DMMP adsorbed on alumina. This is not the case in our experiments. Several different experimental techniques were applied in an attempt to observe the species that lead to the formation of the main products of DMMP decomposition on the surface of alumina. None of these methods yielded any results different from observing molecular DMMP adsorbing on the surface of the alumina. From these experiments and the data obtained, the following was concluded. DMMP first adsorbs molecularly on the surface of the alumina. Then there are two likely processes that occur that lead to the formation of methanol and dimethyl ether:

i) The molecularly adsorbed DMMP modifies the surface of alumina and causes it to become more reactive towards in coming DMMP molecules. These incoming DMMP molecules then react with the surface bound DMMP molecules and form dimethyl ether and methanol. This mechanism is commonly known as the Langmuir-Hinshelwood mechanism.

ii) The surface bound DMMP molecules interact with each other and from the decomposition main products- a Rideal-Eley type mechanism. Since all these reactions occur after molecular DMMP has adsorbed on the surface of the alumina, DRIFT spectroscopy cannot see the secondary reactions or dissociated fragments of DMMP on the surface and hence the results obtained only show molecular DMMP.

4.3 Non-aqueous impregnation samples and their interaction with DMMP

The following section will discuss the interaction of DMMP with the samples that were prepared using the non-aqueous impregnation method. In this non-aqueous impregnation method, the copper precursor- copper acetylacetonate was dissolved in acetonitrile and mixed with alumina using the batch impregnation method to increase the copper content on the alumina support.

4.3.1 Drifts spectra of DMMP on NAQ4

Sample NAQ4 was obtained after the fourth cycle of impregnation with the non-aqueous copper mixture. The sample had 1% copper content and a surface area of 135 m^2/g. The sample was light blue in color.

Figure 13 shows the DRIFTS spectra of DMMP adsorbing on the surface of NAQ4. Before the methyl bands appear in the spectrum, a band at 1222 cm^{-1} appears in the spectrum unaccompanied by the methyl stretch bands indicating that that the first mode of attachment onto the surface of NAQ4 is via the P=O bond. To remove the physisorbed DMMP on the surface, the sample was evacuated and chemisorbed DMMP is left behind on the surface of the sample.

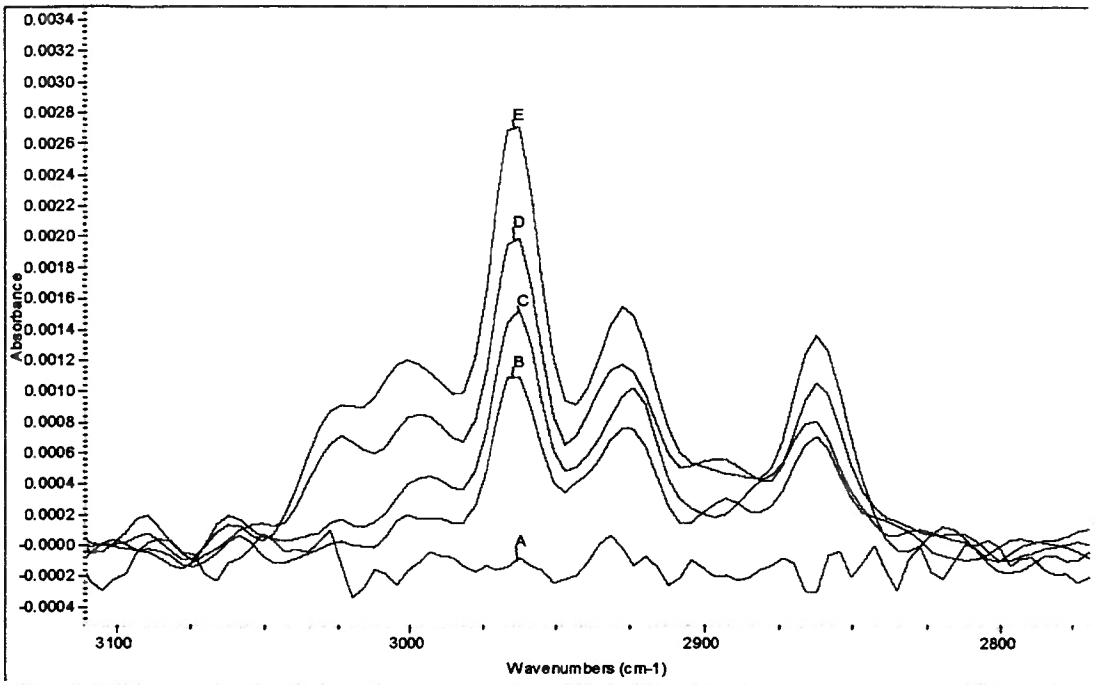

Figure 13. Methyl stretch region of DMMP adsorbed on the vacuum treated surface of NAQ4. Spectrum A = 0 μmoles DMMP, spectrum B = 0. 2 μDMMP, Spectrum C = 0.31 μmoles DMMP, Spectrum D = 0.38 μmoles DMMP, spectrum E = 0.42 μmoles DMMP.

This appearance of the C-H stretching frequencies of DMMP on NAQ4 is similar to that on γ-alumina. The DMMP adsorbs molecularly on the surface of this and the other lower copper loading samples such as NAQ5 and NAQ8.

4.3.2 Interaction of DMMP with the surface of sample NAQ9

Sample NAQ9 is the result of the ninth impregnation cycle that resulted in a green grey colored sample with a copper content of 4.3% and a surface area of 121 m^2/g.

At room temperature, infrared spectra of the initial contact of DMMP with the surface of NAQ9, shown in Figure 14, shows two major bands at 2961 and 2844 cm^1. These bands are accompanied by a 1261 cm^{-1} band in the lower frequency region as shown in Figure 14, spectrum B. Spectrum D in both Figures 14 and 15 show, in addition

to the 1261 peak, a 1317 cm^{-1} and 1215 cm^{-1} peak. These latter frequencies are consistent with molecular DMMP on the surface of the sample.

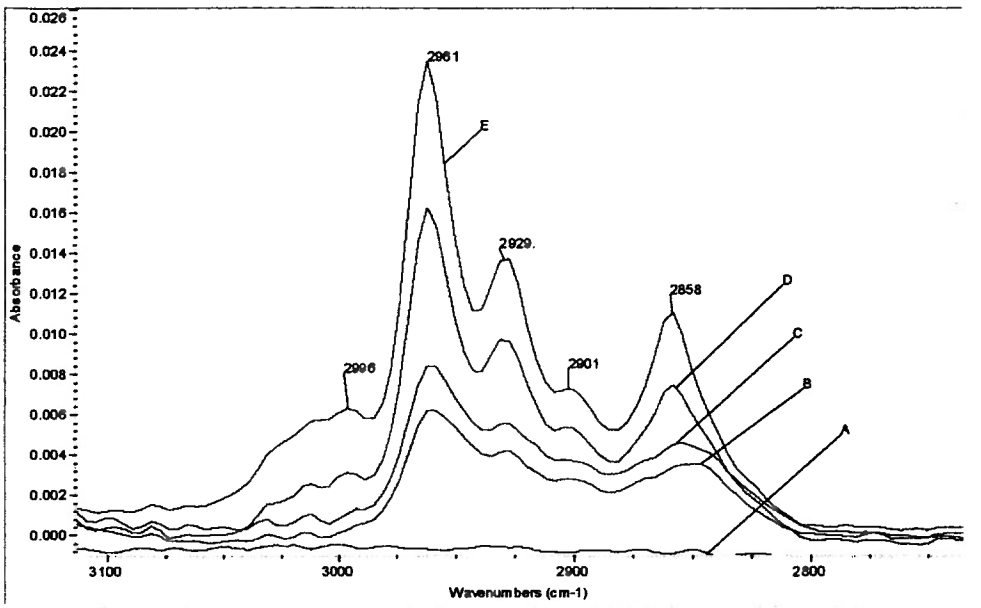

Figure 14. Methyl stretch region of DMMP adsorbed on the surface of NAQ9 at 25 °C. Spectrum A = 0 μmoles DMMP, Spectrum B = 0.03 μmoles DMMP, spectrum C= 0.05 μmoles DMMP, Spectrum D =0.08 μmoles DMMP, spectrum E = 0.1 μmoles.

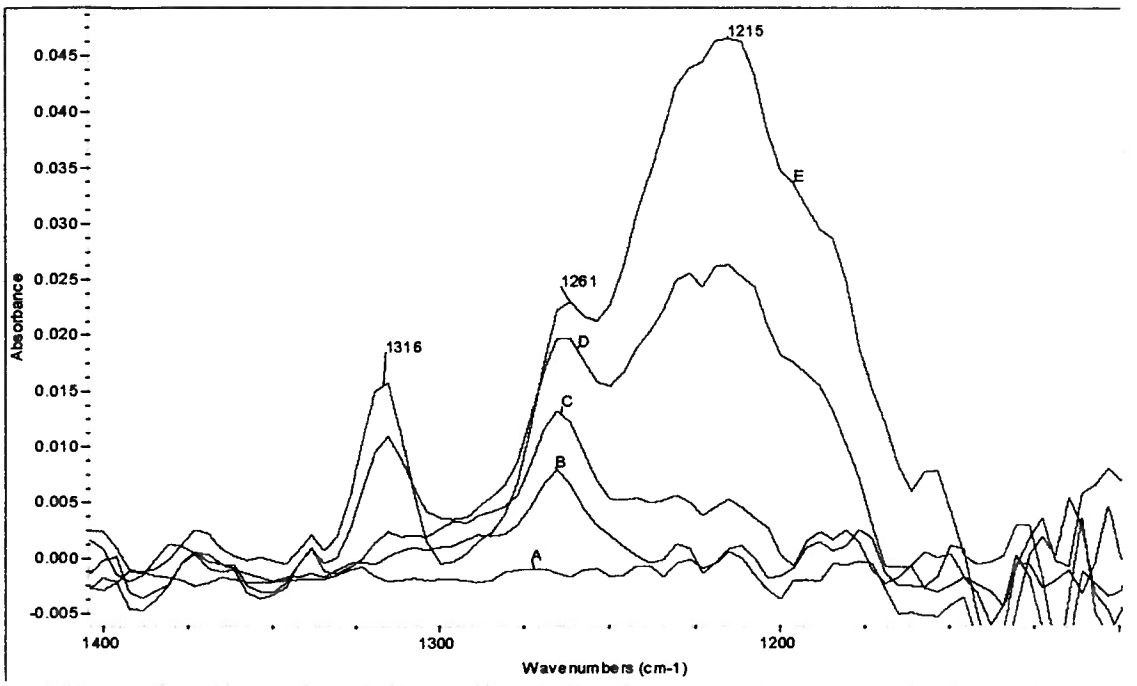

Figure 15. Lower frequency region of DMMP adsorbed on the surface of NAQ9 at 25 °C. Spectrum A = 0 μmoles DMMP, Spectrum B = 0.03 μmoles DMMP, spectrum C= 0.05 μmoles DMMP, spectrum D =0.08 μmoles DMMP, spectrum E = 0.1 μmoles DMMP.

These data are consistent with an alternative adsorption mechanism on the surface of the material that does not involve the interaction of the P=O bond and the surface. The 1261 cm^{-1} band is close to the P=O bond frequency of liquid DMMP in CCl_4. Mitchell et al. observed a similar band when DMMP was adsorbed on iron oxide[11]. They observed a 1255 cm^{-1} band that shifted to 1277 cm^{-1} when the sample was flushed with nitrogen gas for 1 hour. This band was assigned to a shifted P=O vibration due to an adsorption mechanism that involves a nucleophilic attack on the phosphorus atom that leads to a surface bound dissociated DMMP molecule such as the one shown in structure 1.

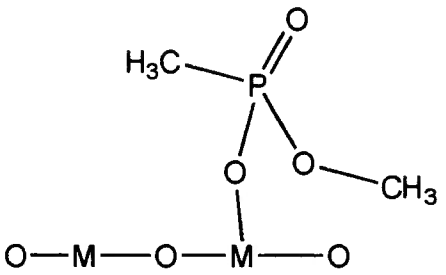

Structure 1

In the case of NAQ9, the 1261 cm^{-1} band is not accompanied by a 1317 cm^{-1} band, which indicates cleavage of the P-CH_3 bond. The surface species responsible for this feature in the spectra cannot be due to the species shown in structure 1 since this species still retains the P-CH_3 bond. Rather a better representation of the surface species observed in Figure 14 is shown in Structure 2.

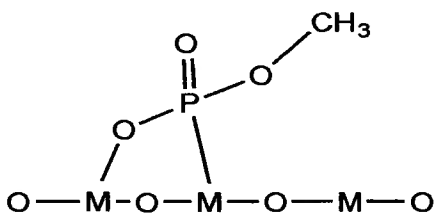

Structure 2

4.3.2.1 DRIFTS results of NAQ9 at 50 °C

The spectra of DMMP following its addition on the surface of NAQ9 at 50 °C are shown in Figure 16. The spectra show the methyl stretch vibrations of the methyl groups on DMMP. When DMMP is adsorbed on a surface molecularly, the ratio of the intensity

of the bands of the CH_3O and CH_3P is 2:1, since there are two methoxy methyl groups and one methyl-P group. When the intensity of this ratio changes to 1:1, or the bands appear to be equal in intensity, then this indicates a loss of a methoxy group. Figure 16 shows spectrum that has methyl stretch bands with the same intensity indicating a loss of a methoxy group. In the lower frequency region, the 1317 cm^{-1} (deformation mode of P-CH_3) and the 1220 cm^{-1} (P=O stretch) are present, leading to the conclusion that the DMMP adsorbs in a dissociative manner cleaving a methoxy group and leaving a surface bound methyl methylphosphonate species.

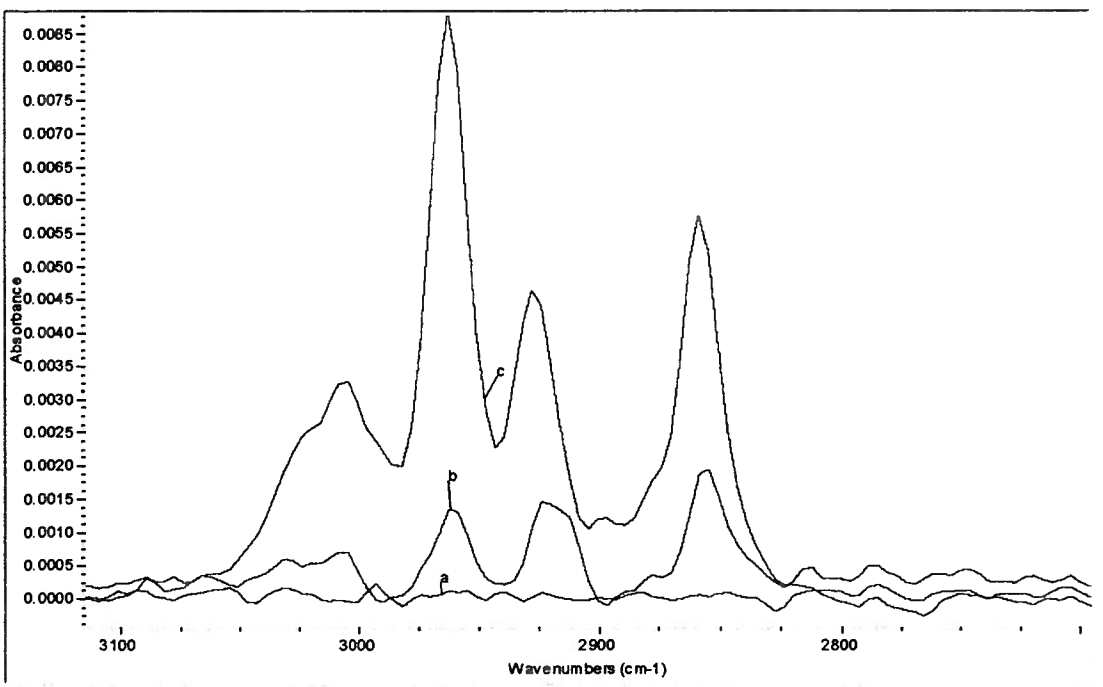

Figure 16. Methyl stretch region of DMMP adsorbed on the surface of NAQ9 at 50 °C. Spectrum a = 0 µmoles DMMP, spectrum b = 0.05 µmoles DMMP, spectrum c = 0.1 µmoles DMMP.

This surface structure has been observed on metal oxides such as lanthana, magnesia and alumina[13] at temperatures above 100 °C.

4.3.2.2 DRIFTS results of the interaction of DMMP with the hydrated surface of sample NAQ9

Water vapor was added to the surface of NAQ9 in an attempt to cause it to react more aggressively with DMMP. The hydration process was achieved as follows: the sample was heated to 400 °C for one hour, and cooled to 100 °C and then water vapor was allowed to come into contact with the surface of the sample for 15-30 min. The sample was then cooled to 50 °C and DMMP was admitted into the cell. Surface hydration had a negative effect on the ability of this catalyst to affect DMMP decomposition. DMMP adds molecularly as shown in Figure 17, even at 50 °C. No formation of a cleaved DMMP molecule was observed when the sample was hydrated.

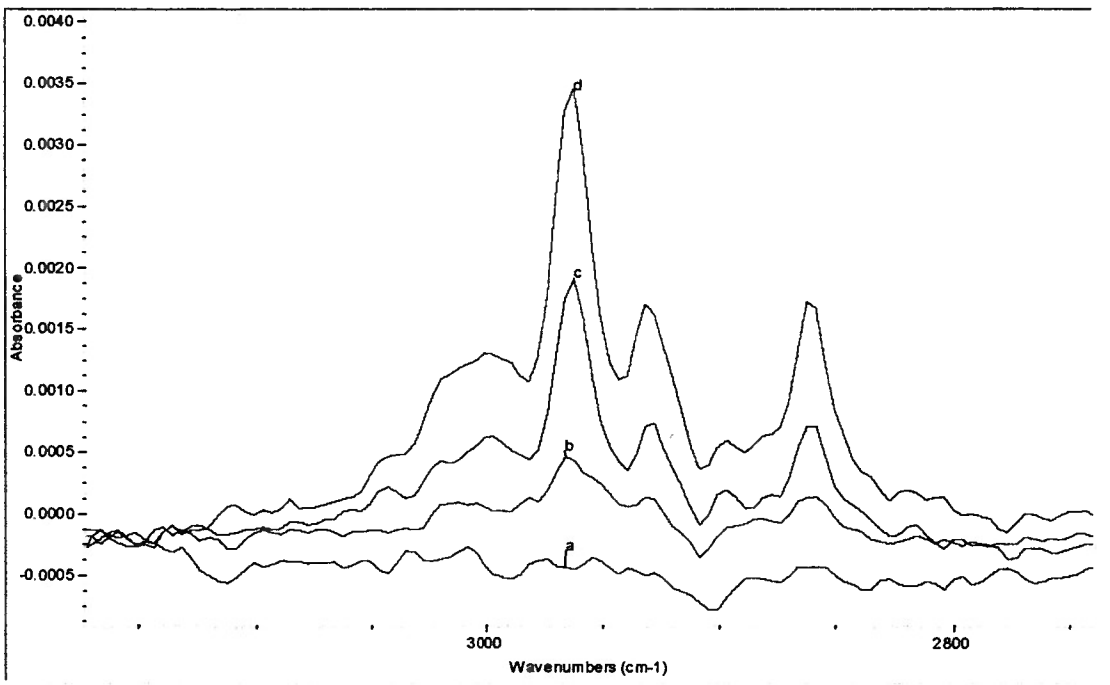

Figure 17. Methyl stretch region of DMMP adsorbed on the hydrated surface of NAQ9. Spectrum a = 0 μmoles DMMP, spectrum b = 0.02 μmoles DMMP, spectrum c = 0.08 μmoles DMMP, spectrum d = 0.1 μmoles DMMP.

4.3.3 DMMP and its interaction with the surface of sample NAQ11

Sample NAQ11 is the result of the eleventh impregnation cycle of the non-aqueous impregnation method. This sample has a brownish grey color and a copper content of 6.23 %. The surface area of the sample is 112.5 m^2/g. To further characterize the sample, carbon monoxide adsorption experiments were conducted on the sample to establish the nature of the copper species on the surface.

4.3.3.1 Carbon monoxide adsorption on the surface of NAQ11

The spectrum of carbon monoxide adsorbed on NAQ11 reduced in methane is shown in Figure 18. A single broad band at 2110 cm^{-1} is observed. A Fourier transform self-deconvolution spectrum of this band shows three peaks at 2098, 2113 and 2123 cm^{-1} that make up the 2110 cm^{-1} band. (A Fourier self-deconvolution is a mathematical calculation performed on a spectrum that synthetically narrows the trace bandwidth and aids in identifying the principal peaks that overlap to make a complex band.) [54, 55] These peaks are consistent with 3 types of copper species on the surface of the alumina. The 2098 cm^{-1} is assigned to a Cu^0- CO species. The 2113 and 2123 cm^{-1} are both assigned to Cu^+-CO linear species in different environments[35] in the alumina matrix.

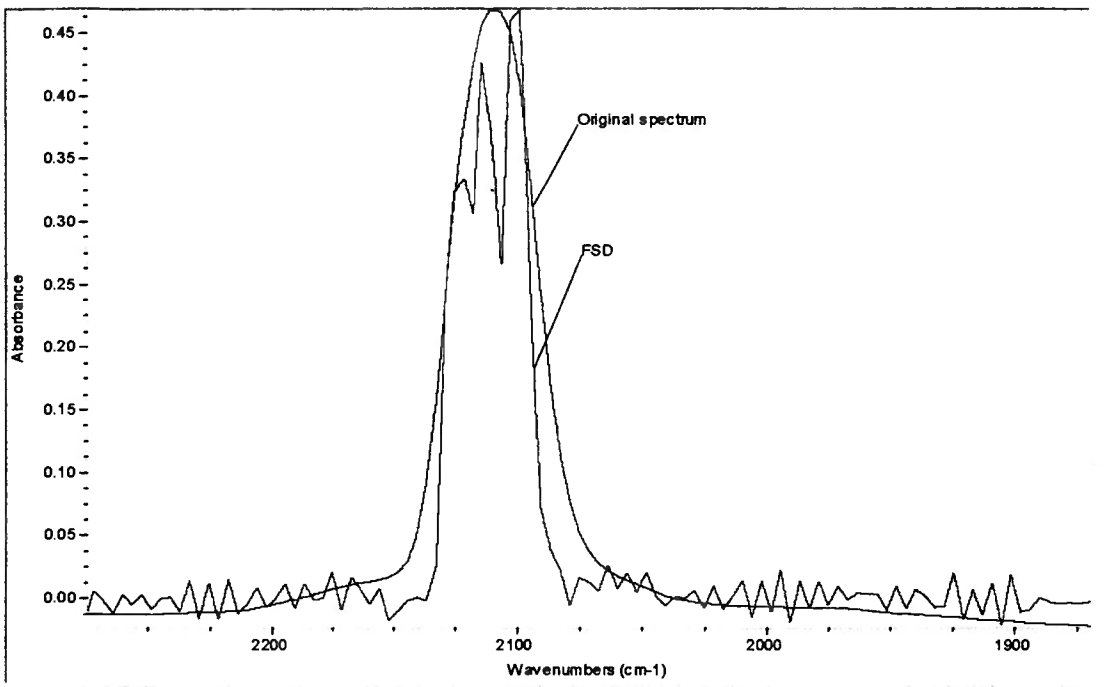

Figure 18. Fourier self-deconvolution spectra of 2110 cm^{-1} CO band on reduced NAQ11. (Not to scale)

4.3.3.2 DRIFTS results of reduced NAQ11 and DMMP

NAQ11, when reduced in methane, shows molecular adsorption of DMMP as shown in Figure 19. Spectrum A show methyl peaks that are similar to those molecular adsorption of DMMP on reduced NAQ11. This indicates that reduced copper supported alumina is not active for DMMP dissociation.

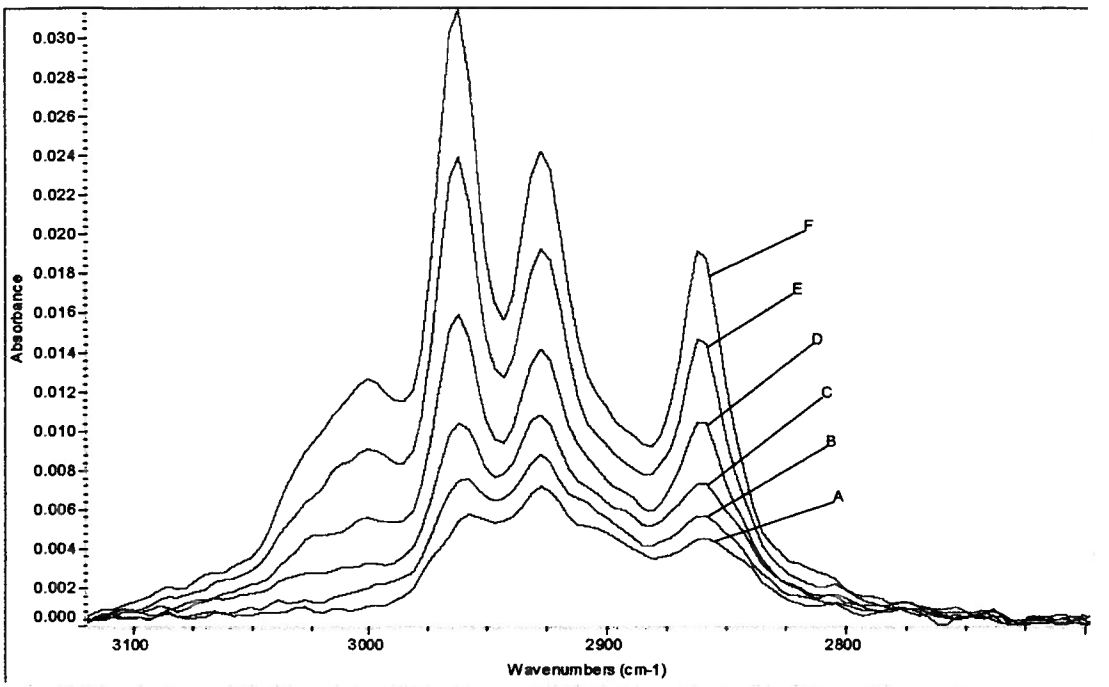

Figure 19. Methyl stretch region of adsorption of DMMP on surface of reduced NAQ11. Spectrum a = 0.02 µmoles DMMP, spectrum b = 0.04 µmoles DMMP, spectrum c = 0.06 µmoles DMMP, spectrum D = 0.08 µmoles DMMP, spectrum e = 0.1 µmoles DMMP, spectrum f = 0.12 µmoles DMMP.

4.3.3.3 Interaction of DMMP on the surface NAQ11 at 25 °C

NAQ11 was heated in vacuum at 400 °C and then allowed to cool to 25 °C in vacuum. DMMP was then allowed to come in contact with NAQ11 at 25 °C and the infrared spectra collected showed two broad bands at the beginning of the adsorption process: one at 2950 cm^{-1} and a broad band at 2822 cm^{-1}. As more DMMP is added onto the surface, the 2820 band shifts to 2859 cm^{-1} with a shoulder at 2820 cm^{-1} and the 2950 band shifts to 2957 cm^{-1} as molecular DMMP adsorbs on the surface of this material shown in Figure 20.

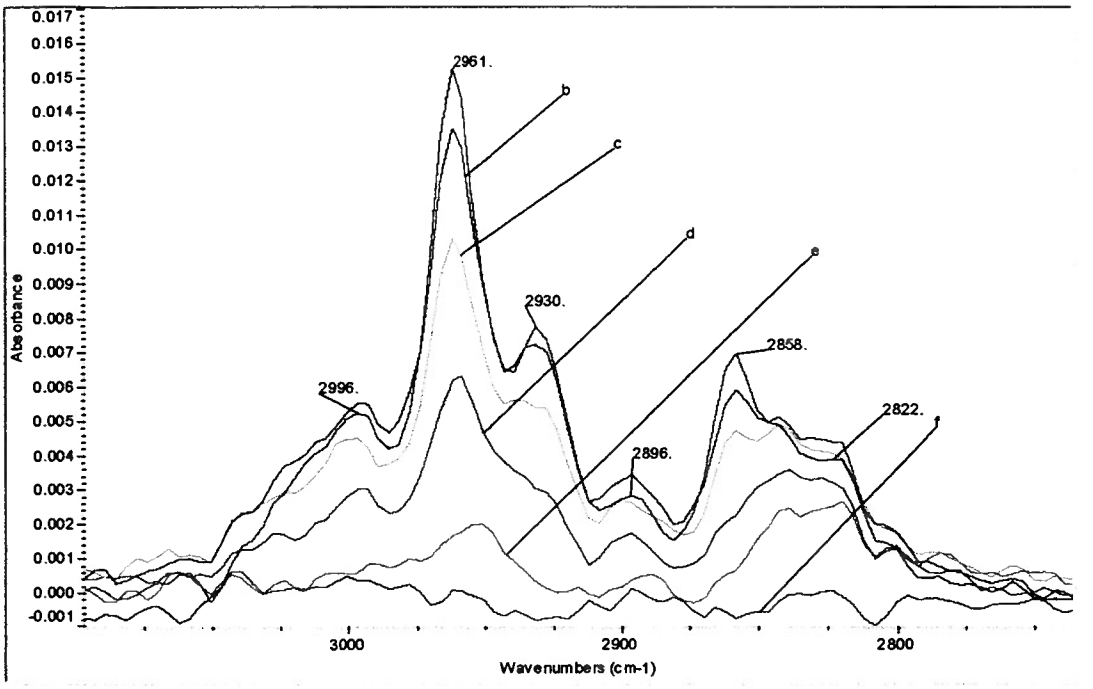

Figure 20. Methyl stretch region of DMMP adsorbed on the surface of NAQ11. Spectrum a = 0.12 µmoles DMMP, spectrum b = 0.1 µmoles DMMP, spectrum c = 0.08 µmoles DMMP, spectrum d = 0.06 µmoles, spectrum e = 0.04 µmoles DMMP, spectrum e = 0.02 µmoles DMMP, spectrum f = 0 µmoles DMMP.

The initial peaks that form on this material are assigned to surface adsorbed methoxy group. This methoxy group is possibly derived from cleavage of a methoxy group of the DMMP molecule.

4.3.3.4 *DMMP adsorption on the surface of NAQ11 at 50 °C*

DMMP was also adsorbed on the surface of NAQ11 at 50 °C after heating the sample in vacuum at 400 °C for 1 hour. The infrared spectra of DMMP interaction with NAQ11 is shown in Figure 21. The four peaks at 3006, 2959, 2826 and 2854 cm^{-1} are assigned to the frequencies of the methyl groups on DMMP. The peaks that represent the 2859 and 2854 cm^{-1} bands are the symmetric and anti-symmetric stretches of the methyl hydrogens attached to the oxygen atom. These two peaks have much higher intensities

than the 3006, and 2854 cm^{-1} bands, which represent the symmetric and anti-symmetric stretches of the methyl hydrogens attached to the phosphorus atom, when the DMMP molecule is intact. The bands that correspond to the C-H stretches of the methoxy bands are reduced by a factor of 2 in intensity indicating loss of one of the C-H groups that contribute to that frequency.

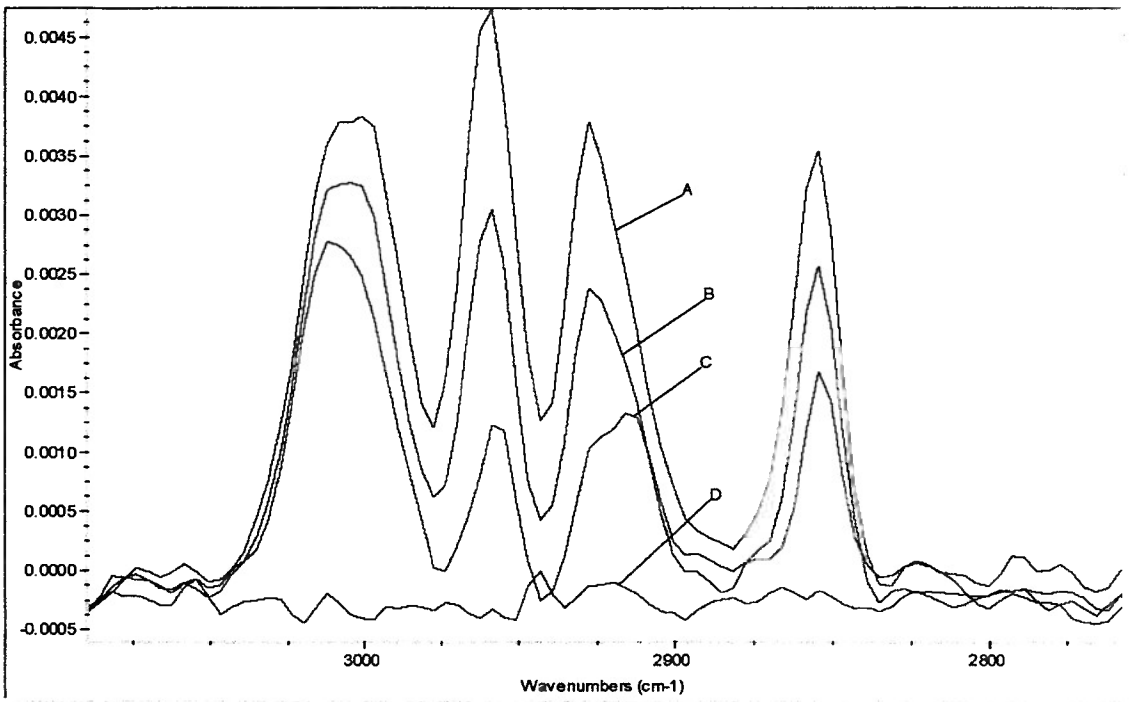

Figure 21. DMMP adsorption on the surface of NAQ11 at 50 °C. Spectrum A = 0.2 μmoles of DMMP, spectrum B = 0.08 μmoles DMMP, spectrum C = 0.04 μmoles DMMP, spectrum D = 0 μmoles of DMMP.

At 50 °C, DMMP interacts with NAQ11, dissociating the molecule and leaving a structure on the surface that has one less methoxy group than molecular DMMP.

4.3.3.5 Heating at high temperatures

After DMMP had been adsorbed on the NAQ11, the sample was evacuated and subsequently heated to 400 °C for 1 hour. This experiment was performed to observe any

changes in the spectra that would indicate further destruction of the adsorbed DMMP molecule. The spectrum that results from this treatment is shown in Figure 22. The spectrum shows a loss of the bands at 2962 and 2850 cm^{-1}. These two band frequencies represent the methoxy stretches (symmetric and anti-symmetric) on the DMMP molecule and their absence indicates that they are not present on the surface adsorbed species on this material. The bands present on the IR spectra, at 3000 and 2908 are the symmetric and anti symmetric stretches of the P-CH_3 moiety. At temperatures as high as 400 °C, the methoxy methyl groups are cleaved from the adsorbed DMMP molecule on the surface but the P-CH_3 bond remains intact.

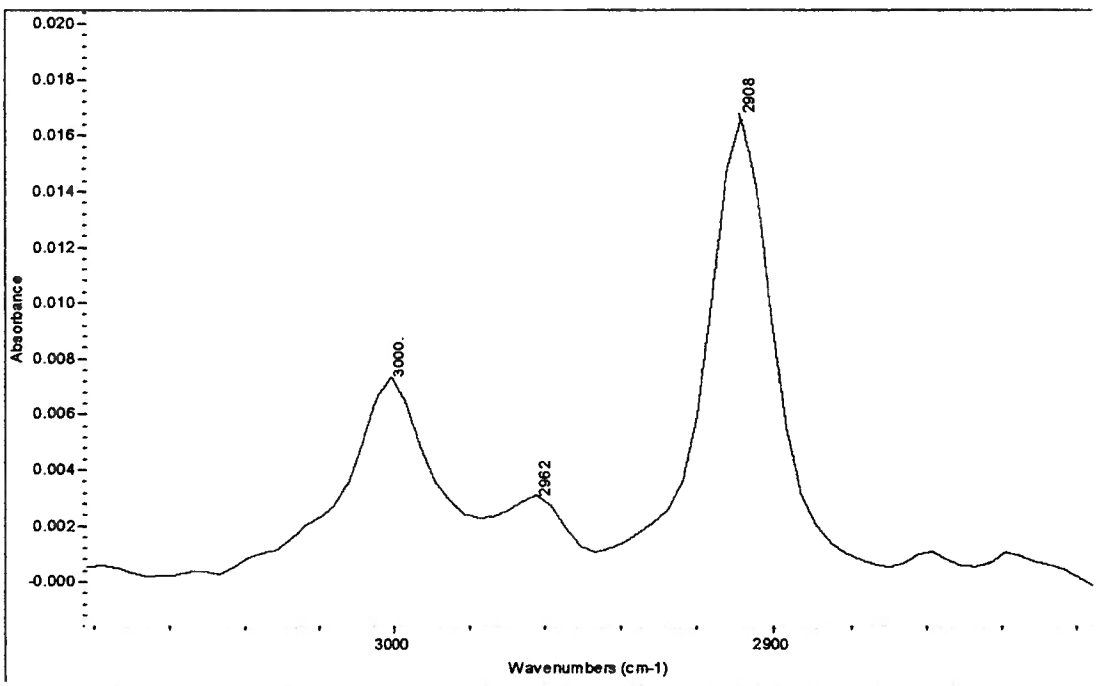

Figure 22. Methyl stretch region of DMMP adsorbed on NAQ11 after heating at 400 °C.

4.3.3.6 Hydration experiments

Water vapor was added to the surface of sample NAQ11, and DMMP administered onto the surface of this catalyst at 50 °C. Figure 22, shows the spectra collected after the surface of sample NAQ11 had been hydrated and DMMP adsorbed on the surface. The spectra show molecular DMMP adsorbing on the surface.

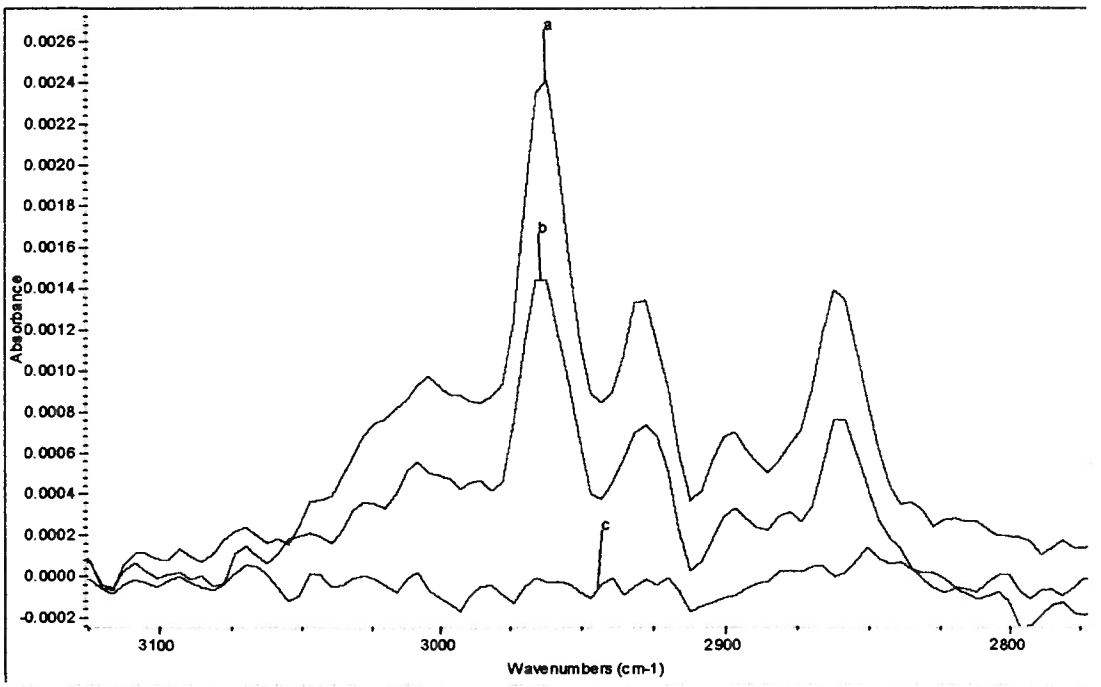

Figure 23. Methyl stretch region of DMMP adsorbed on the hydrated surface of NAQ11. Spectrum a = 0.4 μmoles DMMP, spectrum b= 0.33 μmoles DMMP, Spectrum C = 0 μmoles DMMP

At 50 °C on the surface of NAQ11 without hydration, DMMP adsorbs dissociatively leaving behind surface bound methyl methylphosphonate species. When the sample is hydrated, and DMMP adsorbed on the sample at the same temperature, no dissociative adsorption is observed. It is possible that the water molecules block the active sites on the surface of NAQ11 that lead to the cleavage of one of the methoxy

moieties on the DMMP molecule. This therefore renders the surface of this catalyst unreactive to DMMP dissociation.

4.4 *Aqueous impregnation samples and their interaction with DMMP*

The following section will show and discuss the experimental data obtained from the copper samples that were obtained from the aqueous impregnation method.

4.4.1 DMMP interaction on the surface of sample AQ1

AQ1 has a copper content of 0.64%, is light blue in color and has a BET surface area of 139 m^2/g.

4.4.1.1 Carbon monoxide adsorption on AQ1

Carbon monoxide (CO) adsorbed on the surface of oxidized AQ1 (Figure 24) shows a sharp peak at 2097 cm^{-1} and a shoulder at 2113 cm^{-1}. The 2162 cm^{-1} peak indicates gas phase CO. There are two types of copper present in this material as shown by CO adsorption. The species that adsorbes CO at 2098cm^{-1} and another independent species that adsorbs CO at 2113 cm^{-1}. The 2098 cm^{-1} band position is assigned to a Cu^0-CO species. The 2113 cm^{-1} is assigned to a Cu^+-CO species in a reducing environment.

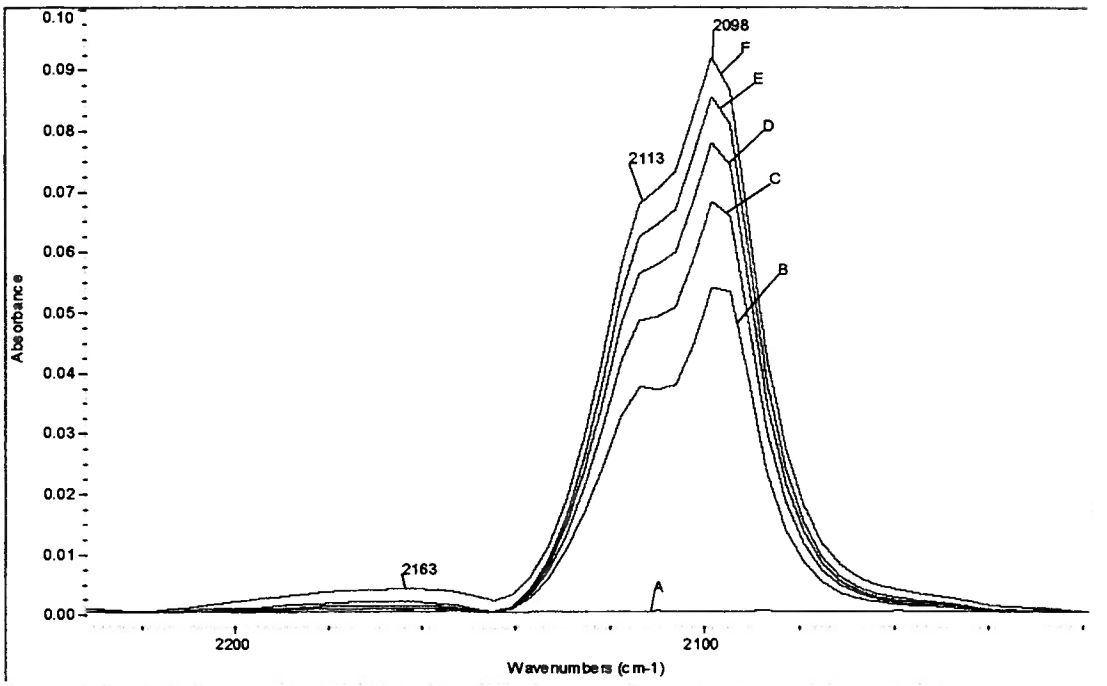

Figure 24. Carbon monoxide adsorbed on surface of AQ1. Spectrum A = 0 Torr CO, spectrum B = 10 Torr CO, spectrum C = 20 Torr CO, spectrum D = 40 Torr, spectrum E = 60 Torr CO, spectrum F = 100 Torr CO.

4.4.1.2 Adsorption of DMMP on AQ1

When DMMP is adsorbed on the surface of oxidized AQ1, non-dissociative adsorption occurs as shown in Figure 25. The pattern of adsorption of DMMP on this sample is similar to that observed the surface of γ-alumina.

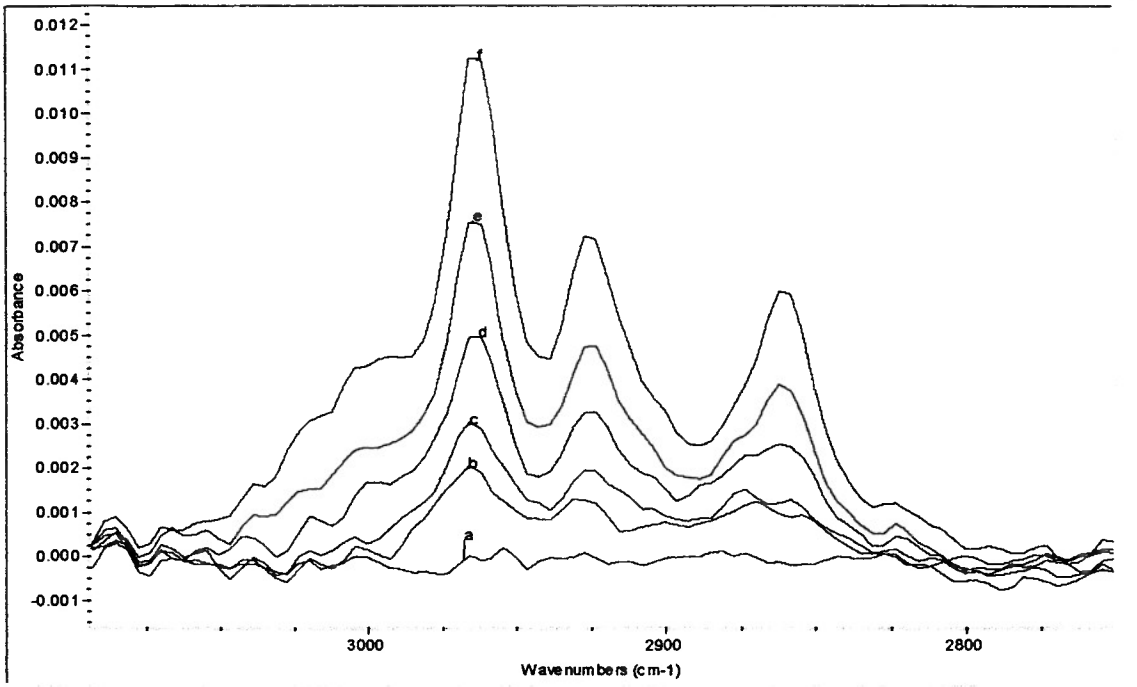

Figure 25. Methyl stretch region of DMMP adsorbed on the surface of AQ1. Spectrum a = 0 μmoles, Spectrum b = 0.17 μmoles, Spectrum C = 0.21 μmoles DMMP, Spectrum D = 0.27 μmoles, Spectrum e =0.32 μmoles , Spectrum f = 0.35 μmoles

4.4.2 Interaction of the surface of sample AQ2 and DMMP

Sample AQ2 was obtained after the second cycle of impregnation during the aqueous impregnation method. This sample was green in color and had a surface area of 138 m^2/g and a copper content of 1%.

4.4.2.1 Carbon monoxide adsorption on the surface of sample AQ2

The infrared spectra of carbon monoxide adsorbed on the surface of oxidized AQ2 are shown in Figure 26. The spectra show two peaks at 2115 cm^{-1} and 2098 cm^{-1}. These two peaks indicate that there are two copper species that adsorb CO at different frequencies. The 2115 cm^{-1} is assigned to a Cu^{+}-CO species and the 2098 cm^{-1} is assigned to a Cu^{0}-CO species.

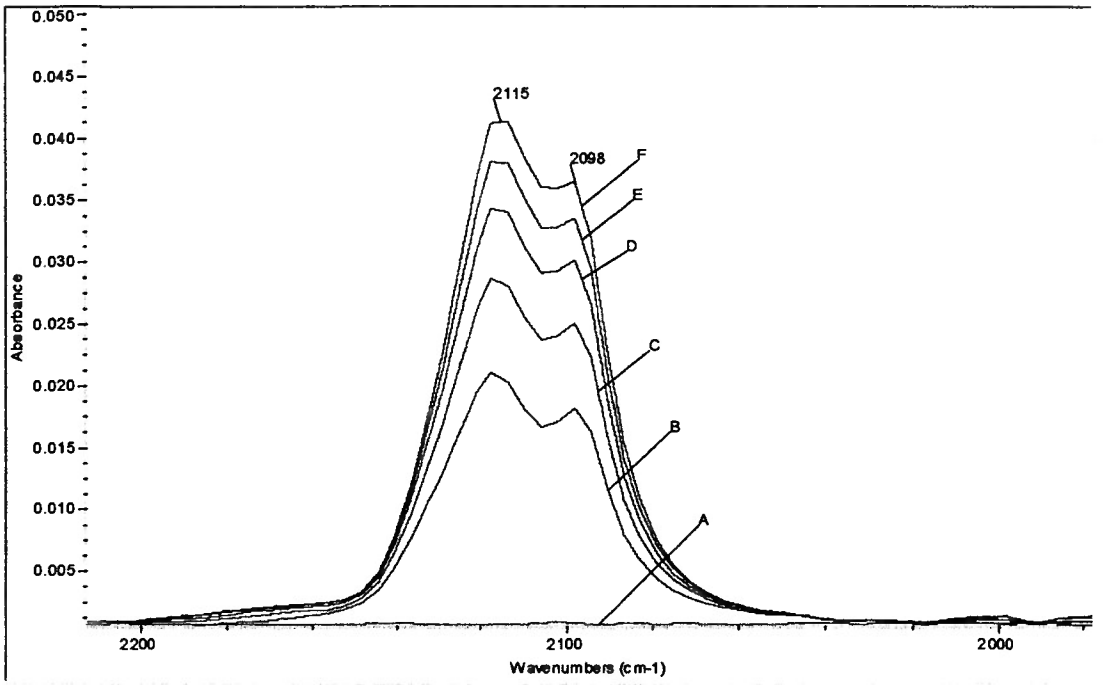

Figure 26. Adsorption of carbon monoxide the oxidized surface of AQ2. Spectrum A = 0, Torr CO, spectrum B = 10 Torr CO, spectrum C = 20 Torr CO, spectrum D = 30 Torr CO, spectrum E = 40 Torr CO, spectrum F = 50 Torr CO.

The infrared spectra of carbon monoxide adsorbed on the reduced surface of AQ2 show two peaks at 2113 and 2103 cm^{-1} as shown in Figure 27. The adsorption profile is different in that there seems to be more 2103 cm^{-1} after reduction than after oxidation. The overall intensity of the band also increases due to more reduced copper species on the surface of the sample.

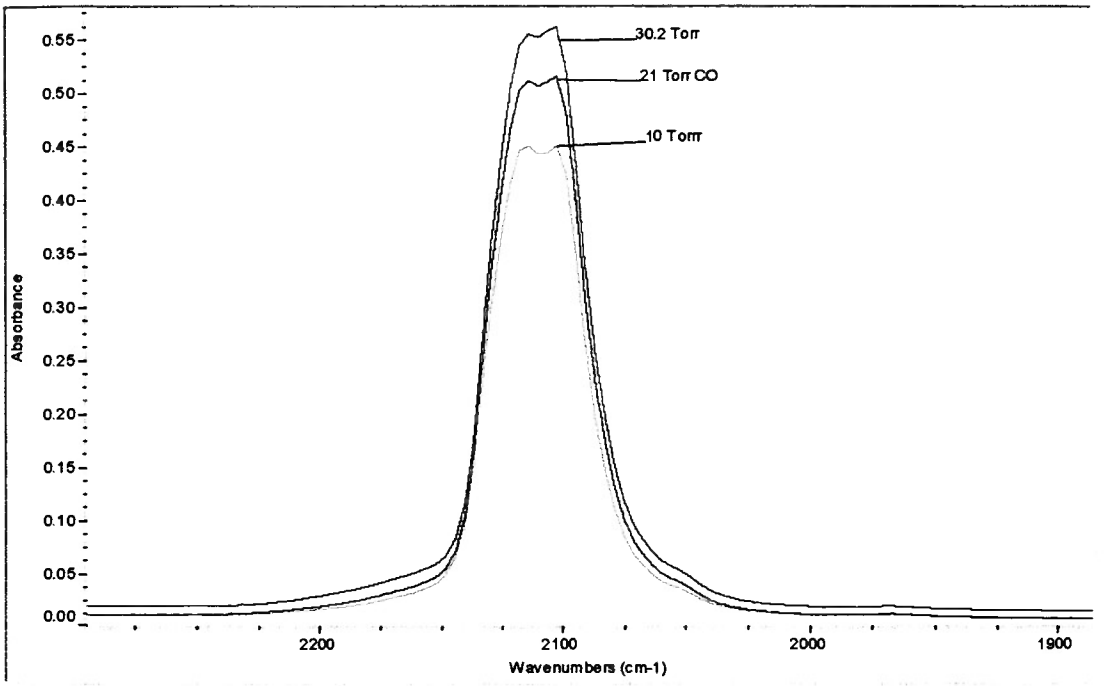

Figure 27. Carbon monoxide adsorbed on the reduced surface of AQ2.

The reduced catalyst interacts with CO in the same manner as the oxidized sample indicating two types of copper on the surface. The copper species that is characterized by the 2113 cm^{-1} peak remains unchanged by reduction or oxidation processes. The copper species characterized by the 2103 cm^{-1} on the reduced sample is probably the same as the 2096 cm^{-1} species on the oxidized sample. The surface of this sample is populated by Cu^{+} and Cu^{0} species even in an oxidizing atmosphere. It is possible that CO may induce an reduction of Cu^{+} to Cu^{0} on contact with this species.

4.4.2.2 DMMP adsorption on AQ2

DMMP adsorbed on the surface of AQ2 is shown in Figure 28. Spectrum A and B show molecular DMMP on the surface of the sample. Spectrum C, which represents

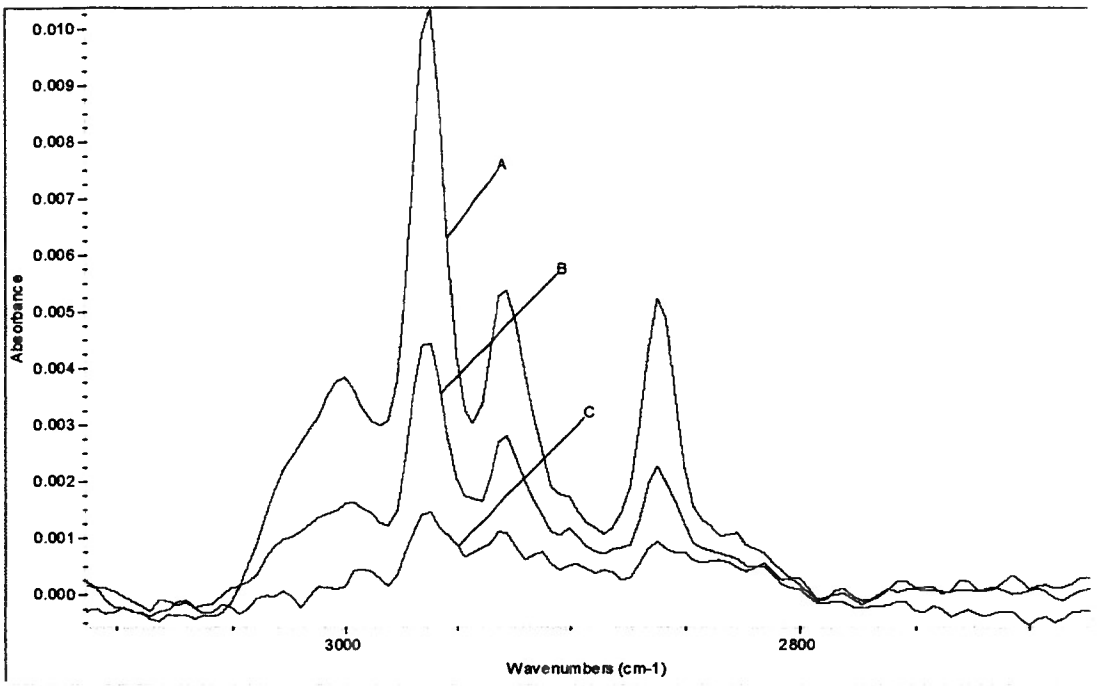

Figure 28. Methyl stretch region of DMMP adsorbed on surface of AQ2 . Spectrum A = 0.22 μmoles of DMMP, spectrum B = 0.19 μmoles and spectrum C = 0.099 μmoles DMMP.

about 0.099 μmoles of DMMP adsorbed on the surface of the sample, shows a broad band at 2859 cm^{-1} and a very weak peak at 2908 cm^{-1} which is consistent with the assignment of a combination of a methyl methylphosphonate species and surface methoxy group on the surface. Figure 29 shows the lower frequency region of Figure 28 which shows the peaks that correspond to molecular DMMP at 1317 and 1213 cm^{-1}.

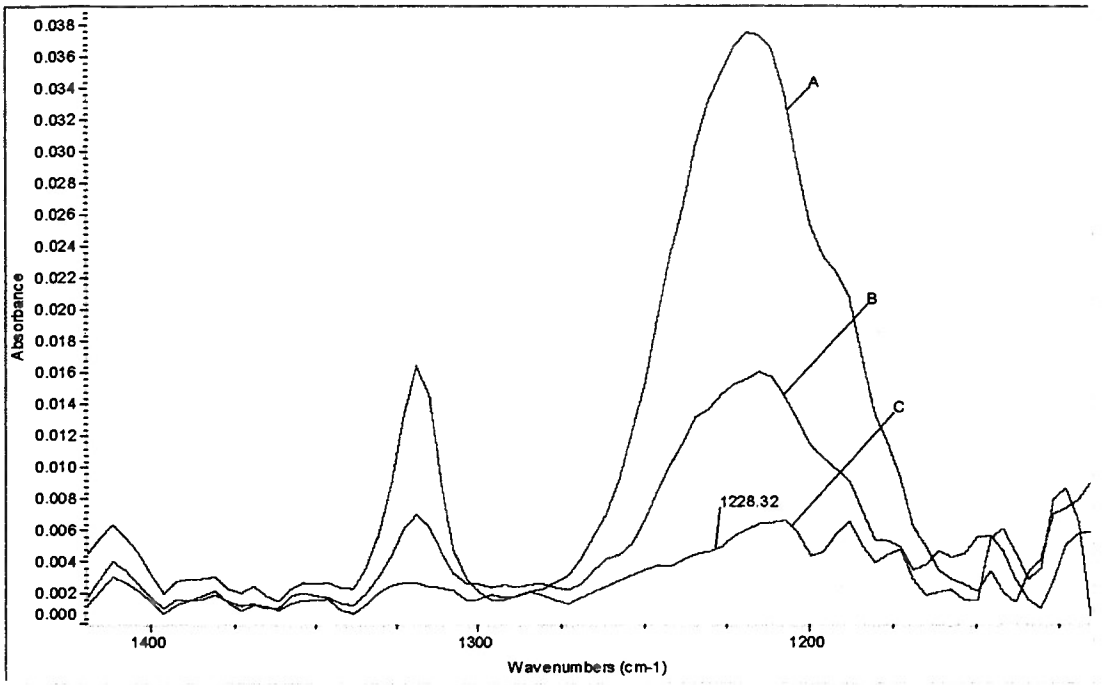

Figure 29. Lower frequency region of DMMP adsorbed on the surface of AQ2.

4.4.2.3 Addition of CO on oxidized AQ2 after DMMP addition

After oxidation of AQ2, DMMP was adsorbed on the surface of the catalyst. CO was then added to the sample after DMMP was adsorbed. The CO band profile when compared to the sample without DMMP had the same shape but the intensity of the absorption was reduced as shown in Figure 30. The reduced intensity of the band could be a result of either of the following two scenarios: copper atoms are participating in the adsorption of the DMMP molecules on the surface or the DMMP molecules accumulated on the surface block the copper atoms that would otherwise be available to adsorb carbon monoxide molecules.

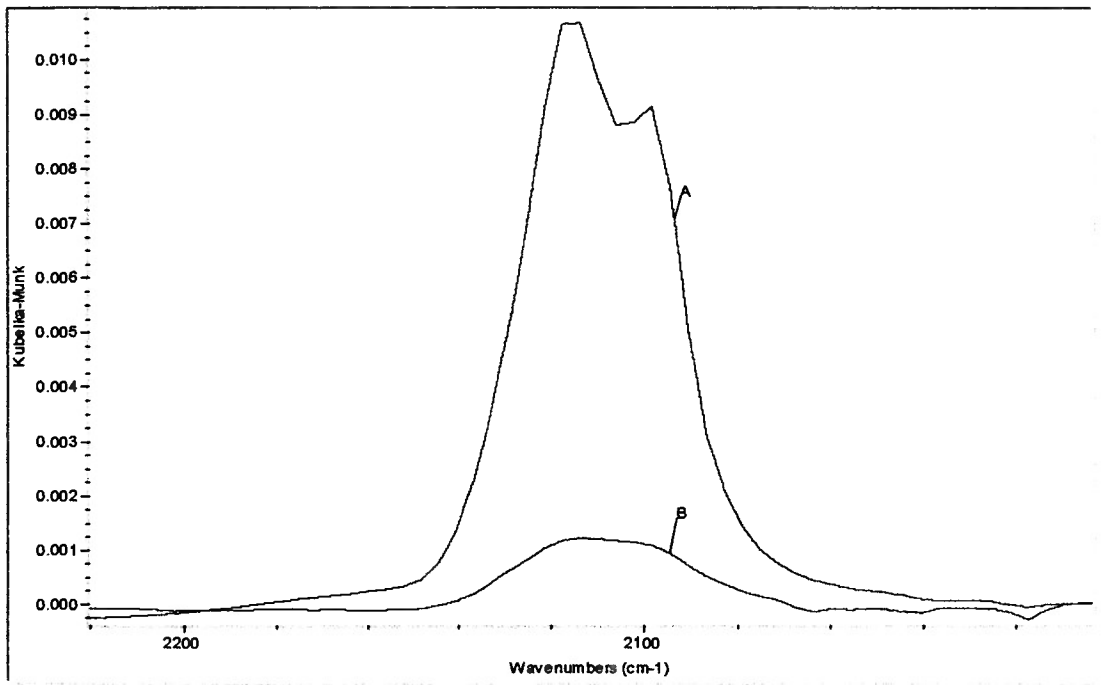

Figure 30. CO adsorbed on the oxidized surface of AQ2 before and after DMMP adsorption. Spectrum A shows 40 Torr of CO adsorbed on a clean oxidized surface of AQ2. Spectrum B shows 40 Torr of CO adsorbed on oxidized AQ2 after DMMP adsorption.

As shown from previous experiments, when the predominant copper species on the surface of the catalyst is in a reduced state, DMMP does not adsorb dissociatively, it adsorbs molecularly. The pattern of the infrared absorption bands of DMMP adsorbed on AQ2 resembles that of DMMP adsorbed on γ-alumina.

4.4.3 *Sample AQ3 and its interaction with DMMP*

Sample AQ3 which has a grey color, was obtained after the third aqueous impregnation cycle. The sample has a copper content of 1.5 % and a surface area of 133 m^2/g.

4.4.3.1 X-ray diffraction data of AQ3

Powder X-ray diffraction is an X-ray technique to look at powders and detect any bulk copper oxide structures present on the surface. γ-Alumina is amorphous and therefore shows no peaks for X-ray diffraction measurements. Pure copper oxide, however, has two peaks that appear at 2θ values of 35.6 and 38.8 °.[56] The X-ray diffraction pattern of this sample does not show any bulk or crystalline CuO indicating that the copper oxide on the surface of this catalyst is well dispersed.

4.4.3.2 Carbon monoxide adsorption

The FT-IR spectra of carbon monoxide adsorbed on the *oxidized* surface of AQ3 at room temperature shown in Figure 31, show a single peak at 2101cm^{-1} which is comprised of two peaks 2113 and 2102 cm^{-1} determined by Fourier self-deconvolution.

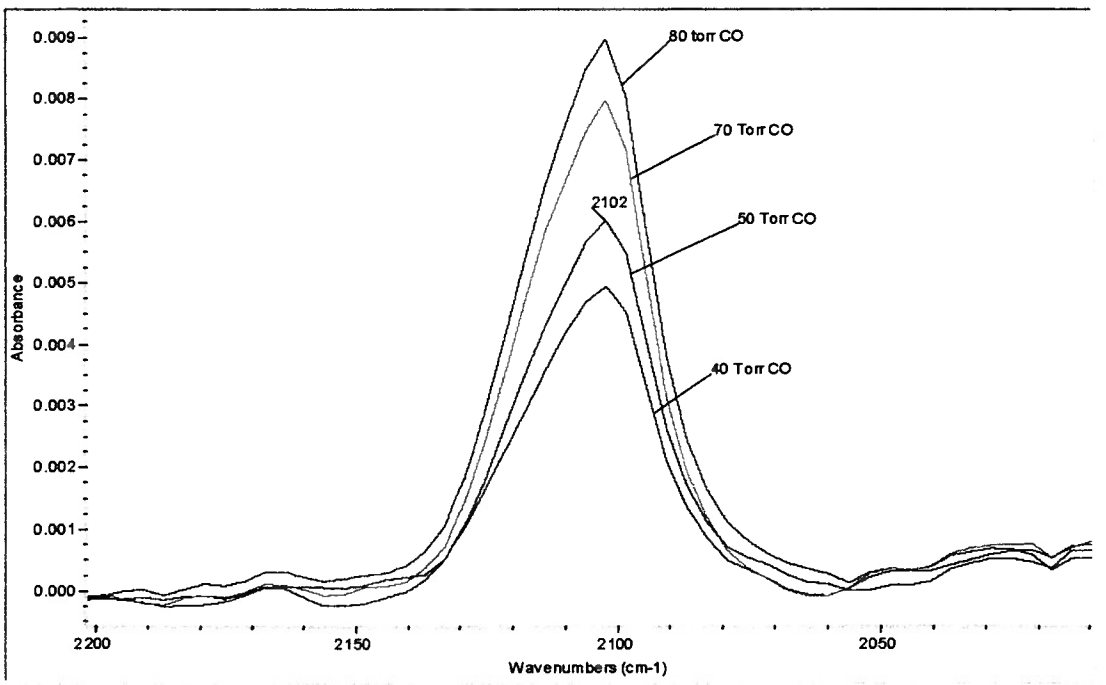

Figure 31. Carbon monoxide adsorbed on the oxidized surface of AQ3.

On the surface of *reduced* AQ3, CO adsorption infrared spectroscopy shows a band at 2101 cm^{-1}. This band is made up of two peaks, one at 2121 and one at 2101 cm^{-1}, shown in Figure 32, which are revealed after Fourier self-deconvolution. These two peaks are caused by linear adsorption of CO on two different types of monovalent copper ions. Padley et al. studied Cu/Al_2O_3 and observed similar peaks when CO was adsorbed on copper supported alumina. They assigned the peak at 2121 cm^{-1} peak to a Cu^+-CO in an environment that contains both Cu^+ and Cu^{2+} vicinal sites. Since the peak at 2101 cm^{-1} is close to the 2099 cm^{-1} peak observed by Padley and workers, it is assigned to a Cu^0-CO species.[39]

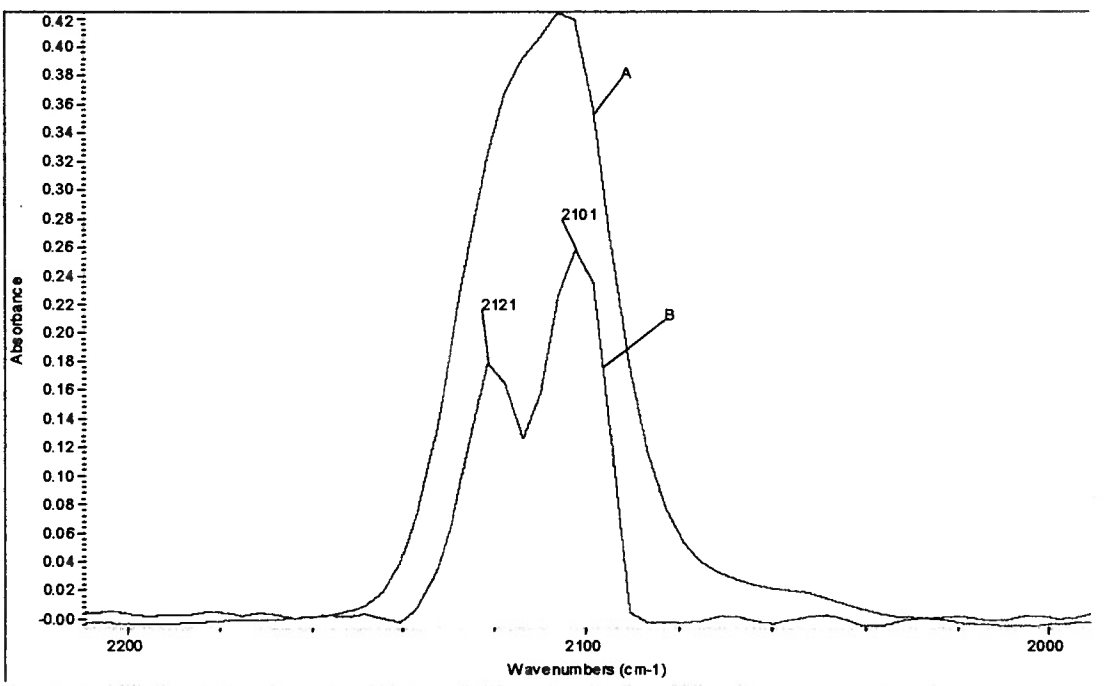

Figure 32. CO adsorbed on the reduced surface of AQ3 and the corresponding Fourier self deconvolution (FSD). Spectrum A represents 60 Torr of CO on the sample. Spectrum B is the corresponding FSD.

After reduction, the sample was re-oxidized after desorbing CO and then CO was re-administered onto the surface of the sample. A single band at 2117 cm^{-1} was observed. In Figure 33, the Fourier self-deconvolution spectrum suggests that there are three peaks that constitute the 2117 cm^{-1} band. The peaks are found at the following frequencies 2135, 2120 and 2102 cm^{-1}. Padley et al. also observed two of these bands on a re-oxidized copper sample. The absorption at 2135 cm^{-1} was assigned to a Cu^{+}-CO species where the copper is in an oxidizing environment

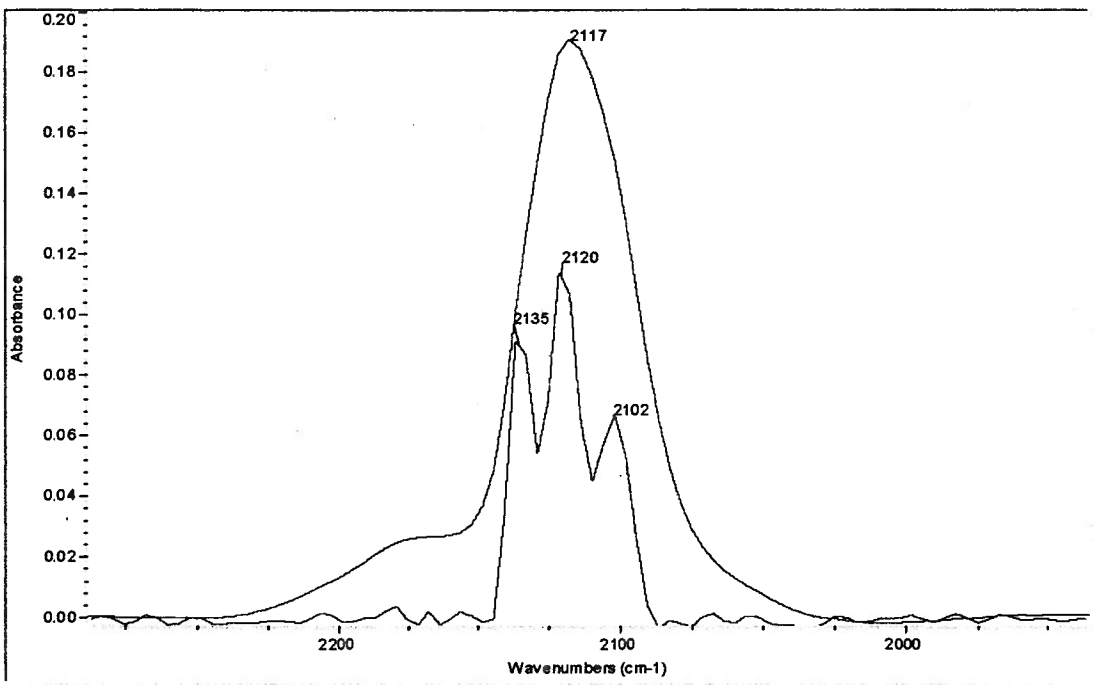

Figure 33. CO adsorbed on the surface of re-oxidized AQ3.

4.4.3.3 Nitric oxide adsorption

Nitric oxide (NO) was adsorbed on the oxidized surface of AQ3. No bands due to the formation of an NO surface complex were observed. Several authors have observed dissociation of the NO molecule over reduced copper catalysts at room temperature. Iwamoto and coworkers[53] reported observing N_2 and N_2O after passing NO over reduced CuZSM-5. Padley et al.[39] also observed the same reaction products after passing NO over alumina supported copper at 308K. It is possible that the lack of NO peaks over AQ3 is due to a dissociation of the NO species to N_2 and N_2O. N_2 is not infrared active and will not be observed and the N_2O may not adsorb on the surface and therefore will not be observed.

4.4.3.4 Micro-reactor experiments

Figure 34 shows the DMMP breakthrough point data of AQ3 at 50 °C and 25 °C. The breakthrough point of DMMP is only slightly dependent on temperature in this range and is twice as high as that of alumina meaning that it takes twice as long for DMMP to appear in the detector when AQ3 is in the sample bed in comparison to alumina. The adsorption capacity of this sample is twice as high at that of γ-alumina.

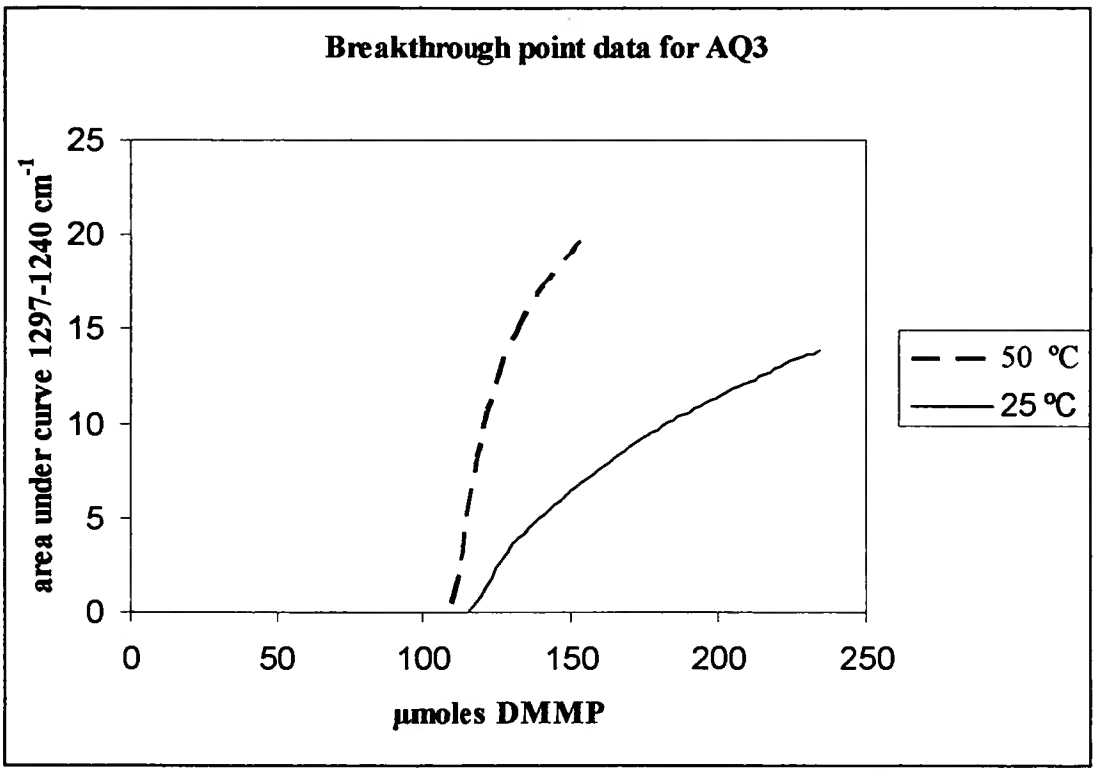

Figure 34. DMMP breathrough data for AQ3 at 25 and 50 °C

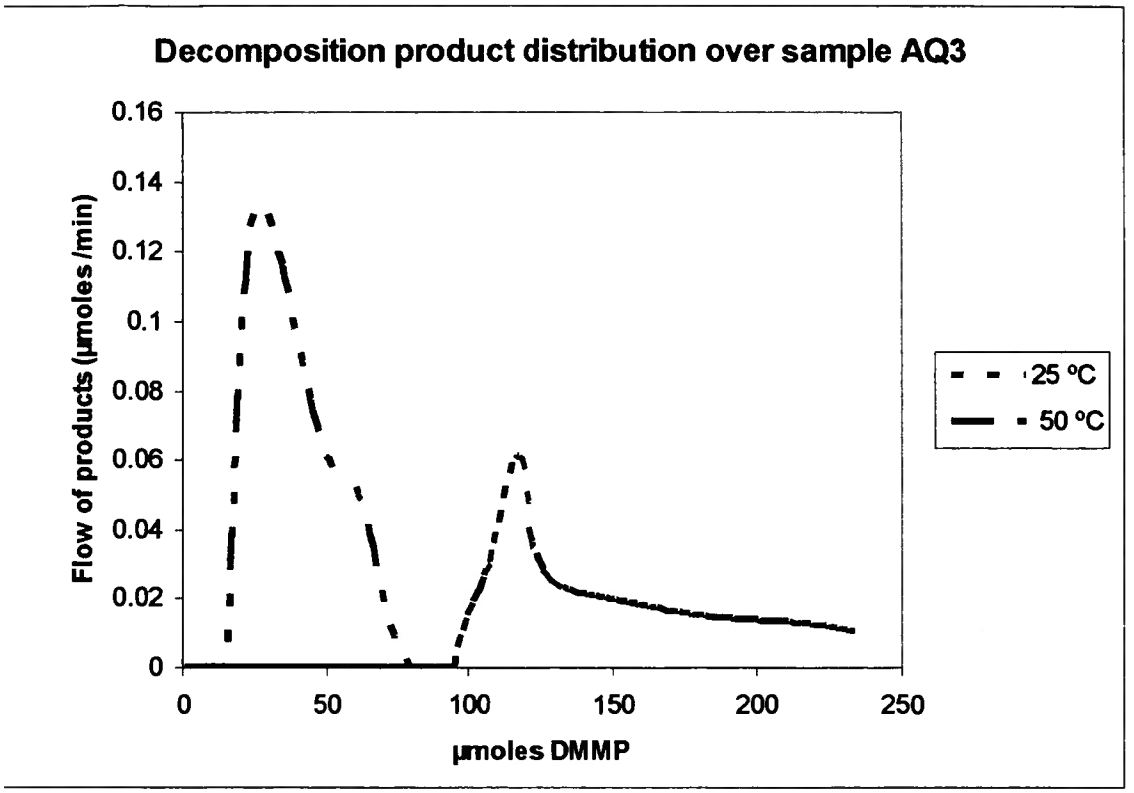

Figure 35. AQ3 product distribution as a function of temperature

During the adsorption process, DMMP also undergoes a decomposition reaction that yields two main products methanol and dimethyl ether. The product distribution data 25 °C and 50 °C are shown in Figure 35. At 50 °C methanol and dimethyl ether are observed whereas at 25 °C only methanol is observed.

At 25 °C, the methanol appears simultaneously with DMMP. The integrated curve indicates that only 3 µmoles of decomposition products are evolved. At 50 °C, methanol and dimethyl ether are evolved before DMMP is detected by the detector and the total amount of products evolved increases to 9 µmoles.

4.4.3.5 DRIFTS spectra of AQ3 with DMMP

Sample AQ3 was heated in vacuum at 400 C for 1 hour and then allowed to cool to 50 °C. DMMP was then allowed to adsorb on the surface and the infrared spectra collected during this experiment are shown in Figures 36 and 37. The data show that DMMP attaches to the surface via the P=O oxygen and the spectra show no evidence of dissociative adsorption.

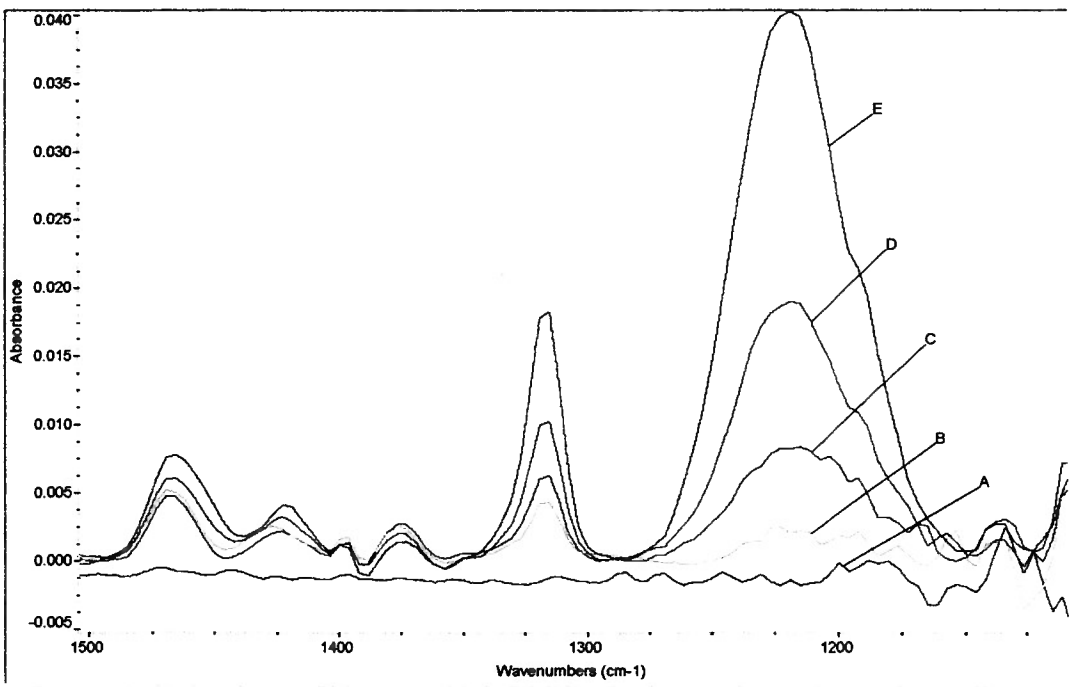

Figure 36. Lower frequency region of adsorbed DMMP on the vacuum treated surface of AQ3 at 50 °C. Spectrum A = 0 μmoles DMMP, spectrum B = 0.04 μmoles DMMP, spectrum C = 0.06 μmoles DMMP, spectrum D = 0.08 μmoles DMMP, spectrum E = 0.1 μmoles DMMP.

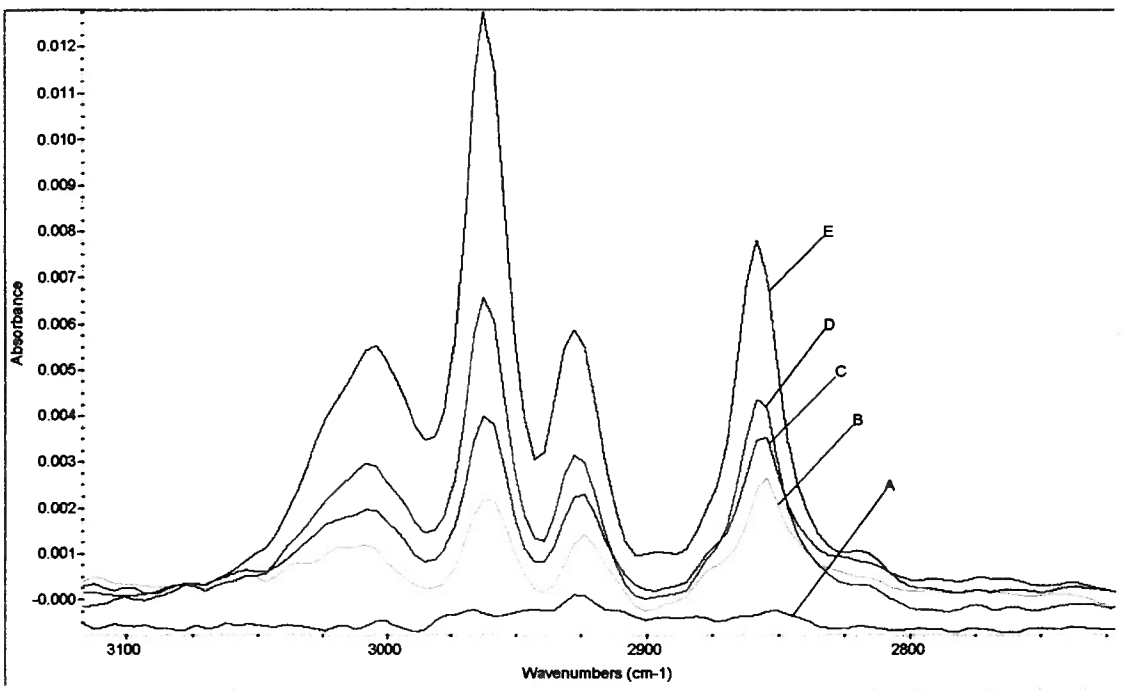

Figure 37. Methyl stretch region of adsorbed DMMP on the vacuum treated surface of AQ3 at 50 °C. Spectrum A = 0 μmoles DMMP, spectrum B = 0.04 μmoles DMMP, spectrum C = 0.06 μmoles DMMP, spectrum D = 0.08 μmoles DMMP, spectrum E = 0.1 μmoles DMMP.

During evacuation, physisorbed DMMP is removed from the surface of the sample and the spectra of the remaining surface species are shown in Figure 38. The spectra show a shoulder in the spectrum at 2816 cm^{-1} which is a band that is assigned to a surface methoxy group.

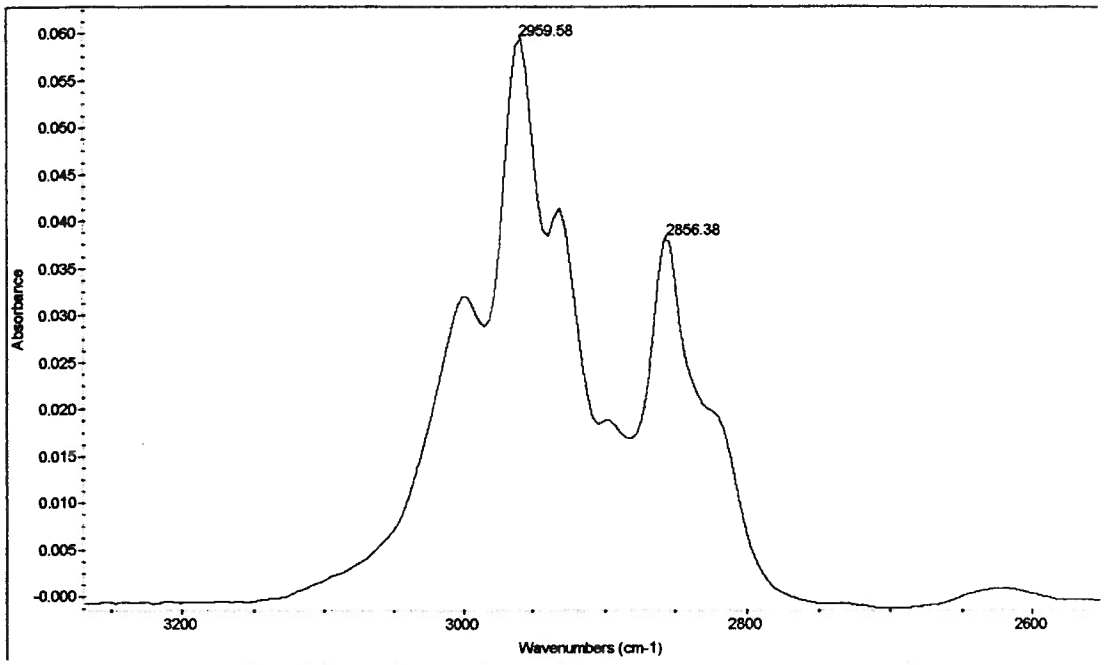

Figure 38. Adsorbed DMMP on the surface of AQ3 during evacuation at 50 °C.

4.4.3.6 DMMP addition on the oxidized surface of AQ3 at 25 °C

The spectra shown in Figures 39 and 40 were collected after AQ3 was oxidized in 20% O_2 (balance helium), at 400 °C for 1 hour and cooled to 25 °C in O_2. Less than half a micromole of DMMP was then allowed to enter the sample chamber and the sample was isolated. The spectra were collected as a function of time. The spectra collected show a sequence of spectra that suggests a mechanism that cleaves all the methyl groups on the DMMP molecule. Figure 39 shows the lower frequency region of DMMP as it adsorbs on the surface of AQ3 as a function of time.

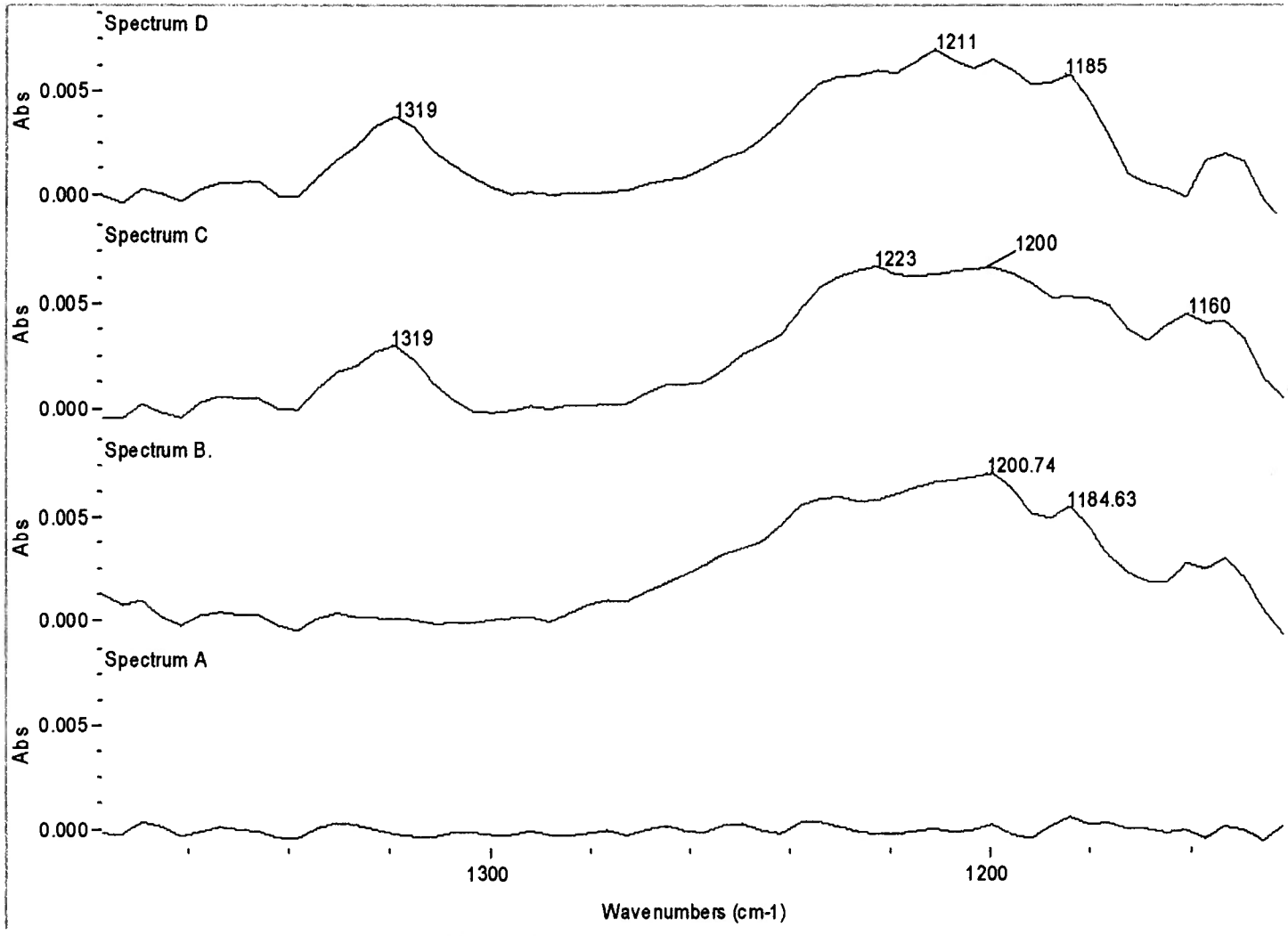

Figure 39. Lower frequency region of DMMP adsorbed on the oxidized surface of AQ3. Spectrum A- No DMMP on the sample, spectrum B collected 5 min after DMMP pulse, spectrum C collected 10 min after DMMP pulse, spectrum D collected 25 min after DMMP pulse.

The first spectrum in Figure 39 represents the clean surface of the sample. The spectrum B was collected 5 min after DMMP was allowed to equilibrate in the cell and shows a broad peak at 1200 cm^{-1}. Spectra C and D were collected 10 and 25 minutes respectively, after DMMP was introduced into the cell and show a sharp peak at 1317 cm^{-1} and a broad peak in the 1200 cm^{-1} region. Figure 40 shows the corresponding methyl stretch region. Spectrum B in the lower frequency region has a phosphate group frequency but no 1317 cm^{-1} band which is indicative of the P-CH_3 deformation mode. The lack of symmetric, anti-symmetric and deformation vibration modes of the methyl groups of DMMP on the surface of this material indicates cleavage of these groups while leaving behind a surface bound phosphate species. This reaction possibly poisons the surface and blocks any sites that would be active for further DMMP decomposition and DMMP then adsorbs molecularly on the surface. After molecular DMMP was adsorbed on the surface of the sample, CO was administered to the sample surface. Figure 41 shows the CO on the surface of AQ3 after DMMP had adsorbed onto the surface of the sample. Three bands are observed as CO adsorbs on the surface of AQ3. The first two at 2170 and 2116 cm^{-1} are due to gas phase carbon monoxide. During the experiment, the 2003 cm^{-1} band is short lived. The band disappears within 10 min of the interaction of the gaseous carbon monoxide with the surface of the sample AQ3. When gas phase CO is evacuated, the 2116 cm^{-1} band remains and is due to linear Cu^{+}-CO. The 2003 cm^{-1} has been previously assigned to a Cu^{0}-CO species by Dandekar and Vannice,[40] who observed this same band on a reduced Cu/Al_2O_3 sample. In our experiments, the 2003 cm^{-1} band is not observed after a reduction process on the surface rather it is observed after an

oxidation process. Therefore the presence of a Cu^0 site is highly unlikely. However, when a two fold bridged CO species occurs on a metallic surface, the infrared frequency shifts to the 2000 cm^{-1} region and below.[47] Hence, the assignment of the band at 2003 cm^{-1} in our case is likely due to a CO bridged across two Cu^{2+} ions. The disappearance of the band is due to the instability of the bridged CO $-Cu^{2+}$ species on the surface.

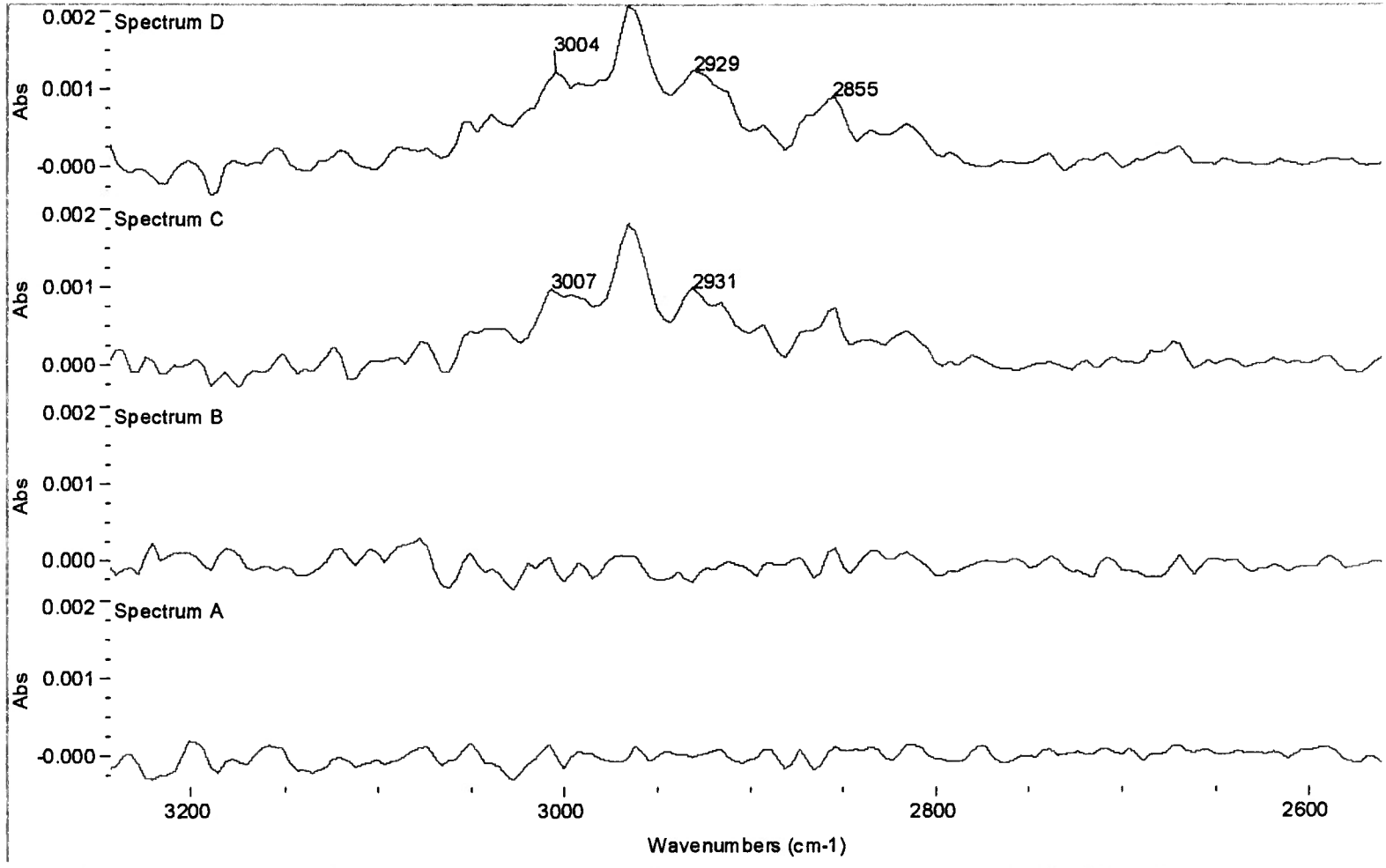

Figure 40. Methyl stretch region of DMMP adsorbed on the oxidized surface of AQ3. Spectrum A- No DMMP on the sample, spectrum B collected 5 min after DMMP pulse, spectrum C collected 10 min after DMMP pulse, spectrum D collected 25 min after DMMP pulse.

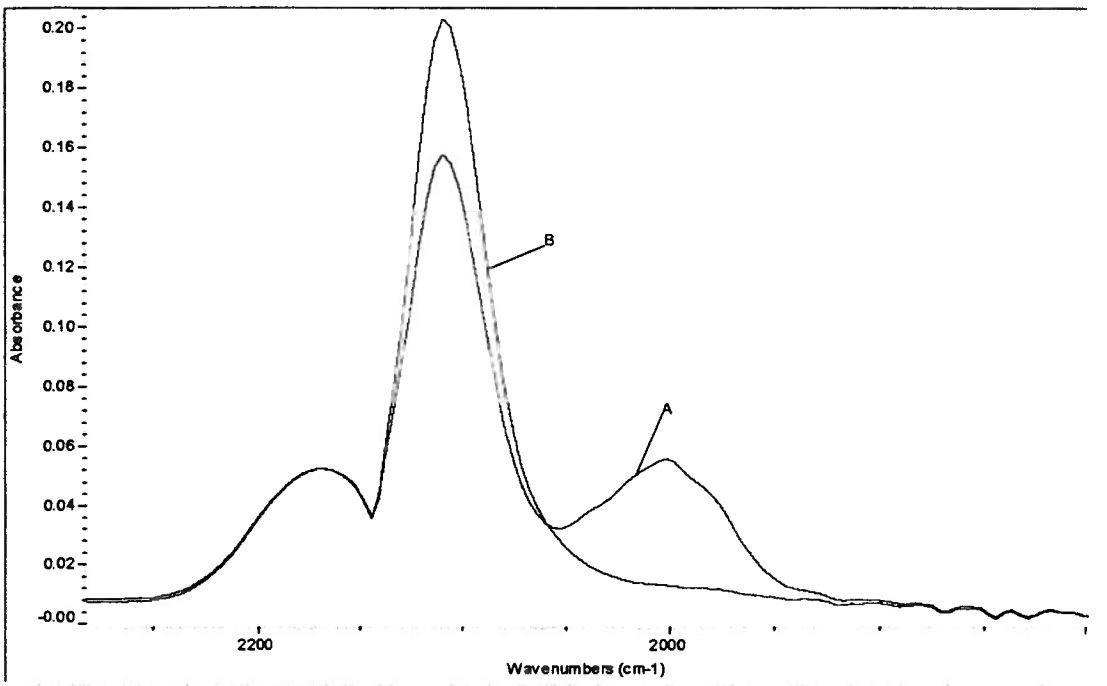

Figure 41. CO adsorbed on the oxidized surface of AQ3 after DMMP adsorption on the surface at 25 °C. Spectrum A was collected immediately after molecular DMMP appeared on the surface. Spectrum B was collected 10 min after admission of CO into the cell.

The DRIFTS experiments show a dissociated DMMP species on the surface of oxidized AQ3 and subsequent adsorption of molecular DMMP. It can be concluded from these results that the first contact of DMMP with the surface of AQ3 leads to complete cleavage of all the methyl groups on the DMMP molecule and a surface phosphate group. After this reaction takes place, DMMP adsorbs molecularly.

4.4.4 Sample AQ4 and its interaction with the DMMP molecule

Sample AQ4 is the result of the fourth impregnation cycle of the aqueous impregnation process. The sample is black in color, has a copper content of 3.5% and a surface area of 128 m^2/g.

4.4.4.1 X-ray diffraction results

The powder X-ray diffraction spectrum of AQ4 shows two peaks at 35.6° and 38.8°. These peaks are indicative of the presence of crystalline CuO on the surface.

4.4.4.2 CO adsorption on the surface of AQ4

When CO is adsorbed on oxidized AQ4, Figure 42, there are two observations to be noted. The first observation, shown in Figure 42 spectrum B, occurs when the O_2 is evacuated for more than 30 min before administering the CO. The two peaks observed in the IR spectrum at 2116 and 2169 cm^{-1} are characteristic of gas phase carbon monoxide. Evacuation of the gas phase CO on this sample results in the observation of a single band at 2116 cm^{-1}. The second observation is shown in Figure 42, spectrum A, and occurs when O_2 is evacuated and CO is immediately administered into the cell. The three peaks observed occur at 2169, 2115 and 2003 cm^{-1}. After 10 min, the 2003 cm^{-1} peak disappears. This band was also observed by Dandekar and Vannice[33], when they adsorbed CO on the surface of a reduced CuO/Al_2O_3, at 173 K and 300K. When the gas phase CO was evacuated, the 2003 cm^{-1} band disappeared at 300 K but remained at 173K. They assigned this band to a linear Cu^0-CO species on the surface of the reduced CuO/Al_2O_3. In our experiment, the temperature of the adsorption was 298 K and the gas phase CO was not evacuated for the 2003 cm^{-1} band to disappear. The sample was oxidized prior to CO administration onto the surface of the sample. The only surface copper species present on the sample surface should be Cu^{2+} and Cu^{+}. Consequently, the presence of a metallic copper species on the surface is highly unlikely. As a result, the

2003 cm^{-1} band is assigned to a two fold bridged CO across two Cu^{2+} sites as shown below.

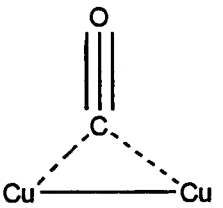

The disappearance of this band can be attributed to the instability of the CO- Cu^{2+} sites.

When the carbon monoxide is evacuated the 2115 cm^{-1} band remains. The intensities of the 2116 cm^{-1} bands, when gas phase CO is mathematically subtracted from the spectra, are similar in both cases indicating that the amount of Cu^{+} species present on the sample is the same when oxidized regardless of the differences in the spectra collected after different evacuation times.

AQ4 was then reduced in methane gas at 450 °C and CO adsorbed on the reduced sample at 25 °C. The infrared spectra collected are shown in Figure 43. Only a single band was observed at 2110 cm^{-1}. There was no evidence of gas phase CO, which suggests that the CO administered onto the sample was linearly adsorbed on the copper sites on the surface of the sample. A small shoulder at 2053 cm^{-1} is also observed and is assigned to a Cu^{0}-CO species. A Fourier self-deconvolution spectrum of the band at 2110 cm^{-1} reveals two peaks at 2105 and 2121 cm^{-1}. These two peaks are assigned to CO linearly adsorbed on Cu^{+} species in dissimilar environments on the alumina surface. During evacuation, the 2110 cm^{-1} shifts to 2117 cm^{-1} and is accompanied by a band at 1973 cm^{-1} as shown in Figure 44. The 2117 cm^{-1} is assigned to a linearly adsorbed Cu^{+}-CO species and the 1973 cm^{-1} is assigned to a carbon monoxide species bridged across two Cu^{+} ions.

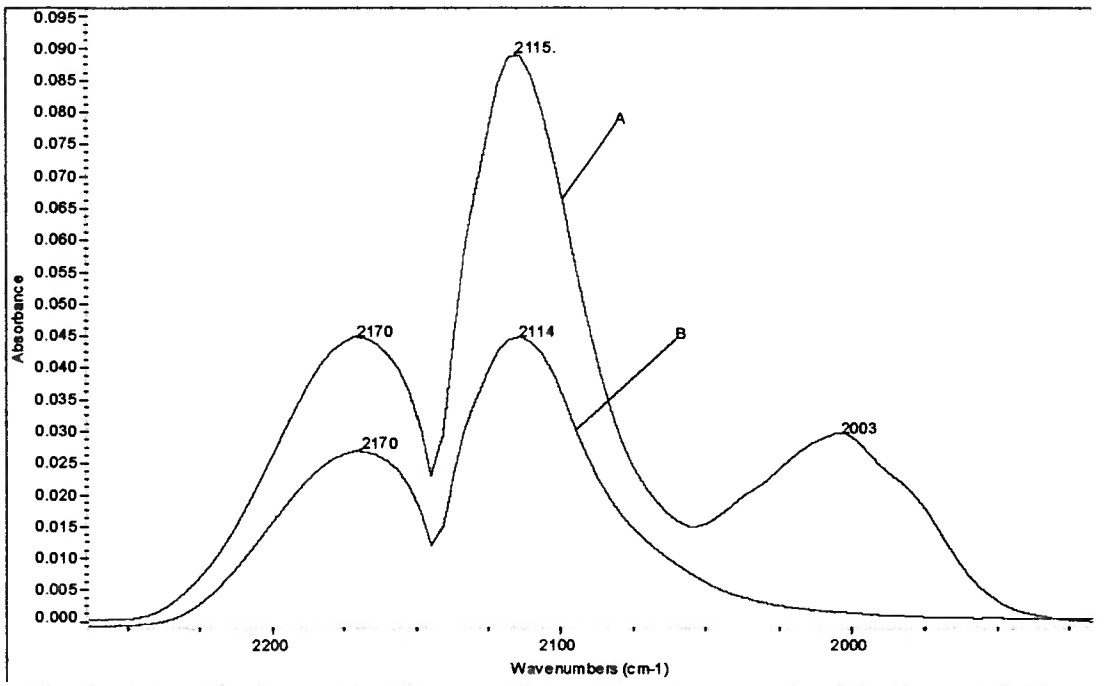

Figure 42. CO adsorbed on the oxidized surface of AQ4. Spectrum A was collected after CO was administered into the cell immediately after O_2 gas was evacuated. Spectrum B was collected after CO was administered into the cell 30 min into evacuation of O_2.

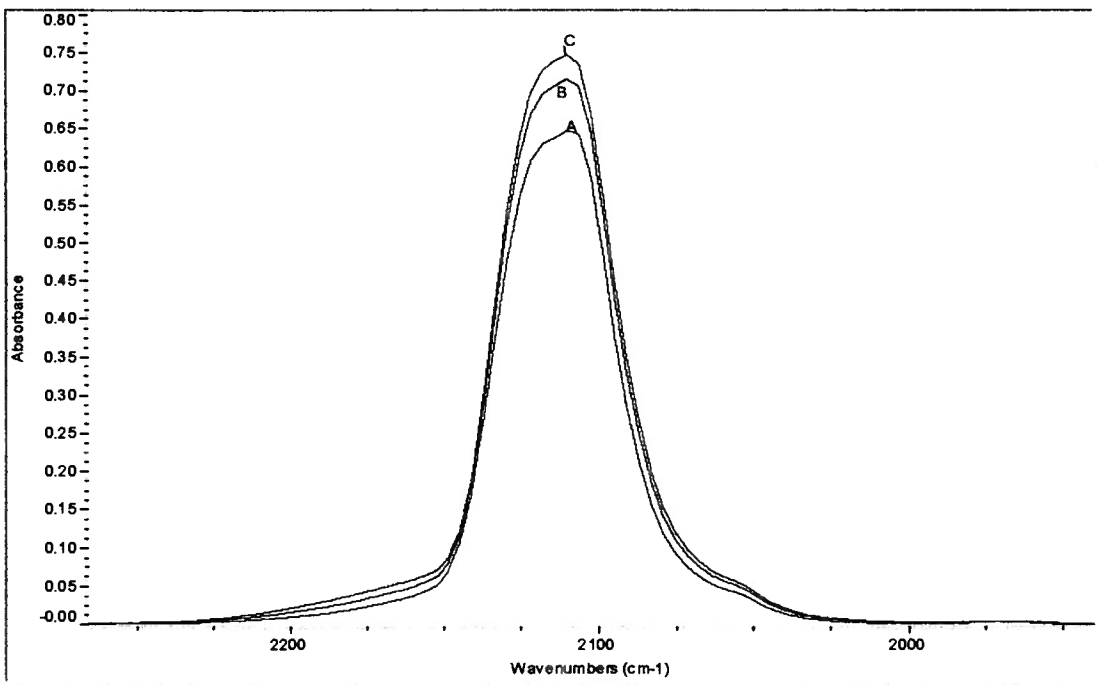

Figure 43. Carbon monoxide adsorbed on the reduced surface of AQ4. Spectrum A = 20 Torr CO, Spectrum B = 40 Torr CO and spectrum C = 60 Torr CO.

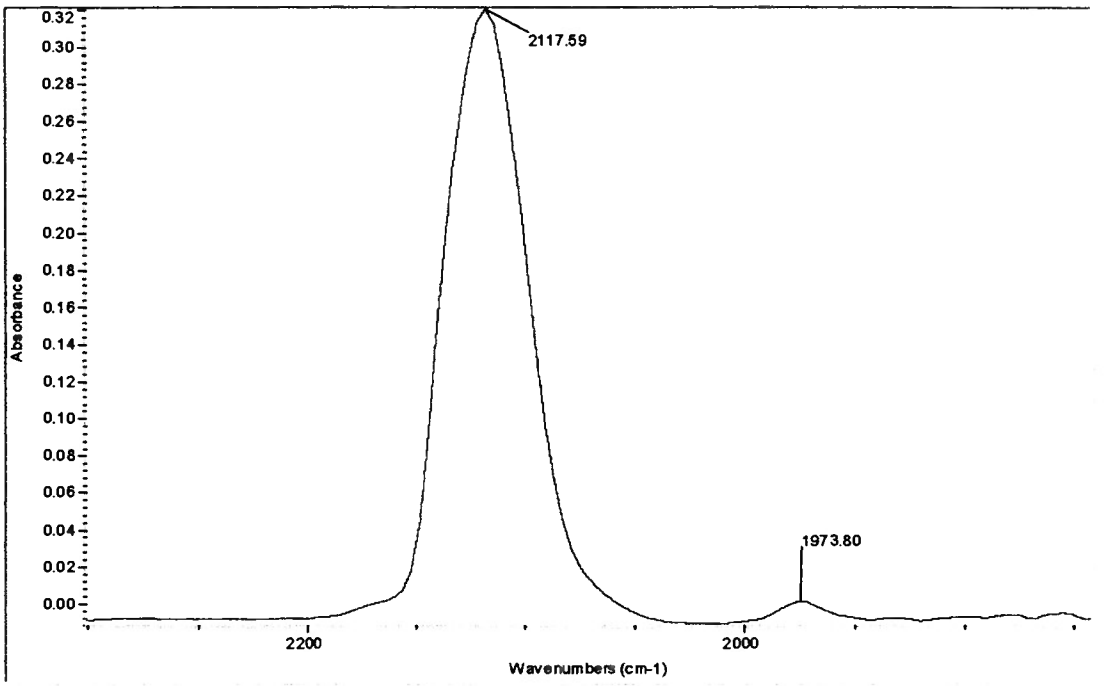

Figure 44. Effect of evacuating gas phase CO on the reduced surface of AQ4 . The 2117 cm^{-1} remains but a new band at 1973 cm^{-1} appears indicating a bridged CO species.

4.4.4.3 Nitric oxide adsorption on the surface of AQ4

NO was admitted onto the surface and evacuated several times before the spectrum in Figure 45 was collected. The first admission on NO did not produce any observable infrared bands in the spectrum. After the fourth admission and evacuation cycle, then the peak at 1866 cm^{-1} was observed and is shown in the spectrum in Figure 45. On evacuation this band disappeared. After evacuation of the NO in the cell, another fresh amount of NO was administered into the cell and the 1866 cm^{-1} peak re-appeared. This peak is assigned to a linear Cu^{2+}-NO species.

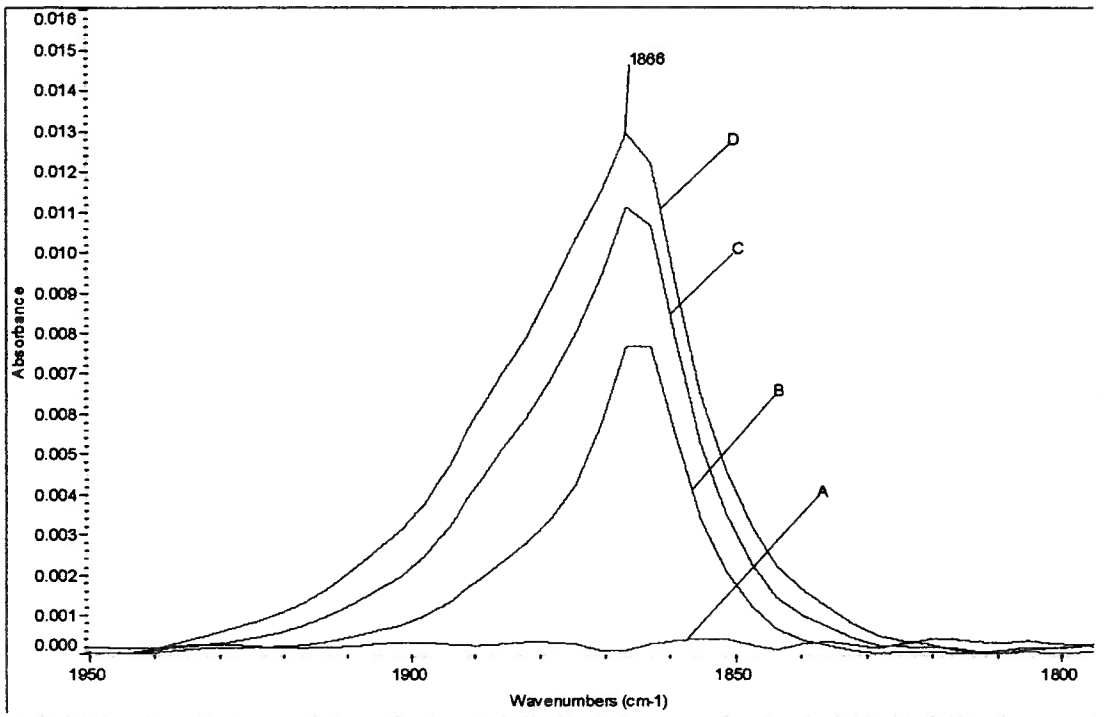

Figure 45. NO on the oxidized surface of AQ4. The different spectra represent different amounts of NO ranging from 10 to 100 Torr. Spectrum A = O Torr NO, B= 12 Torr NO, C= 80 torr NO, D = 100 Torr NO

It is possible that the first pass of NO into the cell caused the NO to dissociate into O_2 and N_2 gas. This reaction has been observed and documented over reduced supported copper catalysts by Reinhard[34] and coworkers and others[37-39].

Figure 46 shows spectra collected after simultaneous adsorption of NO and CO on the surface of AQ4. The spectra shows two prominent peaks one at 2124 cm^{-1} resulting from a CO surface species and the other at 1864 cm^{-1} resulting from a NO surface species. The shoulder at 2170 cm^{-1} is due to gas phase CO. Padley et al. assigned CO frequencies that occurred in the 2120 cm^{-1} region to Cu^{+}-CO species in a Cu^{2+} matrix.

The results of this experiment indicate that the surface of AQ4 is composed of a mixture of Cu^{+1} and Cu^{+2} sites.

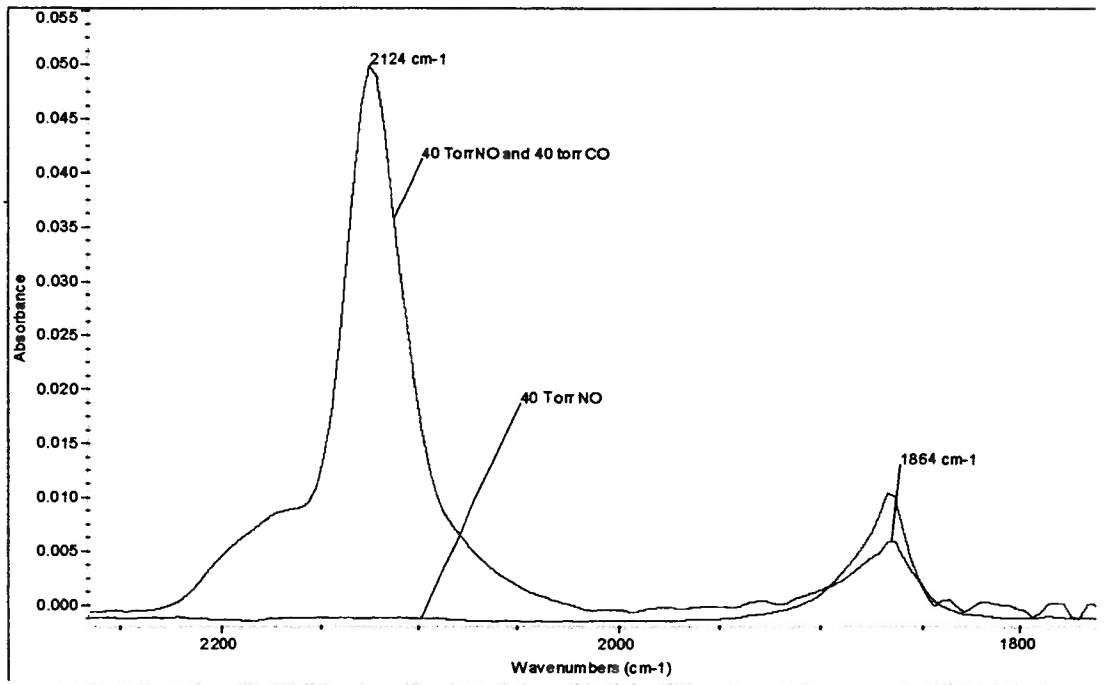

Figure 46. Simultaneous adsorption of NO and CO on the oxidized surface AQ4.

4.4.4.4 Interaction of DMMP and AQ4 using micro-reactor experiments

Micro-reactor experiments were performed on this catalyst in order to observe the products of decomposition. Figure 47 shows the breakthrough points of DMMP over AQ4 at 25 °C and 50 °C. The breakthrough points of DMMP vary at the two temperatures. It takes twice as long for the DMMP to appear in the detector at 25 °C than at 50 °C.

Figure 48 shows the decomposition product distribution as a function of total DMMP passed through the sample. The main product of decomposition for DMMP is

methanol. The methanol production starts before the breakthrough point of DMMP and continues past the breakthough point. At 50 °C however, there was a sharp spike right at the breakthrough point and then the methanol production gradually decreases to zero. This gradual decrease of methanol is due to surface poisoning of the sample.

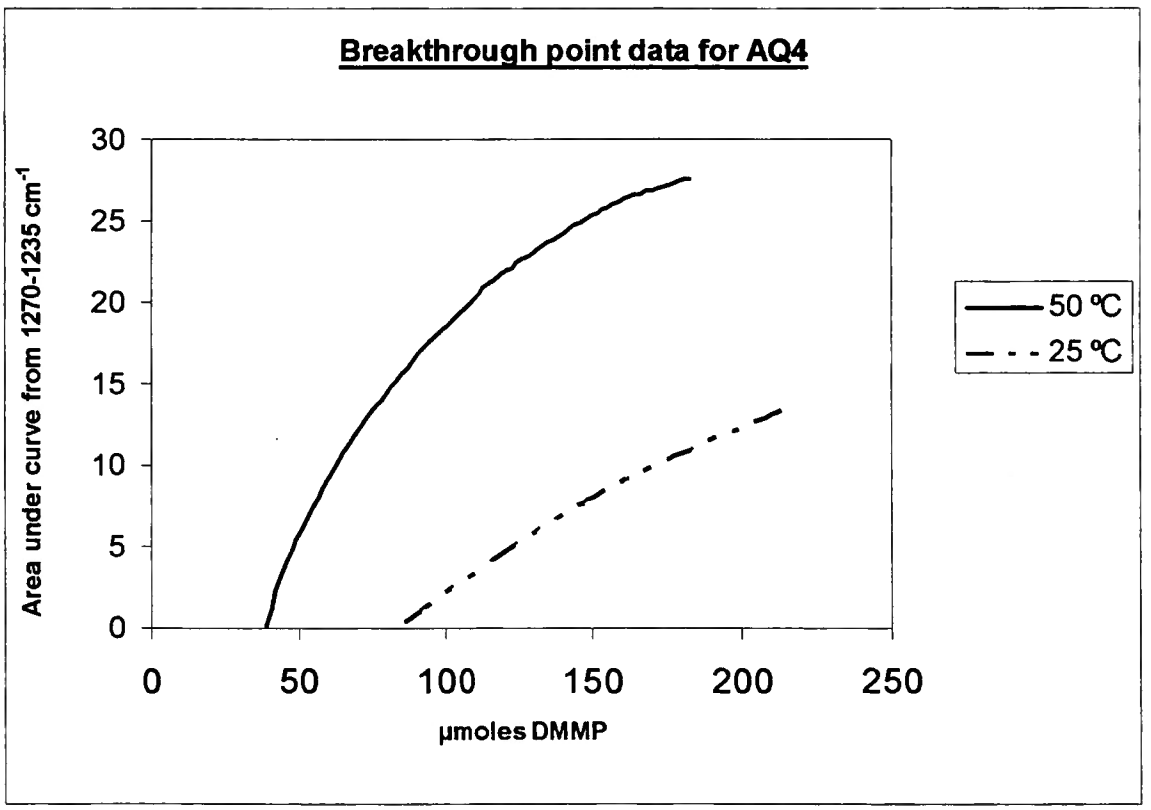

Figure 47. Breakthrough point data for AQ4.

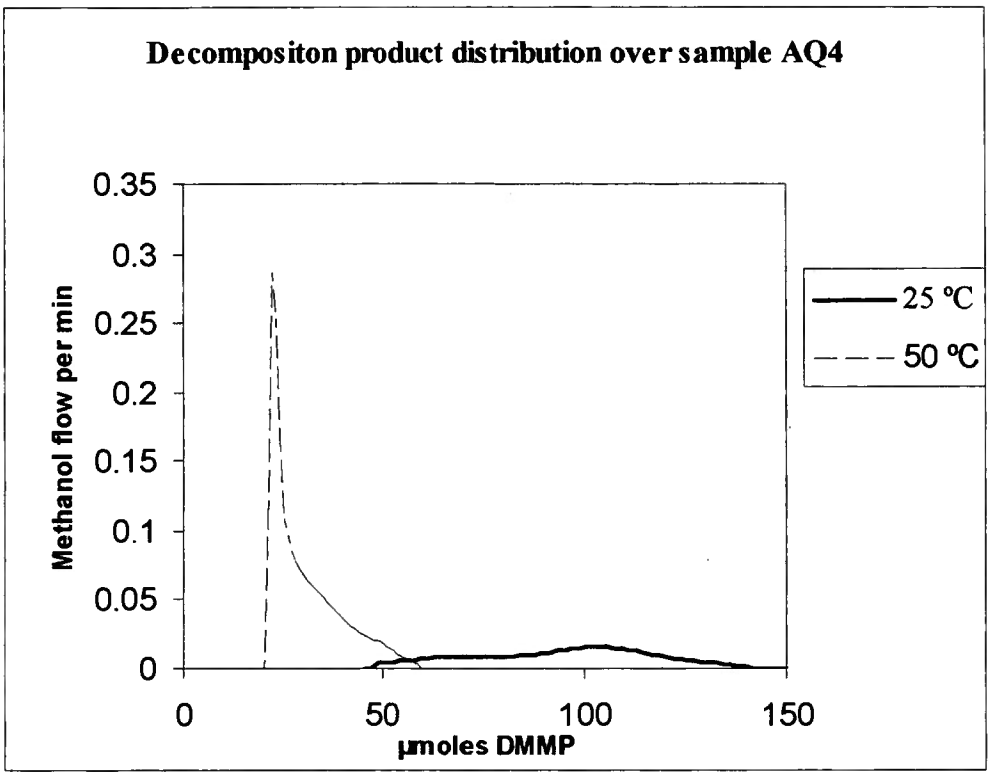

Figure 48. Decomposition products distribution comparison over AQ4

4.4.4.5 DRIFTS spectra of AQ4 with DMMP

Diffuse reflectance infrared spectra of DMMP adsorbed on the surface of AQ4, is shown in Figure 49. Spectrum b in Figure 49 was collected after about 0.02 µmoles of DMMP was admitted into the cell. The infrared spectrum is consistent with a surface structure that resembles a DMMP molecule without a methoxy group. In the lower frequency region there is a 1264 cm^{-1} band that accompanies spectrum b shown in Figure 50. This band has been assigned to a surface structure shown in structure 3 below. This

structure was proposed by Mitchell et al.[11] over iron oxide. As more DMMP begins to accumulate on the surface, this band is hidden under the broad band at 1213 cm^{-1}.

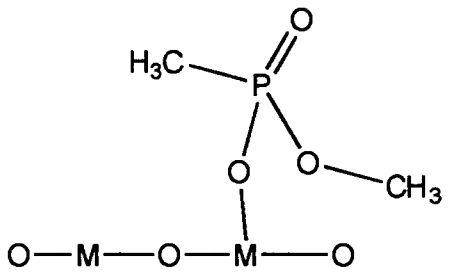

Structure 3

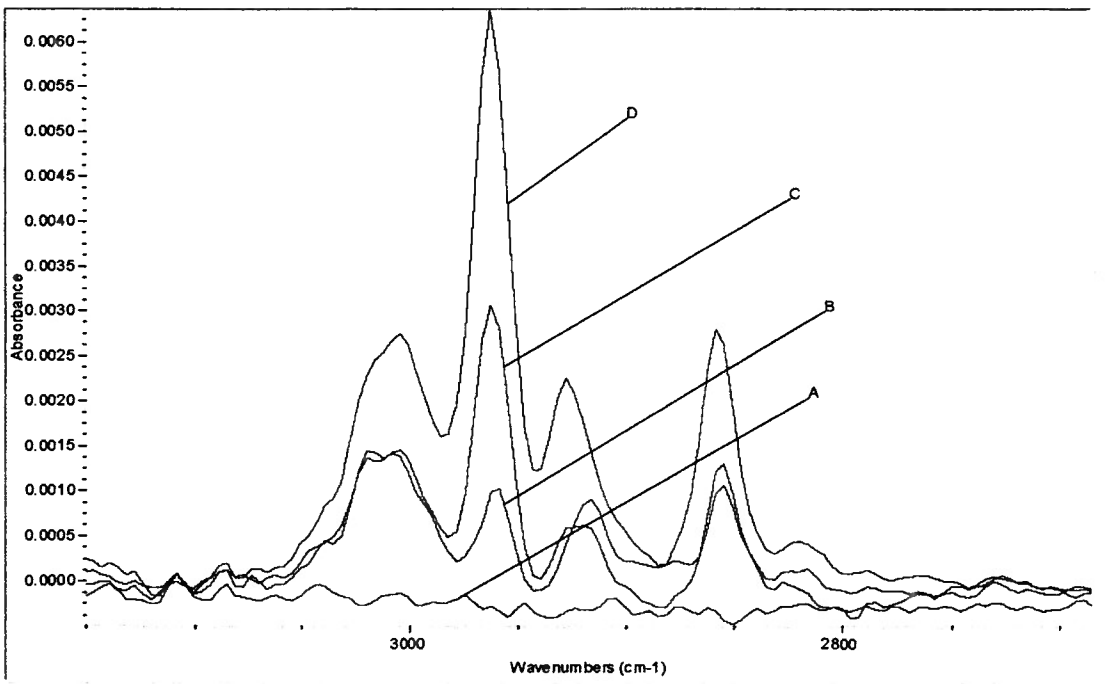

Figure 49. Methyl stretch region of DMMP adsorbed on the surface of AQ4 at 50 °C. Spectrum A through F represent a total of ~ 0.1μmoles of DMMP. Spectrum A = 0 μmoles, spectrum B = 0.02 μmoles, spectrum C =0.065 μmoles and Spectrum D = 0.098 μmoles.

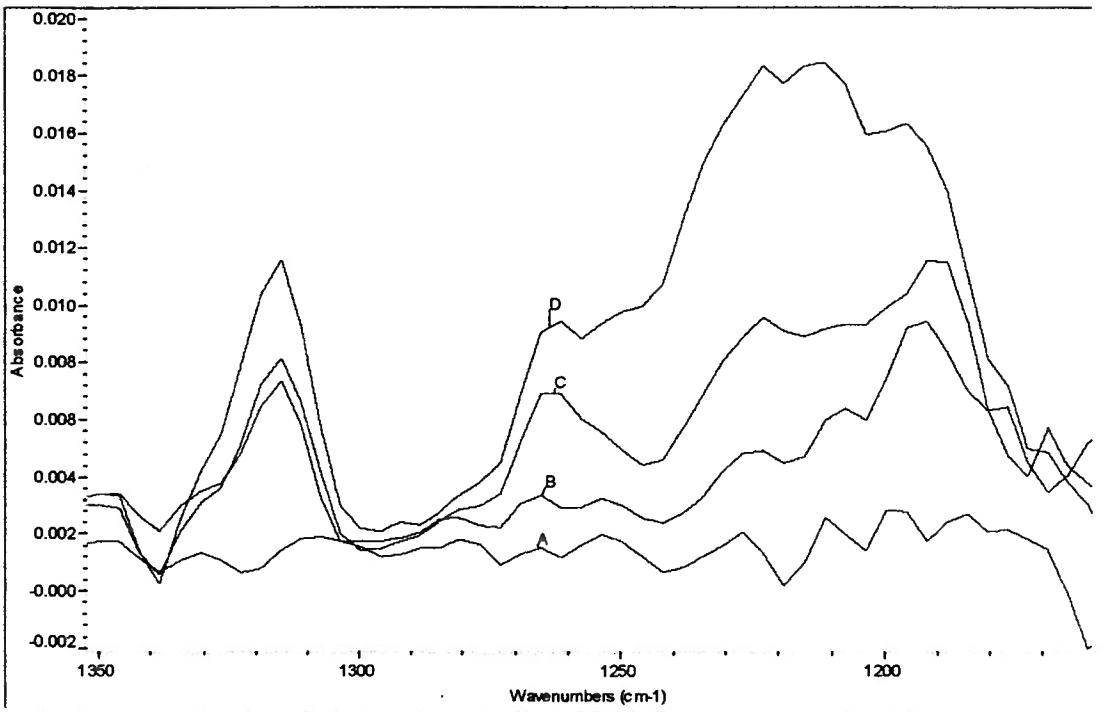

Figure 50. Lower frequency region of DMMPadsorbed on the surface of AQ4 at 50 °C lower frequency region. Spectrum a = 0 µmoles, Spectrum B = 0.02 µmoles, Spectrum C =0.065 µmoles and Spectrum D = 0.098 µmoles.

Supported copper oxide on alumina samples show two types of surface reactions with DMMP that depend on how much copper is present on the surface. At copper coverages of less than 1% for samples prepared via the aqueous impregnation method and less than 2% for the samples prepared via the non-aqueous impregnation method, DMMP adsorbs molecularly (i.e., non- dissociative adsorption). This molecular adsorption proceeds via the phosphoryl oxygen donating electrons to a Lewis acid site on the surface of the supported material, a mechanism suggested by Templeton and Weinberg.[8]

When the copper coverage exceeds the amounts specified above, DMMP may undergo reactions that may cleave the methyl groups on the molecule. The data collected in this work shows that the samples prepared from aqueous impregnation methods with a copper content of 3-4% indicate a reaction that cleaves the methoxy groups on the DMMP molecule and the mechanism of the reaction involves a reorientation of the surface adsorbed structure such that the phosphoryl group remains unperturbed. The energy required to break the P-C is 292 KJ/mol and that required to break the P-O bond is 373 KJ/mol. It is more energetically favorable to cleave the P-CH_3 bond than it is to cleave the P-OCH_3 bond. However, the reaction of DMMP on the surface of copper oxide supported alumina proceeds via the cleavage of the methoxy groups because the methoxy fragment is a good leaving group. The presence of acidic hydrogens on the surface also makes this cleavage more favorable since the hydrogen atoms can be captured by the $^-OCH_3$ leaving group once the phosphorus center has been attacked by a surface nucleophile. The proximity of the copper ions on the surface plays a major role in the commencement of this reaction. The shorter the distance of the copper ions to each other the more likely the methoxy groups on DMMP molecule will be cleaved.

The supported copper oxide supported alumina materials prepared in this work and tested for DMMP decomposition do not show very promising results as alternative viable materials for chemical warfare agent decontamination applications. Although cleavage of the methyl groups on the DMMP molecule was observed for some supported copper samples, the extent of decomposition of the DMMP molecule in comparison to that on γ-alumina is very poor. Consequently, the materials would not suffice to be

applied to small or large scale decontamination efforts where chemical decomposition is the preferred mechanism of action. More work is necessary to develop materials that will have a high conversion rate for the DMMP molecule and molecules with similar structure. The critical issues to be addressed in further designing the mixed metal oxide materials to be applied for decontamination efforts would be as follows:

1) creation of a material with a high density of Lewis acid adsorption sites for the DMMP to attach on to the surface of the material

2) prevention of surface poisoning by phosphate residues created by any decomposition reaction occurring on the surface

3) carefully identifying the appropriate metal oxide or mixed metal oxide combination that would be active for the hydrolysis or oxidative cleavage of the DMMP molecule.

CHAPTER 5

CONCLUSION

Using the successive impregnation method, copper acetylacetonate and copper nitrate were impregnated on high surface alumina. Diffuse reflectance infrared spectroscopy techniques were employed to study the interaction of DMMP with these supported copper oxide materials.

At room temperature, the samples that were prepared using copper acetylacetonate as the precursor showed non-dissociative adsorption for samples with a copper loading as low as 3%. When the copper content reached above 3%, dissociative adsorption of DMMP was observed. In sample NAQ9, the symmetric, anti-symmetric and deformation modes of vibration of the phosphorus bound methyl group are altogether absent in the spectra indicating cleavage of the P-CH_3 bond. At 50 °C, NAQ9 and NAQ11 dissociatively adsorb DMMP via cleavage of the phosphorus bound methoxy group evidenced by the reduction in intensity of the bands that represent the symmetric and anti-symmetric vibration modes.

The copper samples prepared via the aqueous impregnation method using copper nitrate as a precursor also showed similar results to the samples prepared via the non –aqueous impregnation. Samples with a copper loading of 1% or less showed non-dissociative DMMP adsorption. The copper samples that had a copper loading of 1.5% and more showed dissociative adsorption of DMMP. The sample with 1.5% copper content showed complete cleavage of all three methyl groups on the DMMP molecule and a surface phosphate group. The sample with a copper content of 3.64% copper (AQ4) showed cleavage of the phosphorus bound methyl group.

This sample also showed an alternative mode of attachment of DMMP to the surface of the material which did not utilize the oxygen atom on the P=O.

Micro-reactor data on the samples prepared from copper nitrate indicate that the supported copper oxide samples do produce methanol and very little dimethyl ether when DMMP comes in contact with the surface. However, compared to alumina, these copper oxide supported samples have inferior DMMP decomposition properties. This decreased activity is possibly due to the copper oxide occupying the active sites for DMMP decomposition on the alumina surface.

The diffuse reflectance infrared probe molecule experiment results indicate that copper oxide resides on the surface of alumina in both Cu^{+} and Cu^{2+} phases. The Cu^{2+} phase is not easily detected by the carbon monoxide probe at room temperature. However, if the Cu^{2+} ions are in proximity on the surface, an infrared band that is assigned to a two fold bridged CO-Cu^{2+} frequency can be observed. This band is unstable and disappears within a short time after carbon monoxide has been introduced to the surface of the supported copper samples.

5.1 Future Work

The critical issues to be addressed in further designing metal oxide materials to be applied for decontamination efforts require the careful choice of metal oxides or mixed metal oxides that would be effective for the hydrolysis or oxidative cleavage of DMMP and similar molecules. Strong oxidizing agents such as cerium oxide, manganese dioxide, and other metal oxides such as nickel dioxide and cobalt dioxide mixed with copper oxide on the surface of γ-alumina can be suggestions for new materials to be designed for

DMMP decomposition. Other supports other than γ-alumina may also be alternatives. Titanium dioxide, magnesium oxide and silica all have the ability to support other metal oxides on their surfaces and have the ability to possess Lewis acid sites that are necessary for the successful decomposition of the DMMP molecule. Mixing any of the above mentioned supports with other metal oxides could lead to exciting possibilities in designing effective materials for the destruction of the DMMP molecule and molecules of similar structure.

BIBLIOGRAPHY

1. U.S. Arms Control and disarmament Agency. *Convention on the prohibition of the development, production and use of chemical weapons and on their destruction*. Washington:Government Printing Press, 1993.
2. National Research Council. *Review and evaluation of alternative chemical disposal technologies*. Washington: National Academy Press, 1996.
3. Zoledronic acid (Zometa) improved option for hypercalcemia of malignancy. *Am. J. Nurs.* **2001**, *101* (12), 24CCC.
4. Wagner, G.W.; Procell, L.R.; O'Conner, R.J.; Munavali, S.; Carnes, C.L.; Kapoor, P.N.; Klabunde, K.J. *J. Am. Chem. Soc.* **2001**, *123*, 1636-1644.
5. Wagner, G.W.; Koper, O.B.; Lucas, E.; Decker, S.; Klabunde, K.J. *J. Phys. Chem B.* **2000**, *104*, 5118-5123.
6. Vorontsov, A.V.; Davydov, L; Reddy, E. P.; Lion, C.; Savinov, E.N., Smiviniotis, P.G. *New J. Chem.* **2002**, *25* (6), 732-744.
7. Tomkins, B.A.; Sega, G.A.; Macnaughton, S.J. *Anal. Lett.* **1998**, *31* (9), 1603 – 1622.
8. Hedge, R.I.; White, J.M. *J. Phys. Chem.* **1986**, *90*, 2159-2163.
9. Hedge, R. I.; Greenlief, C. M.; White, J. M. *J. Phys. Chem.* **1985**, *89*, 2886-2891.

10. Moravie, R.M.; Fromet, F.; Corset, J. *Spectrochimica Acta.* **1989**, *45A* (10) 1015-1024.

11. Van der Veken, B.J.; Herman, M.A. *Phosphorus and Sulfur*, **1981**, 10, 357-368.

12. Templeton, M.K.; Weinberg, W.H. *J. Am. Chem. Soc.* **1985**, *107*, 97-108.

13. Tesfai, T.M.; Sheinker, V.N.; Mitchell, M.B. *J. Phys. Chem.* **1998**, *102* (38), 7299-7302.

14. Mitchell, M.B.; Sheinker, V.N.; Mintz, E.A. *J. Phys. Chem. B.* **1997**, *101*, 11192-111203.

15. Li, Y-X.; Klabunde K.J. *Langmuir.* **1991**, *7*, 1388-1393.

16. Cao, L.; Segal, S.R.; Suib, S.L.; Tang, X.; Satyapal, S. *J. Catal.* **2000**, *194*, 61-70.

17. Segal, S.R.; Suib, S.L; Tang, X; Satyapal, S. *Chem. Mater.* **1999,** *11*(7) 1687-1695.

18. Segal, S.R.; Cao, L.; Suib, S.L.; Tang, X.; Satyapal S. *J. Catal.* **2001**, *198*, 66-76.

19. Cao, L.; Suib, S.L.; Tang, X.; Satyapal, S. *J. Catal.* **2001**, *197*, 236-243.

20. Yates Jr., J.T.; Rusu, C.N. *J. Phys. Chem. B* **2000**, *104*, 12292-12298.

21. Yates Jr., J.T.; Rusu, C.N. *J. Phys. Chem. B* **2000**, *104*, 12299-12305.

22. Fuller, M.P.; Griffiths, P.R. *Anal. Chem.* **1978**, *50*, 1906-1910.

23. Fuller, M.P.; Grifith, P.R. *Appl. Spectrosc.* **1980**, *34*, 533-539.

24. Kubela, P.; Munk, F., *Z. Tech. Phys.* **1931**, *12*, 593. Kubelka, P. *J. Opt. Soc. Am. Pt.1*, **1948**, *38*, 448.

25. Yang, P. W. and Casal, H. L. *Appl. Spectrosc.*, **1986**, *40*, 1070: Blitz, J. P.; Murthy, R. S. S.; Leyden, D. E. *Appl. Spectrosc.*, **1986**, *40*, 829.

26. Tundo, P. In *Continuous flow methods in organic synthesis*; Ellis Horwood: New York, 1991; pp. 23-26.

27. Peri, J. B. *J. Phys. Chem.* **1965**, *69*, 211, 220, 231.

28. Knözinger, H.; Ratsamy, P. *Catal. Rev.-Sci. Eng.* **1978**, *17*(1), 31-70.

29. Garbowski, E.; Primet, M. *J. Chem. Soc. Chem. Commun.* **1991,** *1*, 11-12.

30. Lee, K.Y.; Houalla, M.; Hercules, D.M.; Hall, W.K. *J. Catal.* **1994**, *145*, 223-231.

31. Morrow, J.R.; Trogler, W.C. *Inorg. Chem.* **1989**, *28* (12), 2330-2333.

32. Morrow, J. R.; Trogler, W. C. *Inorg. Chem.* **1988**, *27*, 3387-3394.

33. Courtney, R.C.; Gustafson, R.L.; Westerback, I.J.; Hyytiainen, H.; Charberek Jr., S.C.; Martell, A.E. *J. Am. Chem. Soc.* **1957**, *79*, 3030-3036.

34. Sohn, H.; Létant, S.; Sailor, M.J.; Trogler, W.C. *J. Am. Chem. Soc.* **2000**, *122*, 5399-5400.

35. Busca, G. *J. Mol. Catal.* **1987**, *43*, 225.

36. London, J.T.; Bell, A.T. *J. Catal.* **1973**, *31*, 32 and 96.

37. Lokhov, Y.A; Morozo, L.N.; Davydov, A.A.; Kostrov, V.V. *Kinet Katal.* **1980**, *21*, 943.

38. Reinhard H.; Urbach H.P.; Knözinger H. *J. Chem Soc. Faraday Trans.*, **1992**, *88*(3), 322-360.

39. Padley, M.B.; Rochester, C.H.; Hutchings, G.H.; King, F. *J. Catal.* **1994**, *148*, 438.

40. Dandekar, A.; Vannice, M.A. *J. Catal.* **1998**, *178*, 621-639.

41. Johnson, D.W.; Matloob, H.; Roberts. *J. Chem. Soc., Faraday Trans.* 1, **1979**, *75*, 2143.

42. Wendelken, J. F. *Appl. Surf. Sci.*, **1982**, *11/12*, 172.

43. Balkenende, A.R; Gijzeman, O.L. J.; Gues, J.W. In *Catalytic science and Technology;* Yoshida S.; Takezawa N.; Ono T.; Kodansha, Ed.; Tokyo and VCH, Weinheim, 1991, p.177.

44. Glocker, G. *J. Phys. Chem.* **1958**, *62*, 1049.

45. Boggs, J.E.; Grain, C.M.; Whiteford, J.E. *J. Phys. Chem.* **1957**, *61*, 481.

46. Eischen R.P.; Pliskin, W.A; Francis, S.A. *J. Chem. Phys.* **1954,** *22*, 194.

47. Nguyen, T.T.; Shepard, N.; R.E. Hester, R.H.J. Clark, Eds., *Advances in Infrared and Raman spectroscopy* Vol.5, Heyden, London 1978, pp.112-117.

48. Horn, K. and Pritchard, J. *Surf. Sci.* **1976**, *55*, 701.

49. Pritchard, J., Catterick, T., and Gupta, R.K. *Surf. Sci.* **1976**, *54*, 1.

50. Chen, L.Y.; Horiuchi, T.; Osaki, T.; Mori, T. *Appl. Catal. B. Environ.* **1999**, *23*, 259-269.

51. Berkowitz, J. *J.Chem. Phys.* **1959**, *30*, 858.

52. *Tables of Interatomic distances and configuration in molecules and ions*; Sutton L.E.; Jenkins E.; Mitchell A.D.; Cross L.C; Ed.; The Chemical Society; London, 1958; pp M46.

53. Iwamoto, M.; Yahiro, H.; Mizuno, N.; Zhang, W.X.; Mine, Y.; Furukawa, H.; Kagawa, S. *J. Phys. Chem.* **1992**, *96* (23), 9360.

54. Lokhov, Y.A; Morozo, L.N.; Davydov, A.A.; Koshov, V.V. *Kinet. Katal.* **1979**, *20*, 1239.

55. Fu, Y.; Tian, Y.; Lin, P. *J. Catal.* **1991**, *132*, 85.

56. Hierl, R.; Urback, H. P.; Knozinger, H. *J. Chem. Soc.,Faraday Trans.*, **1992**, *88* (3), 355.

57. . Griffiths, P.R; Pariente, G. *Trends in Anal. Chem.* **1986**, 5 (8).

58. Peter R. Griffiths and James A. de Haseth. *"Fourier Transform Infrared Spectroscopy"*: John D. Wiley & Sons. 1986. Chapters 1 and 3.

59. Yang, Y.C.; Baker , J.A.; Ward, J.R. *Chem. Rev.* **1992**, *92*,1729-1743.

60. Obee, T.N.; Satyapal, S. *J. Photochem. Photobiol. A chem.* **1998**, *118*, 45-51.

61. Itoh, T; Hisada, H; Usui, Y; Fuji, Y. *Inorganica Chimica Acta.* **1998,** *283* (1), 51-60.

62. J.A. Kerr in CRC handbook of chemistry and physics, 1999-2000: *A ready reference book of chemical and physical data (CRC handbook of chemistry and physics*, D.R. Lide, (Ed.), CRC press, Boca Raton, Florida, USA, 81st edition, 2000.